VOLUME 1

Neonatal and Perinatal Medicine

Atlas of the Newborn

Rudolph

VOLUME 1

Neonatal
and
Perinatal
Medicine

Atlas of the Newborn

Arnold J. Rudolph, M.D.
(Deceased)
Professor of Pediatrics
Baylor Medical College
Houston, Texas

VOLUME 1

Neonatal
and
Perinatal
Medicine

Atlas of the Newborn

Arnold J. Rudolph, M.D.
(Deceased)

1997

B.C. Decker Inc.
Hamilton • London

B.C. Decker Inc.
4 Hughson Street South
P.O. Box 620, L.C.D. 1
Hamilton, Ontario L8N 3K7
Tel: 905 522-7017
Fax: 905 522-7839
e-mail: info@bcdecker.com

Printed in Canada

96 97 98 99 00/BP/987654321

ISBN 1-55009-031-3

Sales and distribution

United States
Blackwell Science Inc.
Commerce Place
350 Main Street
Malden, MA 02148
U.S.A.
Tel: 1-800-215-1000

Canada
Copp Clark Ltd.
200 Adelaide Street West
3rd Floor
Toronto, Ontario
Canada M5H 1W7
Tel: 416-597-1616
Fax: 416-597-1617

Japan
Igaku-Shoin Ltd.
Tokyo International P.O. Box 5063
1-28-36 Hongo, Bunkyo-ku
Tokyo 113, Japan
Tel: 3 3817 5680
Fax: 3 3815 7805

U.K., Europe, Scandinavia, Middle East
Blackwell Science Ltd.
c/o Marston Book Services Ltd.
P.O. Box 87
Oxford OX2 0DT
England
Tel: 44-1865-79115

Australia
Blackwell Science Pty, Ltd.
54 University Street
Carleton, Victoria 3053
Australia
Tel: 03 9347 0300
Fax: 03 9349 3016

Foreword

Sir William Osler stated, "There is no more difficult task in medicine than the art of observation." The late Arnold Jack Rudolph was an internationally renowned neonatologist, a teacher's teacher, and, above all, one who constantly reminded us about how much could be learned by simply observing, in his case, the newborn infant.

This color atlas of neonatology represents a distillation of more than 50 years of observing normal and abnormal newborn infants. The *Atlas* begins with a section on the placenta, its membranes, and the umbilical cord. Jack Rudolph delighted in giving a lecture entitled "Don't Make Mirth of the Afterbirth," in which he captivated audiences by showing them how much you could learn about the newborn infant from simply observing the placenta, its membranes, and the umbilical cord.

In a few more than 60 photomicrographs, we learn to read the placenta and gain insight into such disorders as intrauterine growth retardation, omphalitis, cytomegalic inclusion disease, congenital syphilis, and congenital neuroblastoma. Congenital abnormalities of every organ system are depicted along with the appearance of newborn infants who have been subjected in utero to a variety of different drugs, toxins, or chemicals. We also learn to appreciate the manifestations of birth trauma and abnormalities caused by abnormal intrauterine positioning.

More than 250 photographs are used to illustrate the field of neonatal dermatology. The collection of photographs used in this section is superior to that which I have seen in any other textbook or atlas of neonatology or dermatology; this section alone makes this reference a required addition to the library of any clinician interested in the care of infants and children. Photographs of the Kasabach-Merritt syndrome (cavernous hemangioma with thrombocytopenia), Klippel-Trénaunay syndrome, Turner's syndrome, Waardenburg's syndrome, neurocutaneous melanosis, mastocytosis (urticaria pigmentosa), and incontinentia pigmenti (Bloch-Sulzberger syndrome) are among the best that I have seen.

Cutaneous manifestations are associated with many perinatal infections. The varied manifestations of staphylococcal infection of the newborn are depicted vividly in photomicrographs of furunculosis, pyoderma, bullous impetigo, abscesses, parotitis, dacryocystitis, inastitis, cellulitis, omphalitis, and funisitis. Streptococcal cellulitis, *Haemophilus influenzae* cellulitis, and cutaneous manifestations of listeriosis all are depicted. There are numerous photomicrographs of congenital syphilis, showing the typical peripheral desquamative rash on the palms and soles, as well as other potential skin manifestations of congenital syphilis which may produce either vesicular, bullous, or ulcerative lesions. The various radiologic manifestations of congenital syphilis, including pneumonia alba, ascites, growth arrest lines, Wegner's sign, periostitis, and syphilitic osteochondritis, are depicted. Periostitis of the clavicle (Higouménaki's sign) is shown in a photograph that also depicts periostitis of the ribs. A beautiful photomicrograph of Wimberger's sign also has been included; this sign, which may appear in an infant with congenital syphilis, reveals radiolucency due to erosion of the medial aspect of the proximal tibial metaphysis.

The *Atlas* also includes a beautiful set of photographs which delineate the ophthalmologic examination of the newborn. Lesions which may result from trauma, infection, or congenital abnormalities are included. There are numerous photographs of the ocular manifestations of a variety of systemic diseases, such as Tay-Sachs disease, tuberous sclerosis, tyrosinase deficiency, and many more. Photographs of disturbances of each of the various organ systems, or disorders affecting such organ systems, also are included along with numerous photographs of different forms of dwarfism, nonchromosomal syndromes and associations, and chromosomal disorders. In short, this *Atlas* is the complete visual textbook of neonatology and will provide any

physician, nurse, or student with a distillation of 50 years of neonatal experience as viewed through the eyes of a master clinician.

Arnold Jack Rudolph was born in 1918, grew up in South Africa, and graduated from the Witwatersrand Medical School in 1940. Following residency training in pediatrics at the Transvaal Memorial Hospital for Children, he entered private pediatric practice in Johannesburg, South Africa. After almost a decade, he left South Africa and moved to Boston, where he served as a Senior Assistant Resident in Medicine at the Children's Medical Center in Boston, Massachusetts, and subsequently pursued fellowship training in neonatology at the same institution and at the Boston Lying-In Hospital, Children's Medical Center and Harvard Medical School under Dr. Clement A. Smith.

In 1961, Dr. Rudolph came to Baylor College of Medicine in Houston, Texas, the school at which he spent the remainder of his career. He was a master teacher, who received the outstanding teacher award from pediatric medical students on so many occasions that he was elected to the Outstanding Faculty Hall of Fame in 1982. Dr. Rudolph also received numerous awards over the years from the pediatric house staffs for his superb teaching skills.

He was the Director of the Newborn Section in the Department of Pediatrics at Baylor College of Medicine for many years, until he voluntarily relinquished that position in 1986 for reasons related to his health. Nevertheless, Jack Rudolph continued to work extraordinarily long hours in the care of the newborn infant, and was at the bedside teaching both students and house staff, as well as his colleagues, on a daily basis until just a few months before his death in July 1995.

Although Dr. Rudolph was the author or co-author of more than 100 published papers that appeared in the peer-reviewed medical literature, his most lasting contribution to neonatology and to pediatrics is in the legacy of the numerous medical students, house staff, fellows, and other colleagues whom he taught incessantly about how much one could learn from simply observing the newborn infant. This *Atlas* is a tour de force; it is a spectacular teaching tool that has been developed, collated, and presented by one of the finest clinical neonatologists in the history of medicine. It is an intensely personal volume that, as Dr. Rudolph himself states, "is not intended to rival standard neonatology texts," but rather to supplement them. This statement reveals Dr. Rudolph's innate modesty, since with the exception of some discussion on pathogenesis and treatment, it surpasses most neonatology texts in the wealth of clinical information that one can derive from viewing and imbibing its contents. We owe Dr. Rudolph and those who aided him in this work a debt of gratitude for making available to the medical community an unparalleled visual reference on the normal and abnormal newborn infant.

Ralph D. Feigin, M.D.
June 13, 1996

Preface

I first became attracted to the idea of producing a color atlas of neonatology many years ago. However, the impetus to synthesize my experience and compile this current collection was inspired by the frequent requests from medical students, pediatric house staff, nurses and others to provide them with a color atlas of the clinical material provided in my "slide shows." For the past few decades I have used the medium of color slides and radiographs as a teaching tool. In these weekly "slide shows" the normal and abnormal, as words never can, are illustrated.

"I cannot define an elephant but I know one when I see one."[1]

The collection of material used has been added to constantly with the support of the pediatric house staff who inform me to "bring your camera" whenever they see an unusual clinical finding or syndrome in the nurseries.

A thorough routine neonatal examination is the inalienable right of every infant. Most newborn babies are healthy and only a relatively small number may require special care. It is important to have the ability to distinguish normal variations and minor findings from the subtle early signs of problems. The theme that recurs most often is that careful clinical assessment, in the traditional sense, is the prerequisite and the essential foundation for understanding the disorders of the newborn. It requires familiarity with the wide range of normal, as well as dermatologic, cardiac, pulmonary, gastrointestinal, genitourinary, neurologic, and musculoskeletal disorders, genetics and syndromes. A background in general pediatrics and a working knowledge of obstetrics are essential. The general layout of the atlas is based on the above. Diseases are assigned to each section on the basis of the most frequent and obvious presenting sign. It seems probable that the findings depicted will change significantly in the decades to come. In this way duplication has been kept to a minimum. Additional space has been devoted to those areas of neonatal pathology (e.g., examination of the placenta, multiple births and iatrogenesis) which pose particular problems or cause clinical concern.

Obviously, because of limitations of space, it is impossible to be comprehensive and include every rare disorder or syndrome. I have tried to select both typical findings and variations in normal infants and those found in uncommon conditions. Some relevant conditions where individual variations need to be demonstrated are shown in more than one case.

As the present volume is essentially one of my personal experience, it is not intended to rival standard neonatology texts, but is presented as a supplement to them. It seems logical that references should be to standard texts or reviews where discussion on pathogenesis, treatment, and references to original works may be found.

Helen Mintz Hittner, M.D., has been kind enough to contribute the outstanding section on neonatal ophthalmology.

I have done my best to make the necessary acknowledgements to the various sources for the clinical material. If I have inadvertently omitted any of those, I apologize. My most sincere appreciation and thanks to Donna Hamburg, M.D., Kru Ferry, M.D., Michael Gomez, M.D., Virginia Schneider, PA, and Jeff Murray, M.D., who have spent innumerable hours in organizing and culling the material from my large collection. We wish to thank Abraham M. Rudolph, M.D., for his assistance in reviewing the material. We also wish to thank the following people for their photo contributions to this work: Cirilo Sotelo-Avila, Stan Connor, Avory Fanaroff, Milton Finegold, Brian Kershan, Tom Klima, Susan Landers, Gerardo Cabera-Meza, Ken Moise, Don Singer, Edward Singleton.

It is hoped that this atlas will provide neonatologists, pediatricians, family physicians, medical students and nurses with a basis for recognizing a broad spectrum of normal variations and clinical problems as well as provide them with an overall perspective of neonatology, a field in which there continues to be a rapid acceleration of knowledge and technology. One must bear in mind the caveat that pictures cannot supplant clinical experience in mastering the skill of visual recall.

1. Senile dementia of Alzheimer's type — normal aging or disease? (Editorial) *Lancet* 1989; i:476-477.

Arnold J. Rudolph, M.D.

CONTENTS

Volume I
Neonatal and Perinatal Medicine

Introduction

Although several texts provide extensive written descriptions of disorders o the newborn infant, the senses of touch, hearing and, especially, sight create the most lasting impressions. Over a period of almost five decades, my brother Jack Rudolph diligently recorded in pictorial form his vast experiences in physical examination of the newborn. The *Atlas of the Newborn* reflects a selection from the thousands of color slides in his collection, and truly represents "the art of medicine" as applied to neonatology. A number of unusual or rare conditions are included in this atlas. I consider this fully justified because, if one has not seen or heard of a condition, one cannot diagnose it.

In this, the first in a five-volume series, three main topics are covered. Although it is common practice to discard the afterbirth, or placenta and its membranes, careful examination of this fetal organ often provides insight into conditions affecting the newborn. Thus, it may reveal evidence of intrauterine infection, which may be transmitted to the neonate; of hemorrhage, which may cause asphyxia; or of vascular or developmental anomalies, which may result in intrauterine growth retardation. Many of these placental abnormalities are illustrated in this volume.

Physical forces acting during fetal development, during delivery, or after birth may be responsible for a variety of anomalies in the newborn. The influences of uterine constraint, of fetal position, and of amniotic bands are demonstrated magnificently, with resulting anomalies being related to specific fetal postures. Conditions associated with birth trauma, including fractures, nerve disruptions and other disturbances, are clearly depicted. Many examples of complications resulting from treatment of the newborn, or iatrogenic problems such as vascular complications of umbilical arterial catheterization, are shown graphically.

A major section demonstrates many of the physical anomalies resulting from fetal exposure to various chemicals, such as occurs through maternal drug abuse or administration of pharmacologic agents to the mother during embryonic or fetal development.

This volume will be enormously valuable to obstetricians and neonatologists, as well as to midwives and nurses involved in the delivery and care of the newborn.

Abraham M. Rudolph, M.D.

Chapter 1
The Placenta, Its Membranes, and the Umbilical Cord

The human placenta is a highly sophisticated organ of interface between mother and fetus, often referred to as the "gate-keeper to the fetus." Careful examination of the placenta, its membranes, and the umbilical cord can prove to be a valuable aid in the diagnosis and treatment of the neonate. Gross examination of the placenta takes five minutes, and more sophisticated examination should be considered when there is poor pregnancy outcome, recognizable malformations or abnormalities, multiple gestation, extremes of amniotic fluid volume, severe intrauterine growth retardation, short umbilical cord (< 32 cm), and profound acidemia. The maternal surface of the placenta (decidual plate) is soft, spongy and dark red; and the fetal surface (chorionic plate) is shiny and steel blue to gray. The placenta, membranes, and umbilical cord weigh approximately 400 to 600 g at birth. The ratio of fetal to placental size increases with gestation, being less than or equal to 1:1 at prior to three months, 4:1 at four to six months, and 6:1 at term. Abnormalities in structure can result in an inefficient transport of oxygen and nutrients to the developing baby. Despite this importance, it is one of the least understood and investigated human organs.

1.1

Figure 1.1. A succenturiate (accessory) lobe is common and has no effect on the fetus. This occurs in about 3 to 5% of deliveries. Its importance arises from the fact that it may be retained within the uterus and cause postpartum bleeding. (Sotelo-Avila, C.)

1.2

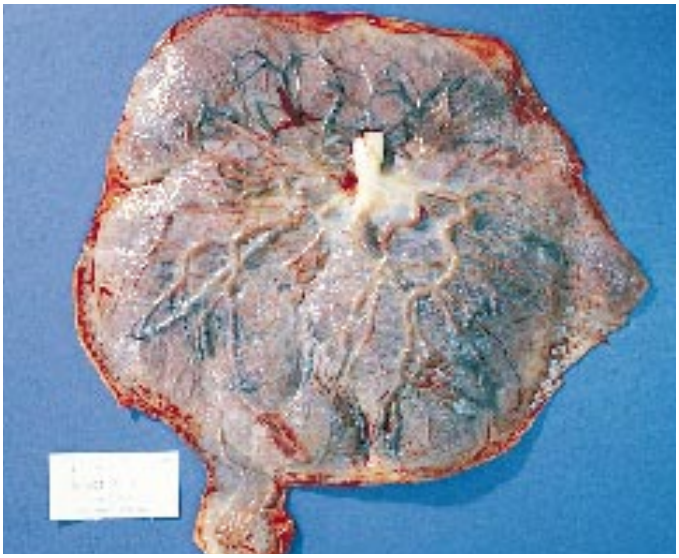

Figure 1.2. Another example of a succenturiate lobe. Note that this is very small and the diagnosis can easily be missed if the placenta is not examined carefully. (Singer, D.)

1.3

Figure 1.3. Fetal surface of a bipartite or bilobed placenta (placenta duplex). The two parts of the placenta are of nearly equal size and this occurs in about 1% of deliveries. Note that the lobes are separated by membranes. The umbilical cord may insert into one or other lobe, or may insert between the two.

1.4

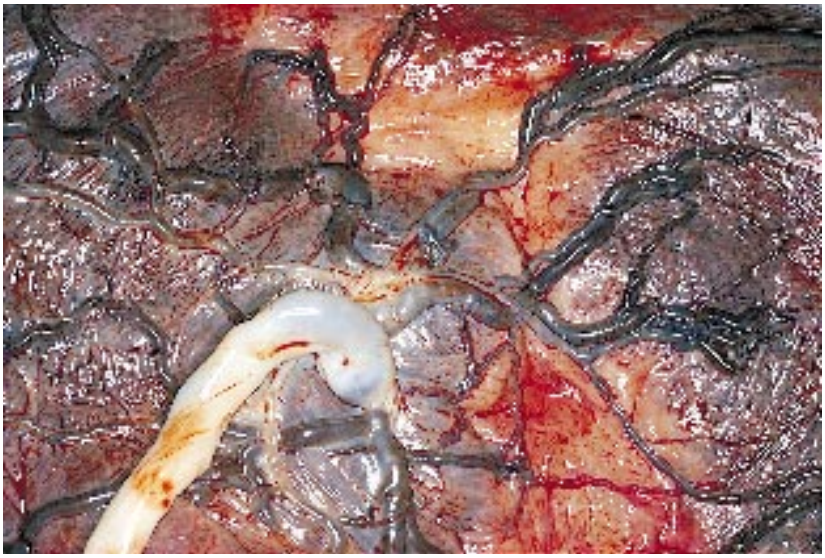

Figure 1.4. A close-up of the same placenta. The risk to the infant is that the vessels crossing the membranes may rupture, resulting in massive blood loss. It is suggested that this condition arises as a result of superficial implantation of the ovum.

1.5

Figure 1.5. Another example of a placenta duplex showing the maternal surface.

1.6

Figure 1.6. In a circumvallate (circummarginate) placenta the fetal surface may be reduced if decidual tissue has made its way between the amnion and chorion. This appears as a yellow, peripheral, hyalinized fold circumscribing the edge of the chorionic plate. This type of placenta has been reported to be a cause of antepartum bleeding and premature labor.

1.7

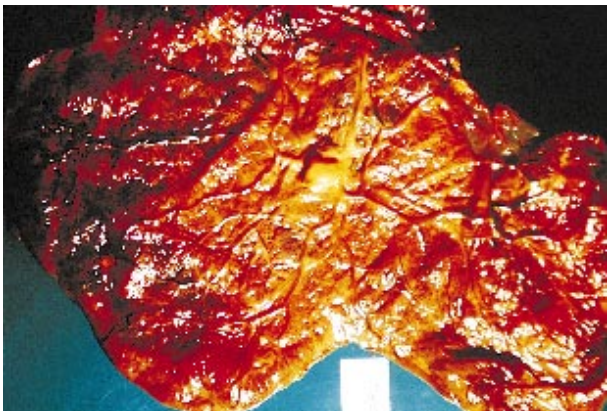

Figure 1.7. This is an example of placenta membranacea (placenta diffusa). These placentas are rare. The ovum implants too deeply, the villae of the chorion fail to regress, and the placental tissue develops over the entire surface of the chorion. The placenta is very thin and is associated with poor fetal growth and antepartum hemorrhage. There may be previa type bleeding.

1.8

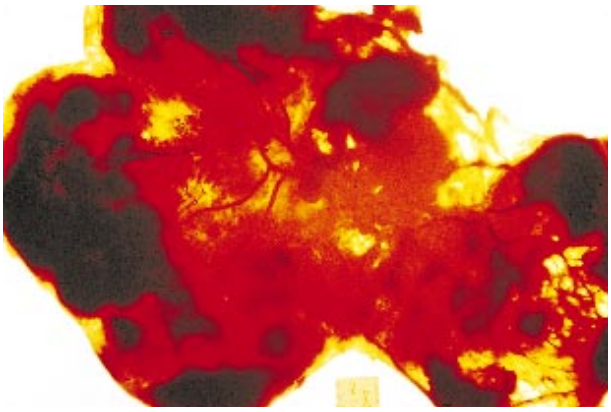

Figure 1.8. Transillumination of the same placenta shows the thinness of this type of placenta and that islets of placental tissue are present throughout the membranes. Pregnancy rarely goes to term and fetal death is common. If pregnancy continues to term, placenta accreta may occur. In this condition, there is failure of separation of the placenta during the third stage of labor and there may be severe postpartum hemorrhage.

1.9

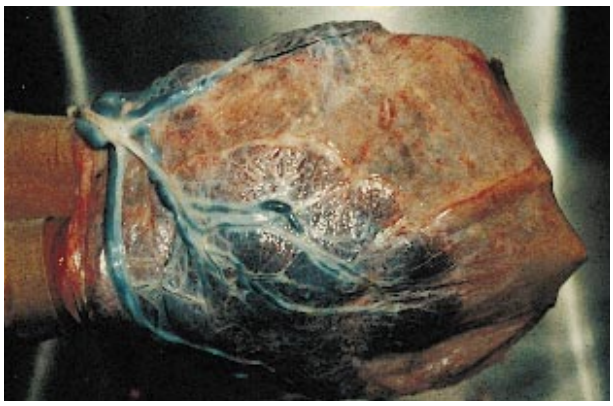

Figure 1.9. An annular ("girdle" or ring-shaped) is a rare form of placenta which resembles a segment of a hollow cylinder. Sometimes a complex ring of placental tissue is seen. More commonly a portion of the ring undergoes atrophy resulting in a placenta which is approximately horseshoe-shaped. This type of placenta is probably a variant of placenta membranacea. Its clinical significance is uncertain but it appears to be associated with a high incidence of both ante- and postpartum bleeding. The fetus is often small for gestational age. (Connor, S.)

1.10

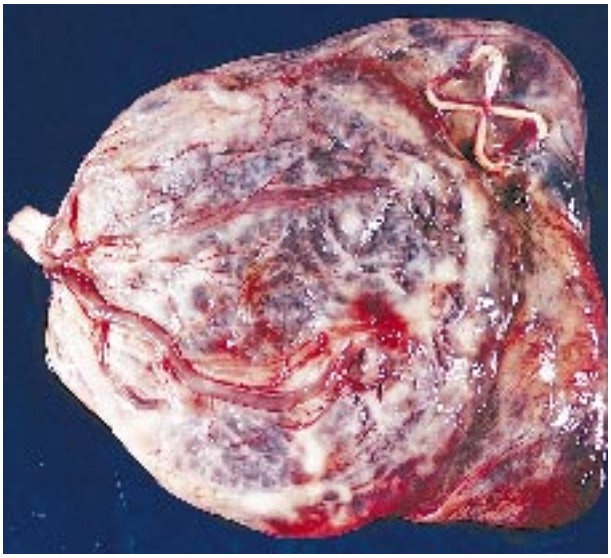

Figure 1.10. This otherwise normal placenta shows the presence of an intrauterine contraceptive device, indicating that it did not prevent pregnancy.

1.11

Figure 1.11. In premature separation of the placenta (abruptio placentae) there may be massive bleeding of maternal origin. Note the massive blood loss on the left of the maternal surface of the placenta. In these cases, there may be severe fetal asphyxia or death. The infant in this case had blood in stool (melena neonatorum) at birth. This was shown to be ingested maternal blood by the Apt test.

1.12

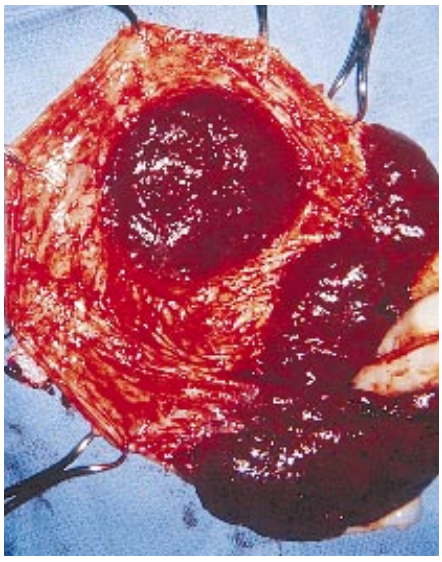

Figure 1.12. Another example of abruptio placentae. A large abruptio placentae may result in poor growth of the infant and fetal blood loss.

1.13

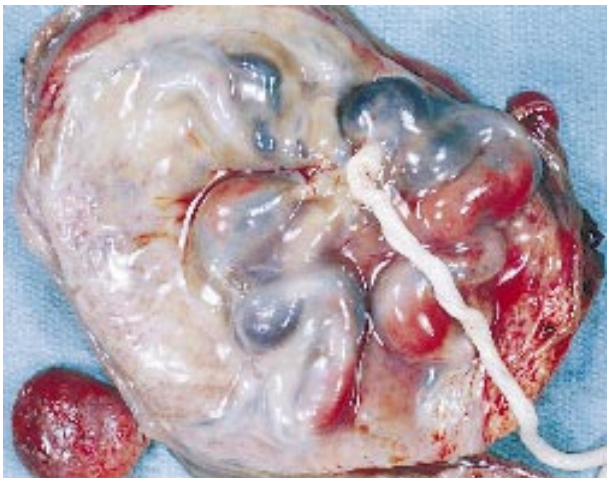

Figure 1.13. Fetal surface of a placenta with a large chorangioma (hemangioma of the placenta). These infants may present with severe nonimmune hydrops fetalis. The majority of cases of hydrops fetalis are now due to nonimmune causes.

1.14

Figure 1.14. Maternal surface of the same placenta. Note the placental enlargement due to the chorangioma and edema. If the placenta is not examined, this cause of nonimmune hydrops fetalis may be missed.

1.15

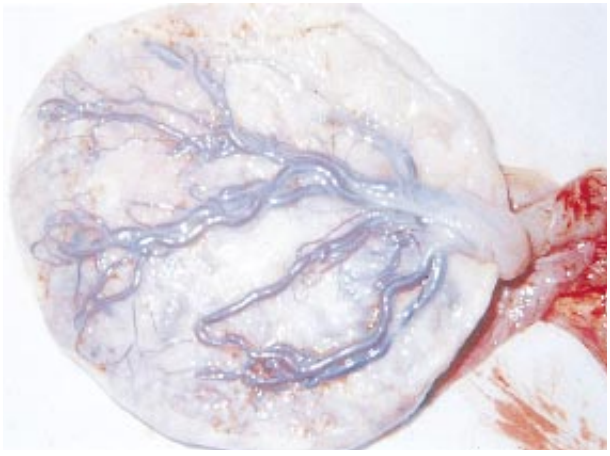

Figure 1.15. A calcified, small placenta. This infant had severe intrauterine growth retardation at term as a result of poor fetal nutrition.

1.16

Figure 1.16. In velamentous insertion of the cord the umbilical vessels traverse the fetal membranes unsupported by either the umbilical cord or by placental tissue. If tearing of these unsupported vessels occurs before or during delivery, it can result in massive fetal blood loss.

1.17

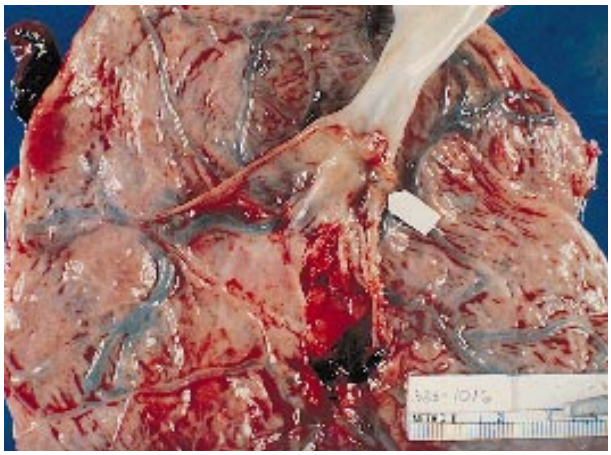

Figure 1.17. Another example of velamentous insertion of the cord. Note the vessels traversing the membranes before inserting into the fetal surface of the placenta. The vessels, lying in loose unsupported tissue, may easily stretch and tear, especially if they cross the cervical os and result in vasa previa with massive blood loss. (Sotelo-Avila, C.)

1.18

Figure 1.18. An example of velamentous insertion of the cord. Note the large vessels exposed in the membranes before they insert into the placental tissue, a section of which is shown at the top. Velamentous insertion of the cord occurs in 0.5 to 1% of singleton births, in 7% of twin births, and in 30 to 40% of triplet births. (Sotelo-Avila, C.)

1.19

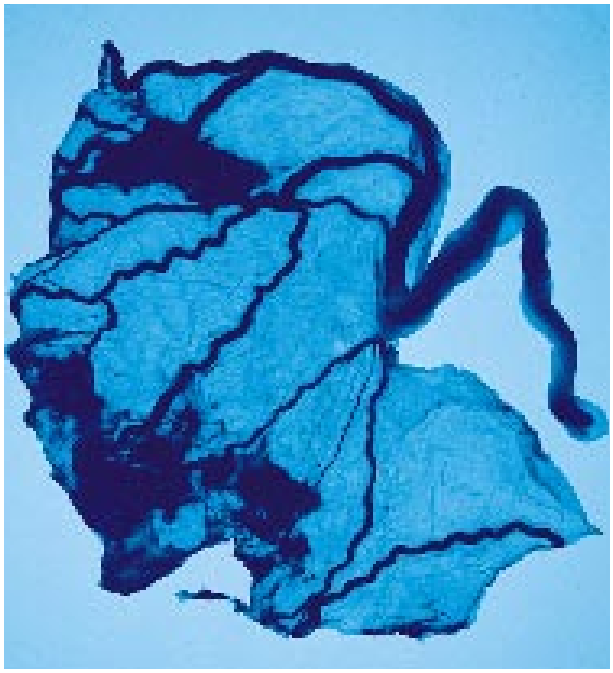

Figure 1.19. Transillumination of the placenta shown in Figure 1.18. (Sotelo-Avila, C.)

1.20

Figure 1.20. Fetus born in a caul. Note that the membranes completely surround the fetus and that the umbilical cord (nuchal cord) encircles the neck twice. A cord around the neck once occurs in about 20%, and twice in about 2% of pregnancies. Whether the cord causes any problems depends on its tightness around the neck. (Klima, T.)

1.21

Figure 1.21. Note the petechiae of the face and head and the subconjunctival hemorrhages in this infant who had a long cord around the neck. The normal umbilical cord is 40 to 60 cm long. Long cords (>70 cm) are more apt to be looped around the neck or an extremity of the fetus or to have true knots. Extremely short cords (<30 cm) may lead to abruptio placentae, inversion of the uterus, and intrafunicular hemorrhage (bleeding within the umbilical cord).

1.22

Figure 1.22. This cord was extremely long and wrapped around the left wrist and several times around the neck resulting in intrauterine death and birth of a stillborn infant. A long umbilical cord has usually been stretched by the movement of an extremely active fetus.

1.23

Figure 1.23. Intrauterine death as a result of a long umbilical cord which wrapped around the neck and then the left leg. As the infant moved in utero, he strangled himself.

1.24

Figure 1.24. A long umbilical cord can encircle an extremity and leave recognizable grooves (furrows) with or without skin ulceration. These are not associated with a poor outcome. In this infant, the cord encircled the right knee very tightly and interfered with the circulation distally.

1.25

Figure 1.25. The severe umbilical cord constriction proximally resulted in intrauterine death of this fetus. (Finegold, M.)

1.26

Figure 1.26. A hematoma of the umbilical cord (intrafunicular hemorrhage) resulted from a short umbilical cord. Short umbilical cords are associated with extreme intrauterine immobility, such as in the fetal akinesia syndrome.

1.27

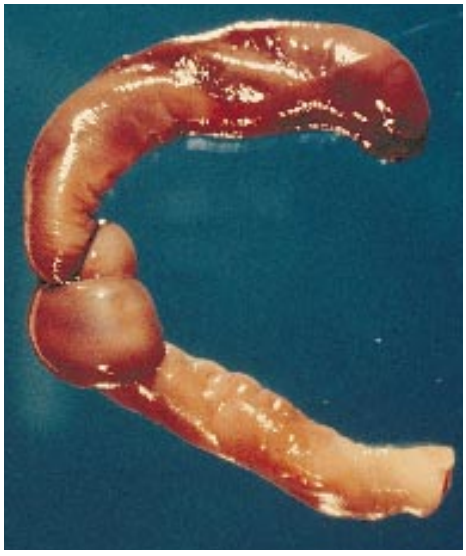

Figure 1.27. A true knot in the umbilical cord of this fetus resulted in intrauterine death. The incidence of true knots in the umbilical cord is 0.1 to 1%, and is strongly associated with long cords and other markers of vigorous fetal activity. It is associated with about 10% of stillbirths. The knots must be very tight to obstruct blood flow. At the site of a long standing knot, such as in this fetus, there is a loss of Wharton's jelly and a constriction of umbilical vessels. Wharton's jelly probably prevents umbilical cord blood vessel compression by diffusing the pressure exerted by knots. The jelly is also slippery and this makes it difficult to maintain a knot.

1.28

Figure 1.28. An example of two true knots in the umbilical cord in an infant who was normal at birth.

1.29

Figure 1.29. Close up of the true knot to the right in Figure 1.28. Note that the Wharton's jelly is normal and that there is no constriction of the cord. This is, therefore, a recent knot. A previously loose knot may be suddenly tightened as the infant descends during delivery.

1.30

Figure 1.30. This umbilical cord transection during amniocentesis occurred several years ago, before ultrasound was used to determine the position of the amniocentesis needle. There was considerable blood loss.

1.31

Figure 1.31. Another example of amniocentesis through a term placenta. The fetus developed tachycardia but was normal at birth. (Moise, K.)

1.32

Figure 1.32. Hematoma from transection of the umbilical cord during amniocentesis. There was marked blood loss and fetal demise.

1.33

Figure 1.33. The diagnosis of single umbilical artery is made by examining a section through the surface of the umbilical cord. This anomaly is present in 0.7 to 1.0% of single placentas and in 3 to 7.0% of multiple birth placentas. The incidence is low in black infants, but is increased in infants with associated congenital malformations. Further investigation is recommended if a single umbilical artery is associated with one other major anomaly.

1.34

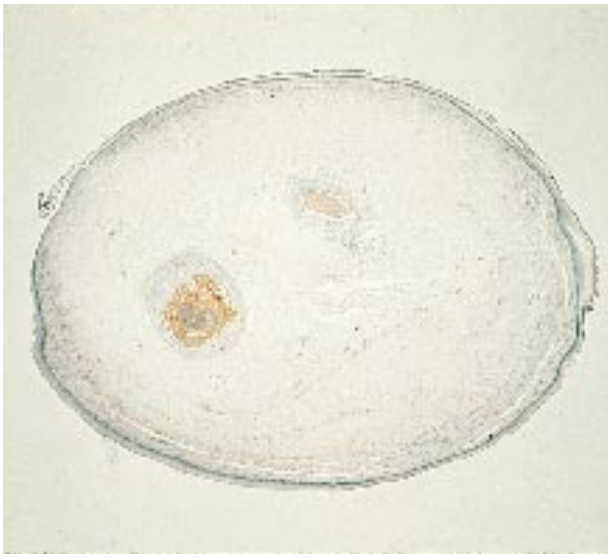

Figure 1.34. A histologic section of an umbilical cord with a single umbilical artery. Note that the thick-walled vessel is the artery and the thin-walled vessel is the vein. It may be associated with abnormal cord length, velamentous cord insertion, or circumvallate placenta. The finding of other congenital malformations is not specific for any one organ system. Cardiac, renal, gastrointestinal, and skeletal malformities have been described. There is an increased incidence of a single umbilical artery in trisomy 13 and 18.

1.35

Figure 1.35. Note the markedly enlarged, edematous umbilical cord due to excess Wharton's jelly in an infant of a diabetic mother. These cords are very friable and tear easily.

1.36

Figure 1.36. A thrombosed vessel in an umbilical cord with little Wharton's jelly. Trauma to the cord is more common when there is a lack of Wharton's jelly. The lack of Wharton's jelly is seen more commonly in postmature infants. A thrombosed vessel in the umbilical cord may compromise fetal well-being.

1.37

Figure 1.37. This thin, narrow umbilical cord with total lack of Wharton's jelly was present at birth in an infant with postmaturity and oligohydramnios. Cord compression is probably more frequent with a narrow cord, perhaps because the Wharton's jelly does not "cushion" the cord.

1.38

Figure 1.38. A drying umbilical cord 4 days after birth. Note that as the cord dries, the Wharton's jelly disappears rapidly.

1.39

Figure 1.39. This infant has a large cyst in the umbilical cord. The chemical composition of the fluid in this cyst was that of serum rather than urine. These cysts are thought to arise from the allantois.

1.40

Figure 1.40. Another example of an umbilical cord cyst which is thought to arise from the allantois. These cysts are of no clinical significance.

1.41

Figure 1.41. Omphalitis and funisitis in an umbilical cord. Omphalitis is an acute inflammation of the skin surrounding the umbilicus. Funisitis is an acute inflammation of the umbilical cord itself. It results from bacteria or mycoplasma in the amniotic fluid attracting fetal neutrophils to migrate out of the umbilical cord vessels. It can be associated with necrosis and calcium deposits within the cord.

1.42

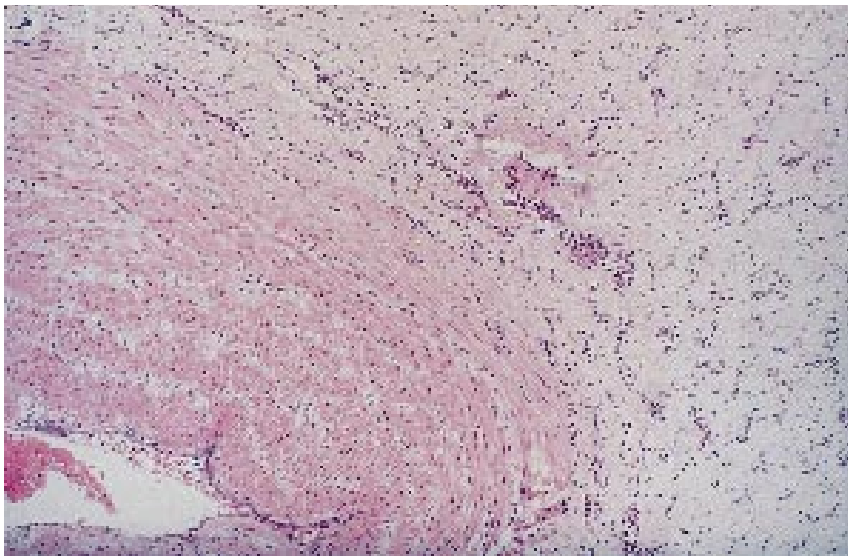

Figure 1.42. Histologic section of an umbilical cord showing funisitis. Note the marked inflammatory reaction surrounding an artery in the cord itself. (Sotelo-Avila, C.)

1.43

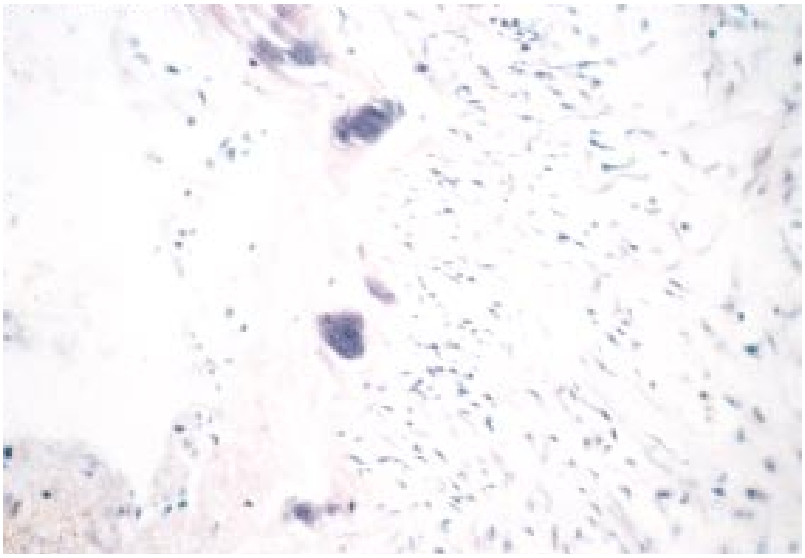

Figure 1.43. Histologic section of an umbilical cord showing marked inflammatory reaction and bacterial colonies (intensely stained blue areas) surrounding a vein in the cord itself.

1.44

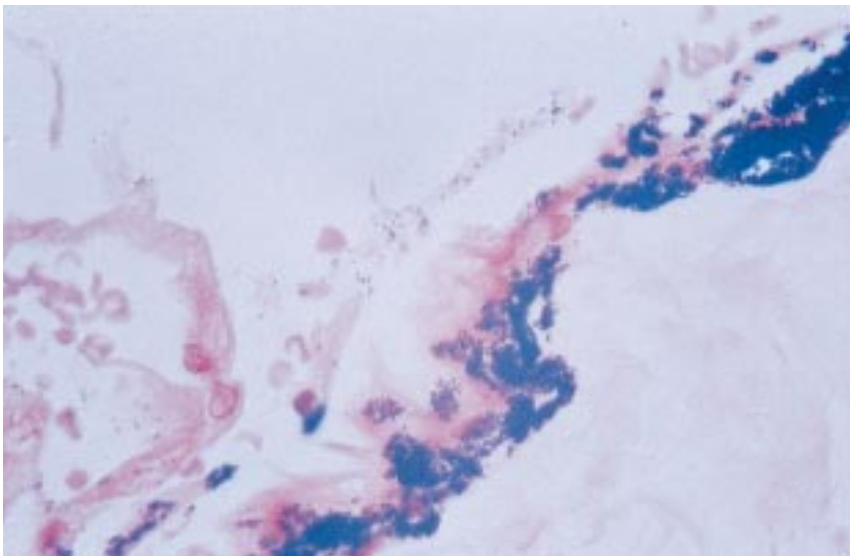

Figure 1.44. Histologic section of the umbilical cord in an infant with congenital listeriosis. Note the gram positive organisms on the surface of the umbilical cord.

1.45

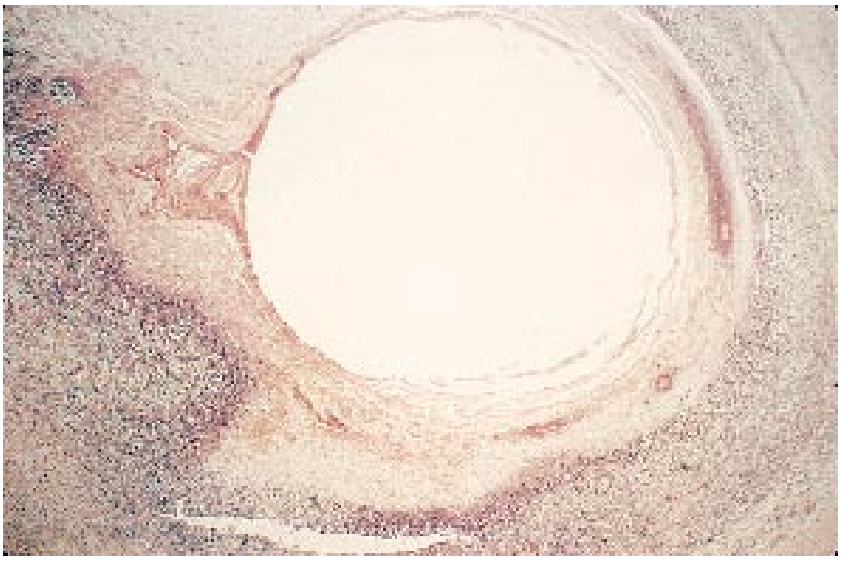

Figure 1.45. Histologic section of funisitis occurring as a result of a catheter in situ in an umbilical vessel.

1.46

Figure 1.46. The external surface of the umbilical cord shows cheesy white areas similar to thrush which suggest the diagnosis of congenital candidiasis. (Sotelo-Avila, C.)

1.47

Figure 1.47. A histologic section of the umbilical cord of the same infant showing funisitis with the hyphae of *Candida* which are stained pink. (Sotelo-Avila, C.)

1.48

Figure 1.48. External surface of an umbilical cord with yellowish brown areas on the external surface which suggest the diagnosis of congenital candidiasis. (Fanaroff, A.)

1.49

Figure 1.49. Fetal surface of a placenta showing chorioamnionitis. Normally, the fetal surface of a placenta is shiny and clear with a prominent vascular pattern. In chorioamnionitis the fetal surface appears dull and opaque with an obscure vascular pattern. The amniotic fluid is cloudy, and the placenta, membranes, and amniotic fluid may have a foul odor. Aspiration in this infected milieu by the fetus may result in neonatal pneumonia, sepsis and/or neonatal meningitis.

1.50

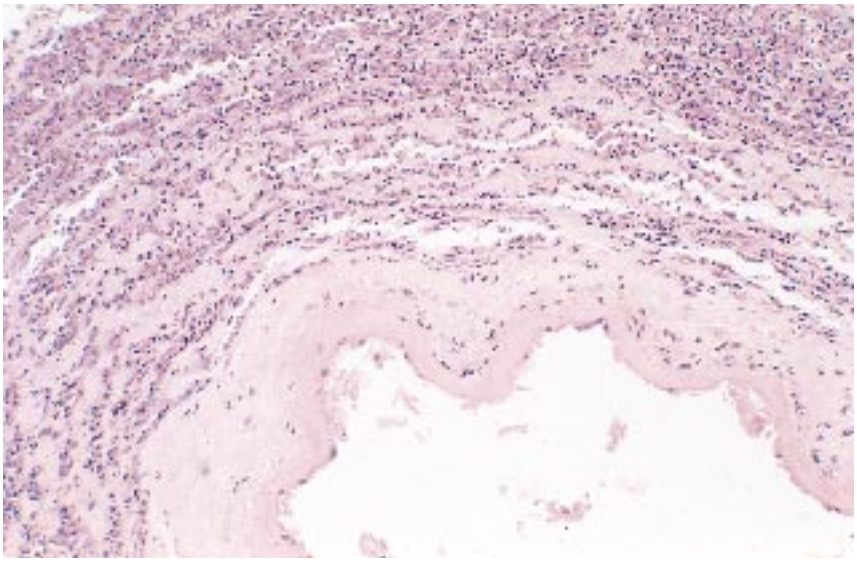

Figure 1.50. Histologic section of the placenta showing chorioamnionitis. Factors associated with increased risk of placental infection include premature and prolonged rupture of the membranes, prolonged labor, placenta previa, and multiple births. Bacterial infections are more common than viral and fungal infections.

1.51

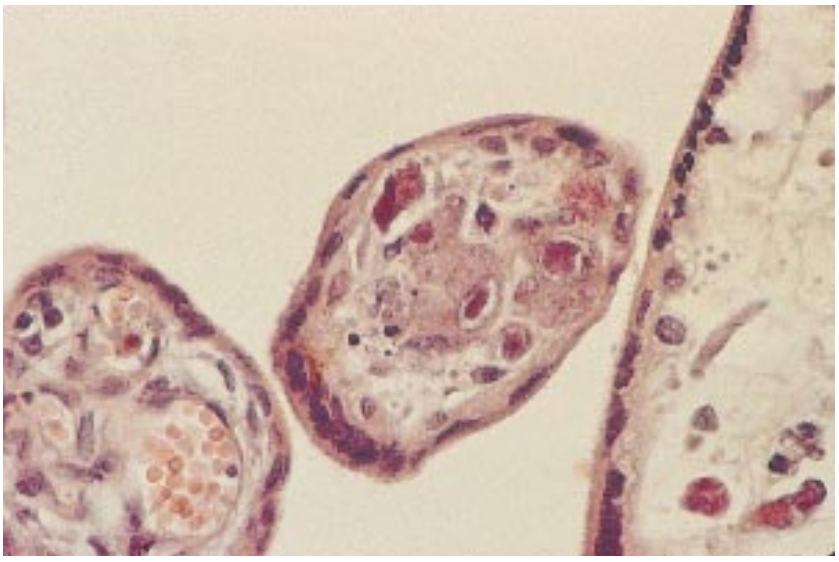

Figure 1.51. Histologic section of a placenta with cytomegalovirus infection. Note the typical "owl's eye" inclusions in the villae. Viral agents reach the fetus by hematogenous dissemination and traverse the placental villae. Since viral lesions tend to be microscopic, gross examination of the placenta is not helpful. (Finegold, M.)

1.52

Figure 1.52. Histologic section of a placenta with congenital syphilis. Note the numerous spirochetes. (Finegold, M.)

1.53

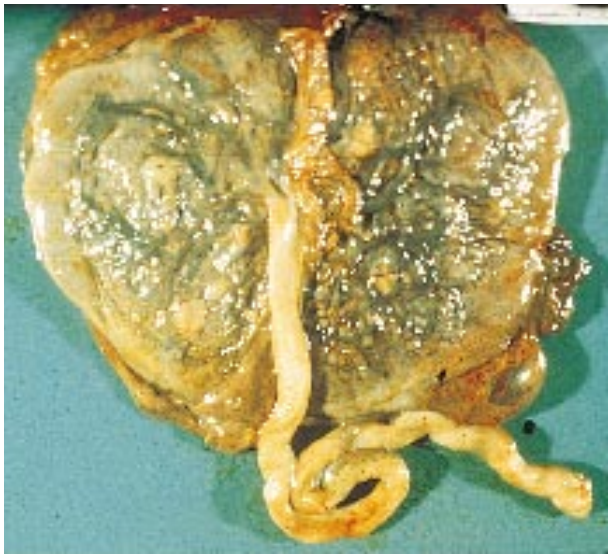

Figure 1.53. The presence of meconium staining of the amniotic fluid occurs with fetal distress and postmaturity. Meconium staining of the placenta may occur within 1 hour. In cases of chorioamnionitis, the fetal surface may be green; in listeriosis, there may be brown or chocolate staining of the amniotic fluid with similar staining of the placenta. (Finegold, M.)

1.54

Figure 1.54. Infant with a large "garment" nevus (bathing trunk nevus). Note the marked breakdown and ulceration of the skin.

1.55

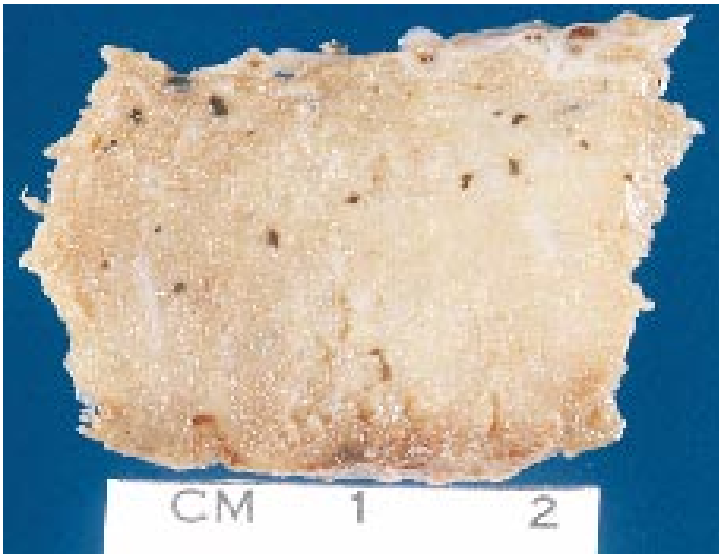

Figure 1.55. Gross section of placenta showing multiple nevi in the same infant shown in Figure 1.54. This emphasizes the importance of examining the placenta in infants born with such abnormalities. (Sotelo-Avila, C.)

1.56

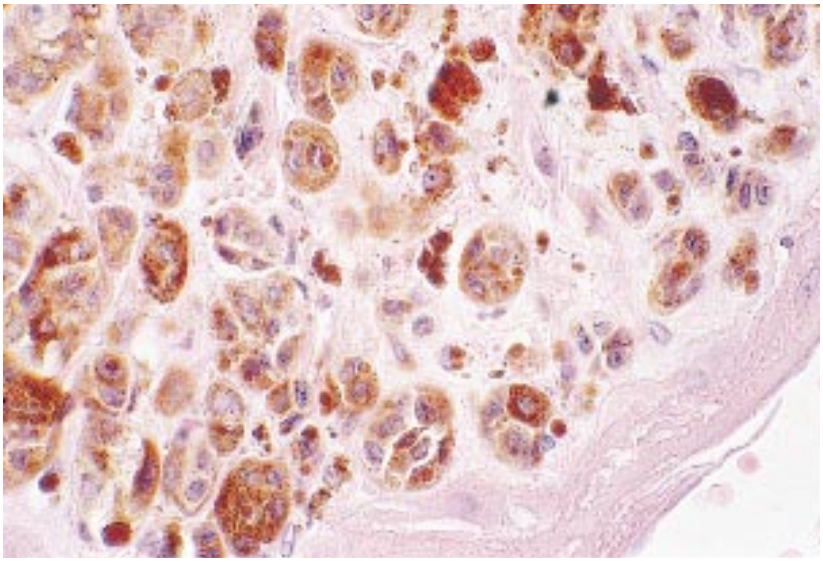

Figure 1.56. Histologic section of melanoma cells from the placenta of the same infant shown in Figure 1.54 and 1.55. Similarly lesions can be seen in the placenta of infants with congenital neuroblastoma. (Sotelo-Avila, C.)

1.57

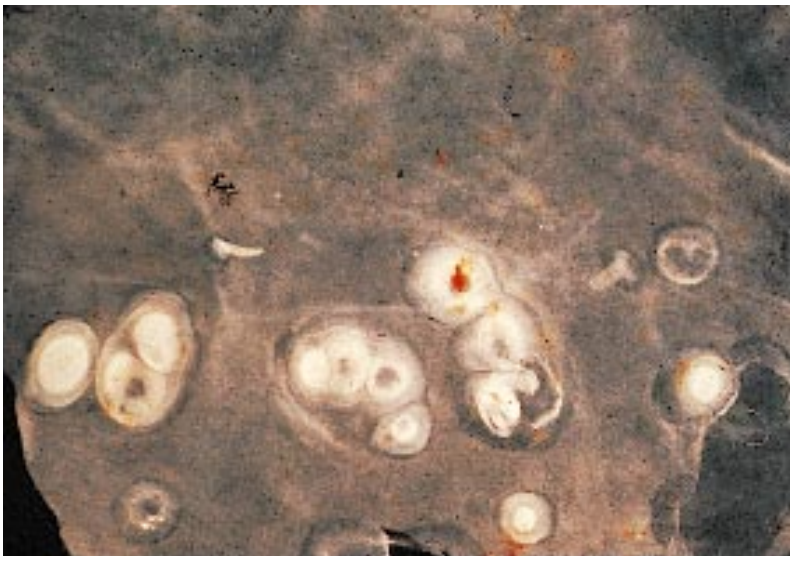

Figure 1.57. Squamous metaplasia of the amnion. In this placenta with squamous metaplasia, the amnion is stripped from the membranes. Note the concentric appearance of these nodules and their frequent umbilication. The amnion is squamous and these areas of metaplasia form with maturity. Note the tiny nodules of keratin irregularly present on the fetal surface.

1.58

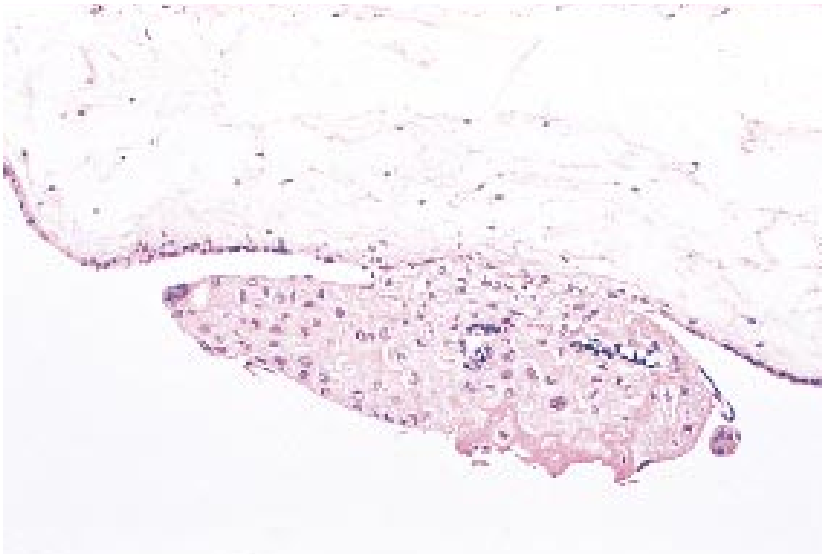

Figure 1.58. Histologic section of the amnion showing the squamous metaplasia. Squamous metaplasia differs from amnion nodosum in that the lesions *cannot* be separated readily, whereas the nodules in amnion nodosum can be picked off of the underlying amnion leaving a semi-transparent, saucer-shaped depression with somewhat ragged edges.

1.59

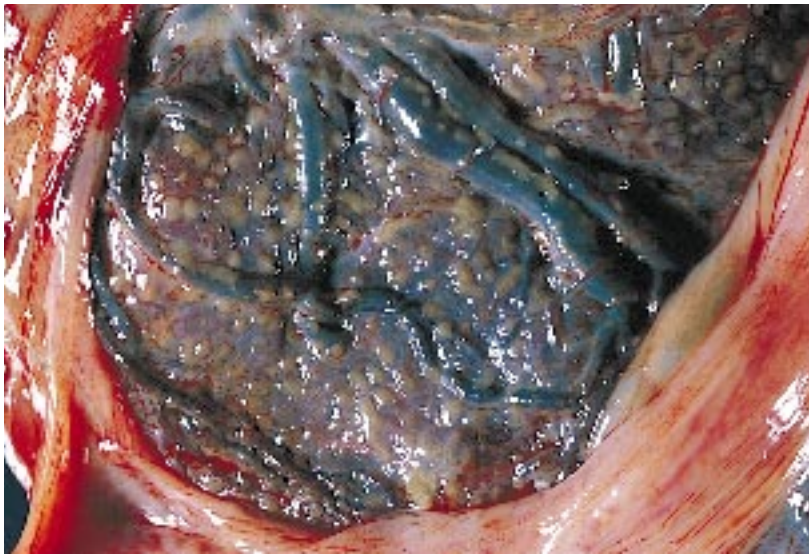

Figure 1.59. Typical amnion nodosum in one twin. This twin was an acardiac monster having no urinary tract. The amnion is rough and shows numerous fine granules which are whitish, opaque, and uniform in size. Frequently the nodules are more irregular in size and slightly yellowish brown. It is unusual to see this degree of amnion nodosum. The other twin was normal.

1.60

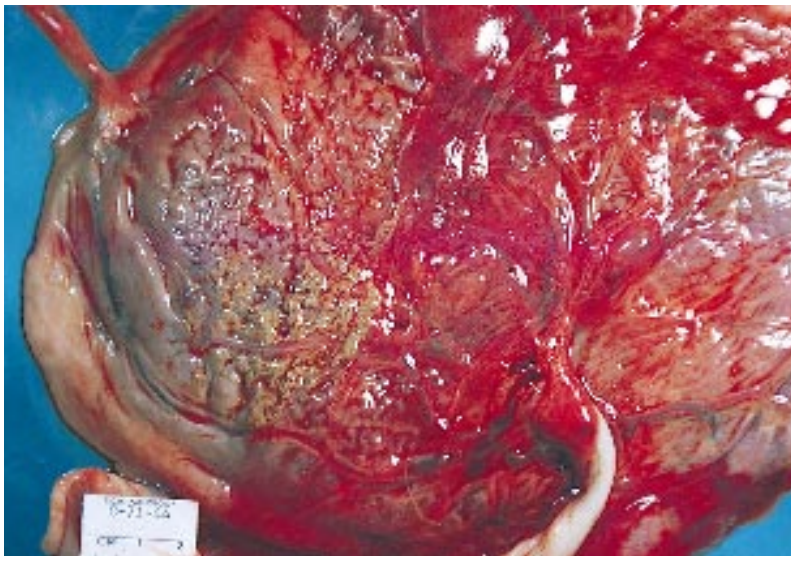

Figure 1.60. Another example of amnion nodosum in a twin placenta. Note the normal umbilical cord and placenta on the right and the small umbilical cord with a thrombosed vessel on the left. This was a twin-twin transfusion syndrome and the twin on the left became a fetus papyraceus. The amnion nodosum lesions are whitish, opaque, and uniform in size.

1.61

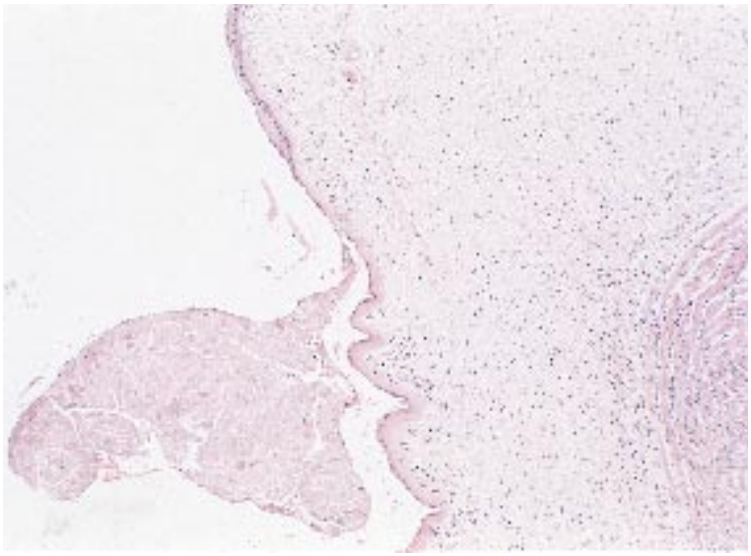

Figure 1.61. Histologic section of a placenta and membranes showing amnion nodosum on the left and chorioamnionitis on the right in an infant with renal dysgenesis and hypoplastic lungs.

1.62

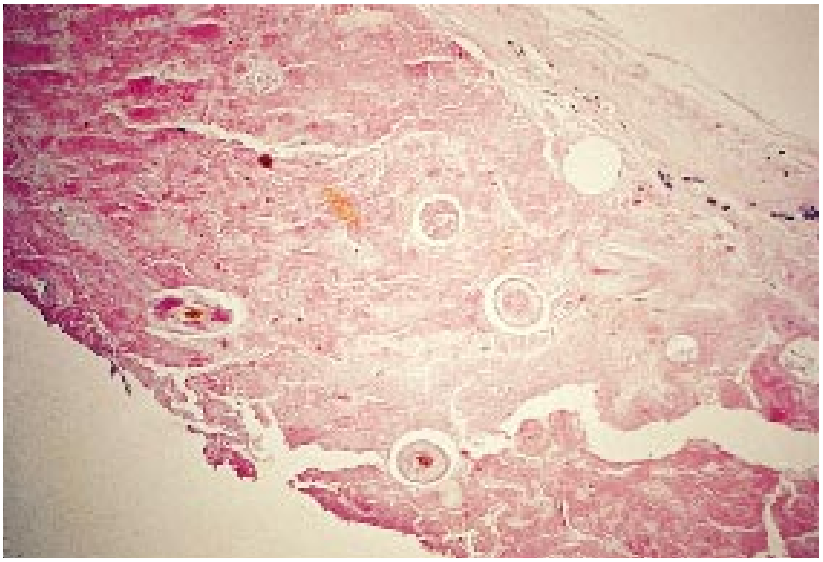

Figure 1.62. High-power histologic section of amnion nodosum which consists of lanugo, vernix caseosa, and squamous epithelial cells. With marked oligohydramnios, the fetal skin rubs against the fetal surface of the placenta and produces these lesions.

Chapter 2
Multiple Births

Multiple gestation occurs frequently in pregnancy. The most common is twinning, which occurs in about one in every 80 pregnancies. There are two types of twins: monozygous or "identical" and dizygous or "fraternal." The monozygous twin rate is 1 in every 200 pregnancies. It results from a single ovulation with subsequent splitting of the developing egg within the first 14 days. There is no familial tendency. Dizygous twinning results from double ovulation and fertilization and is probably determined by higher gonadotropin secretion rates. The rate of dizygous twinning is variable and is influenced by heredity (transmitted autosomally but expressed only in the mother), race (as high as 1 in 23 births in some West African races; as low as 1 in 300 births in Mongolian races), maternal age (increased frequency with increasing age), and drugs (incidence of twinning is 6.6% with the use of Clomid®). Examination of the placenta of multiple births is important because of the two- to three-fold higher incidence of structural defects in monozygous twins and increased potential for successful future transplant between monozygous twins. Monochorionic placentas are invariably fused and about 75% of the infants are identical twins. Dichorionic placentas may be fused or separate. Infants with a dichorionic fused placenta may be identical (monozygous) or fraternal (dizygous). The membrane which separates the two fetal cavities is the key to the evaluation of twin placenta. Typically, this runs across the middle of the fused placenta. In monochorionic twins, with one chorion covering two amnia, the dividing membrane consists of two translucent amnionic layers which can be pulled with ease from the placental surface. In 1% of monozygotic twinning, the placenta will be monochorionic-monoamnionic. In conjoined twinning, the placenta is also monochorionic-monoamnionic. In dichorionic twins, with two amnia, the dividing membrane consists of four layers, two chorionic and two amnionic; it is opaque, thicker, and does not separate from the placental surface without tearing.

2.1

Figure 2.1. These infants are normal, identical triplets born at 32 weeks gestation. They initially had mild respiratory distress, but improved rapidly. (Cabera-Meza, G.)

2.2

Figure 2.2. The fetal surfaces of the placentas of fraternal triplets.

2.3

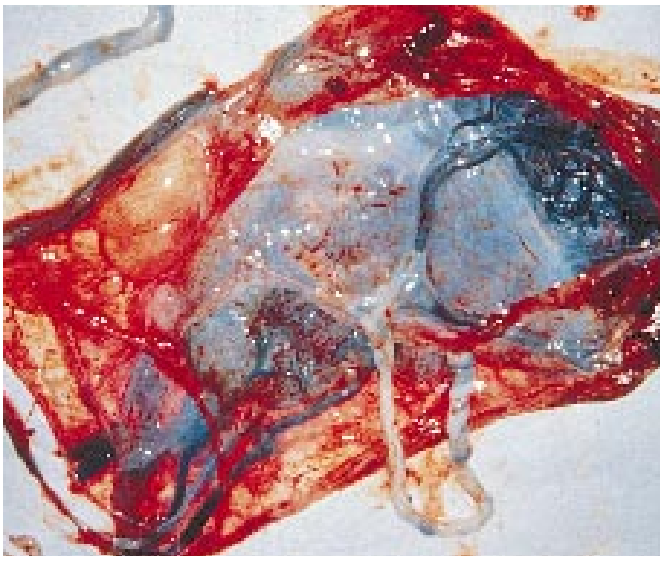

Figure 2.3. A triplet placenta showing a velamentous insertion of the cord in one of the triplets. Note that the placentas are fused and thus the pregnancy could be monozygotic.

2.4

Figure 2.4. The fetal surfaces of two completely separated twin placentas. These are always dizygotic.

2.5

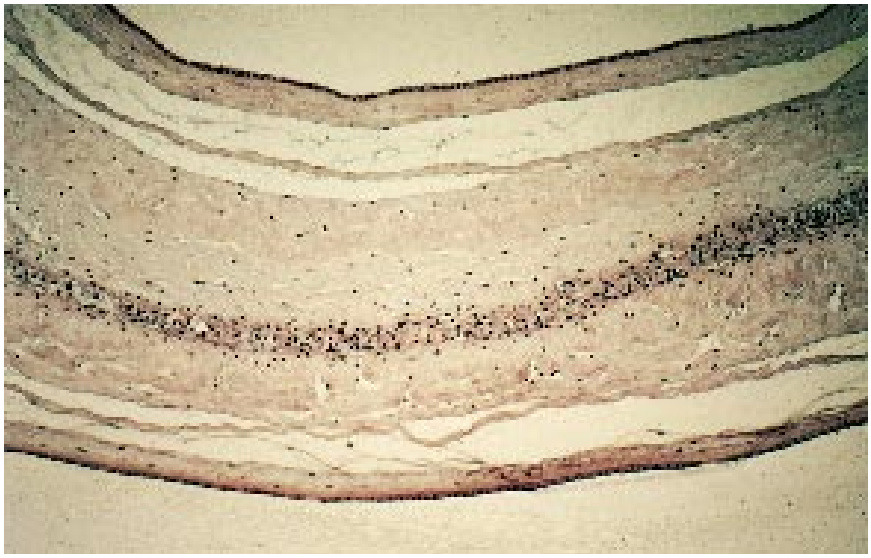

Figure 2.5. This low-power histologic section demonstrates that an amnion can be identified on each side of two choria. Thus, this is an example of a dichorionic-diamnionic placenta. This type of dividing membranes is typically seen in all dizygotic twinning and in about 20 to 25% of monozygotic twinning.

2.6

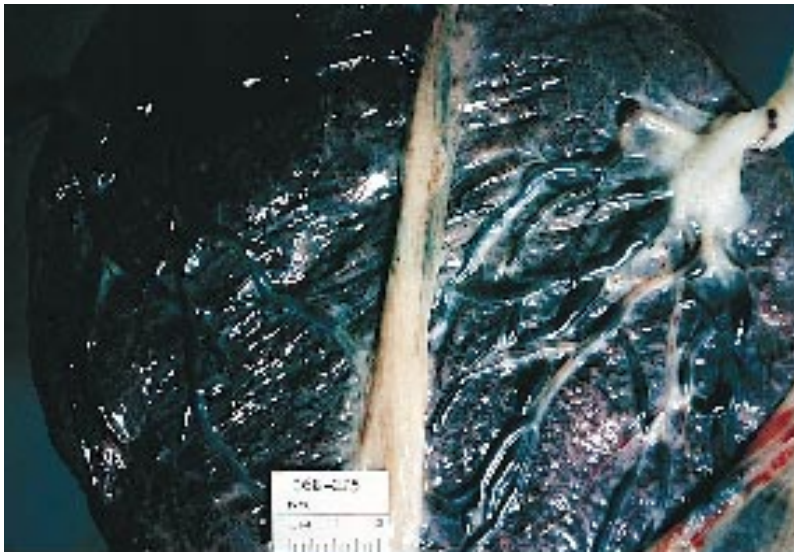

Figure 2.6. The fetal surface of this fused, twin placenta shows the dividing membranes. In this placenta, histologic examination showed that there were two amnia and a single chorion (diamnionic-monochorionic). These twins would thus be monozygotic.

2.7

Figure 2.7. Histology of the membranes of the same placenta shows the double amnion on the outer surfaces with a single chorion (diamnionic-monochorionic).

2.8

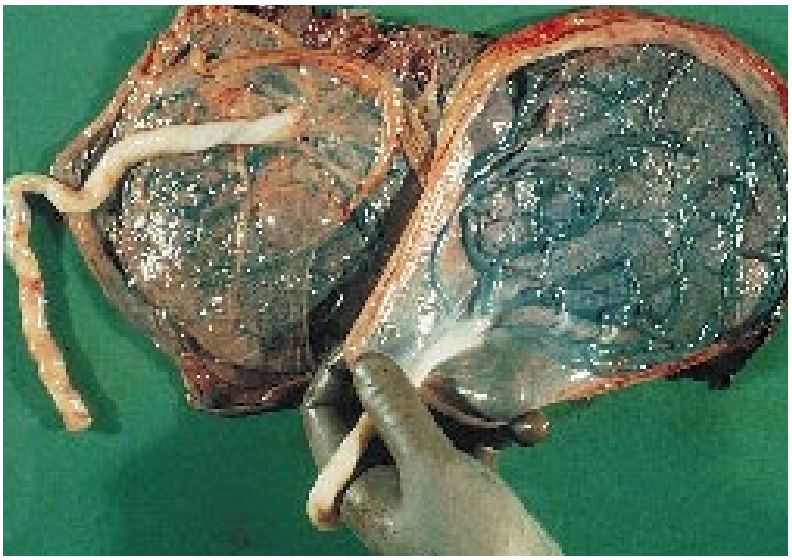

Figure 2.8. On the fetal surface of this fused, twin placenta, the dividing membrane is very thin and clear, suggesting that this is a monozygotic pregnancy. This was confirmed by histologic examination showing a single chorion. (Finegold, M.)

2.9

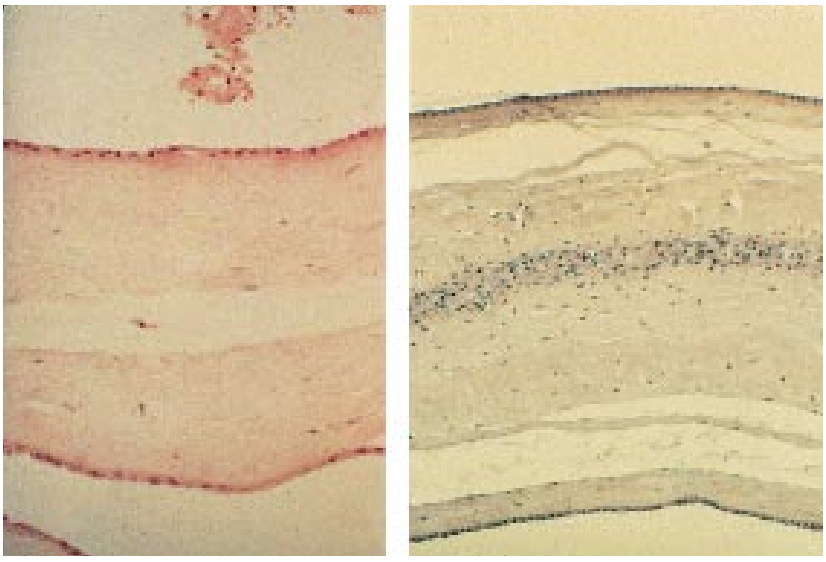

Figure 2.9. The histologic appearance of the dividing membranes in twin placentas are compared in this figure. On the left, note the diamnionic-monochorionic twin placenta, and on the right, note the diamnionic-dichorionic twin placenta.

2.10

Figure 2.10. Note the two umbilical cords inserting into the fetal surface of the placenta without the presence of dividing membranes. This is typical of a monoamnionic-monochorionic twin placenta, which occurs in 1% of twin pregnancies.

2.11

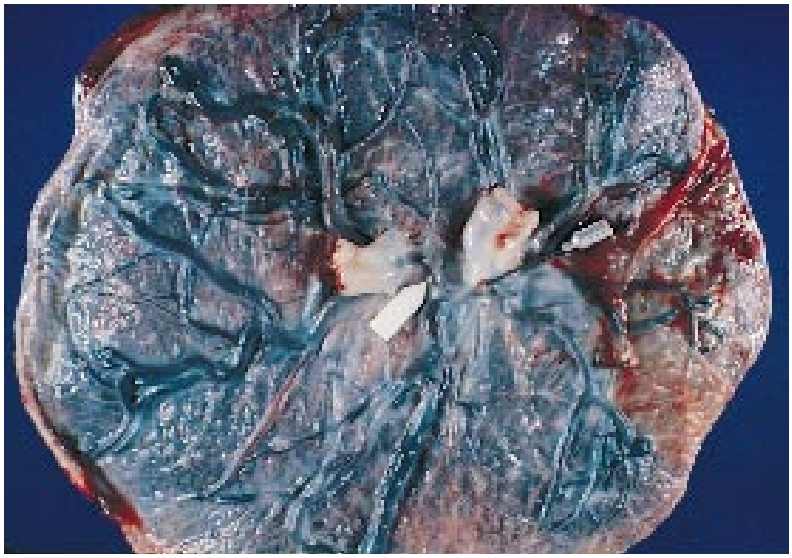

Figure 2.11. The fetal surface of a monoamnionic-monochorionic twin placenta, showing the insertion of two separate umbilical cords. (Sotelo-Avila, C.)

2.12

Figure 2.12. Close-up of the above placenta shows anastomosis of the vessels between the two umbilical cords. This results in a twin (feto-fetal) transfusion syndrome. (Sotelo-Avila, C.)

2.13

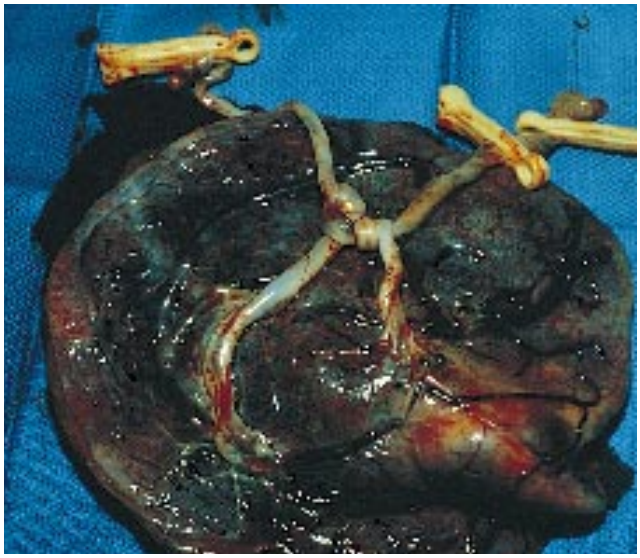

Figure 2.13. The fetal surface of a monoamnionic-monochorionic twin placenta showing the entanglement of the two umbilical cords resulting in fetal anoxia and fetal distress with meconium passage. Note the meconium-stained appearance of the fetal surface of the placenta. Entanglement of the cords is a complication which may occur because of a lack of a dividing membrane in monoamnionic-monochorionic twins. (Karishan, B.)

2.14

Figure 2.14. Another example of entangled cords in a monoamnionic-monochorionic twin placenta.

2.15

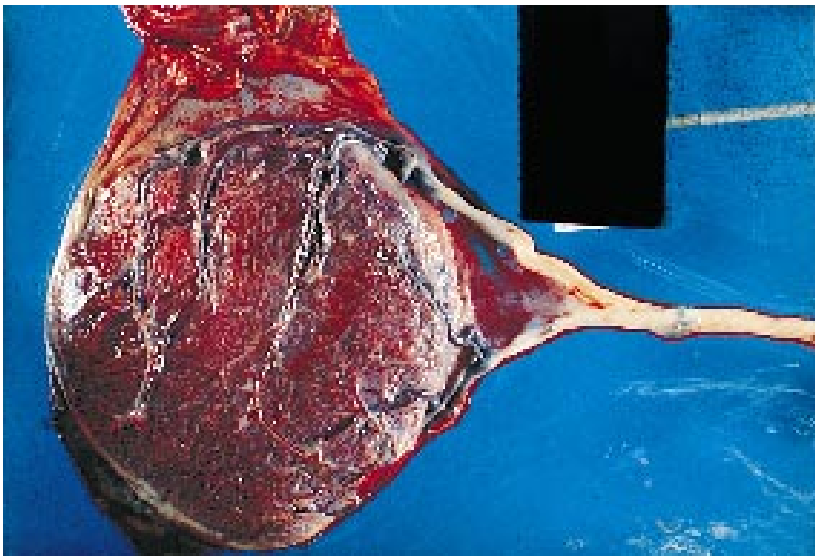

Figure 2.15. The fetal surface of this monoamnionic-monochorionic placenta in conjoined twins shows the insertion of the two umbilical cords, but note that these fuse and present as a single fused cord in thoracopagus twins. (Sotelo-Avila, C.)

2.16

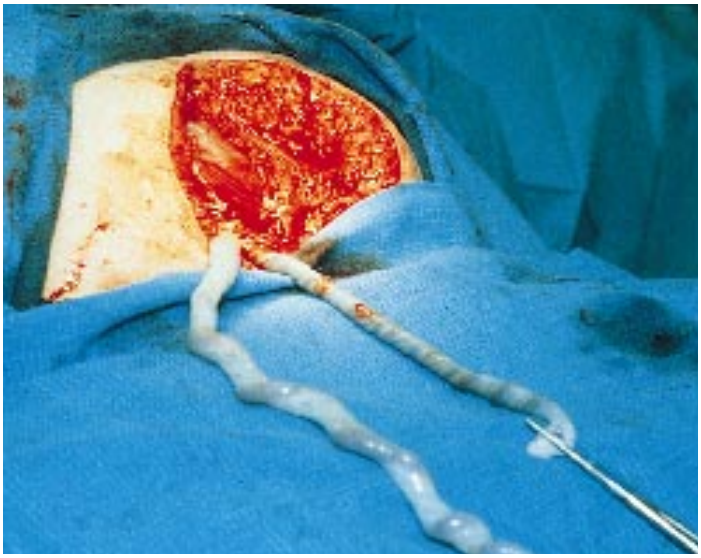

Figure 2.16. The appearance of the umbilical cords in a twin pregnancy. Note the small size of the umbilical cord in the infant who was growth-retarded as compared to the normal size of the umbilical cord in the normal twin.

2.17

Figure 2.17. These infants born as stillbirths at 30 weeks gestation are an example of twin (feto-fetal) transfusion syndrome. In this syndrome, vascular anastomoses permit the transfer of arterial blood under high pressure from the twin on the right (donor) to the low pressure venous system of the other twin (recipient). The donor twin is thus kept hypovolemic, dehydrated, malnourished, or even in shock. His organs are small and his amniotic fluid is decreased. The recipient twin becomes hypervolemic, edematous, and plethoric (polycythemic). His organs are large, he may have congestive failure and his amniotic fluid is increased.

2.18

Figure 2.18. These monozygotic twins at birth represent another example of twin transfusion syndrome. The birth weight of the twin on the left was 3000 g with a central hematocrit of 86%. The birth weight of the twin on the right was 2230 g with a central hematocrit of 27%. Twin transfusion syndrome occurs only in monochorionic twins. It occurs in 15 to 30% of monochorionic pregnancies and is defined in terms of a difference of greater than 250 g birth weight and/or 20% difference in the central hematocrit between the twins. Twins in this syndrome usually do not look identical at birth although in fact they are monozygotic.

2.19

Figure 2.19. In these infants with twin transfusion syndrome, the difference in birth weight was only 180 g and the difference in central hematocrit was 32%. Thus, these infants represent a mild example of twin transfusion syndrome.

2.20

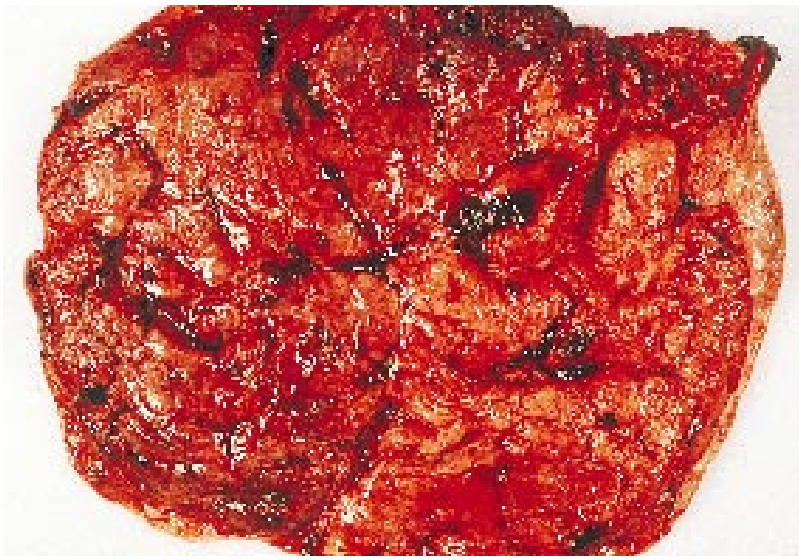

Figure 2.20. The maternal surface of a monozygotic twin placenta in infants who had the twin transfusion syndrome. Note on the left the congested appearance of the portion of the placenta supplying the recipient twin who had a central hematocrit of 69%, and note on the right the much paler appearance of the placenta supplying the donor twin who had a central hematocrit of 45%. (Singer, D.)

2.21

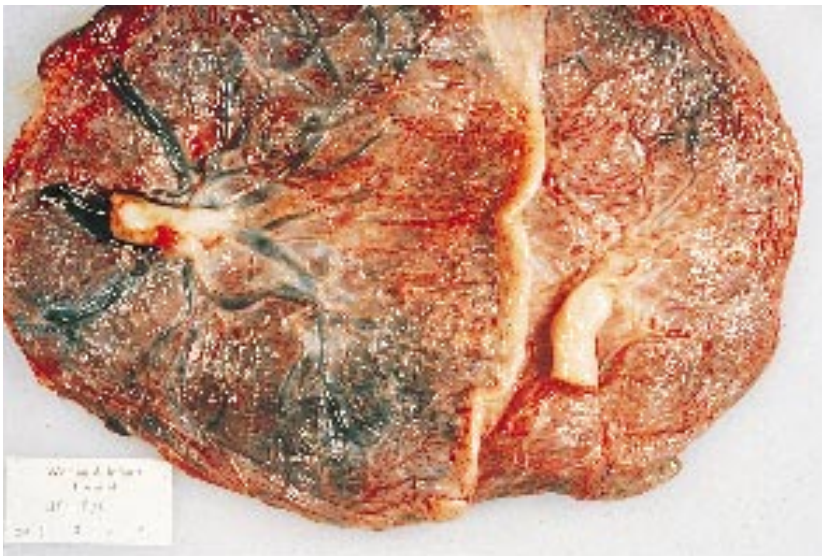

Figure 2.21. The fetal surface of the same placenta as in Figure. 2.20 showing the congested appearance on the left of the recipient portion of the twin placenta and the pallor on the right of the donor portion of the twin placenta. These vascular connections may be artery-to-artery, vein-to-vein, or artery-to-vein. Any form may significantly affect the fetuses physiologically and clinically.

2.22

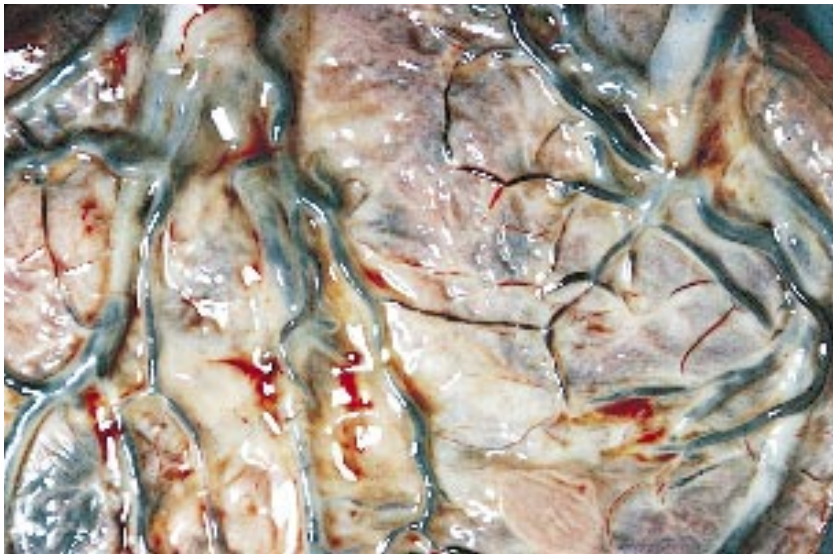

Figure 2.22. The fetal surface of placentas in twin transfusion syndrome showing the anastomoses between the two fetal circulations following the injection of infant formula, which is used as a contrast medium. Note that on the fetal surface of the placenta arteries *always* cross over veins. The anastomosis between an artery on the left and a vein on the right is shown at the junction of the left third and the right two-thirds of the figure.

2.23

Figure 2.23. This close-up view clearly shows the artery-to-vein anastomosis.

2.24

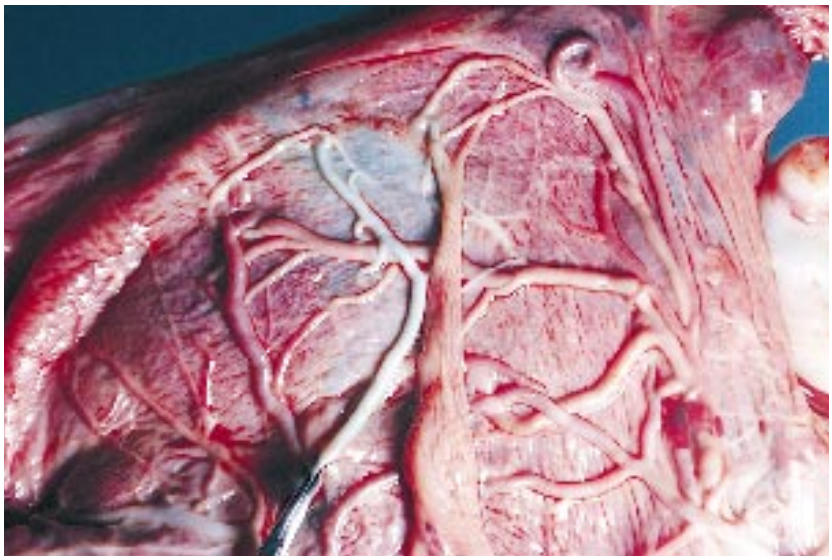

Figure 2.24. Another example of an injection of infant formula filling the arteries which cross over the veins in this vessel anastomosis.

2.25

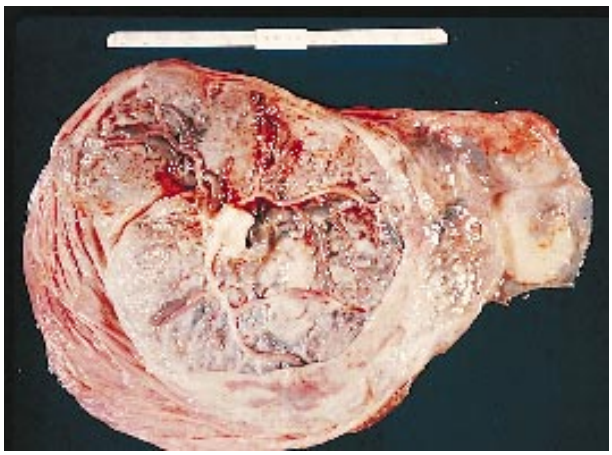

Figure 2.25. In extreme cases the transfusion syndrome may cause the death of one twin resulting in a fetus papyraceus. In this figure, there is an extrachorial placenta with a fetus papyraceus attached.

2.26

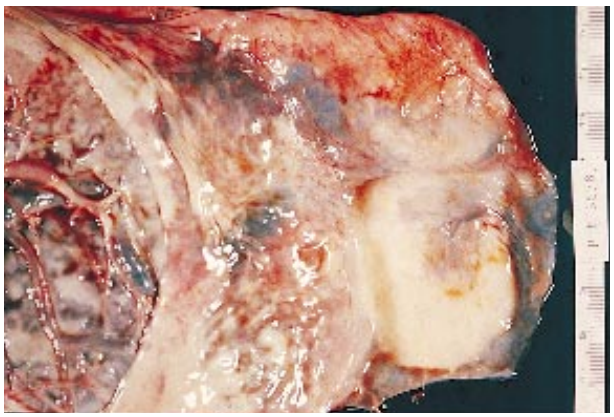

Figure 2.26. Close-up of the extrachorial placenta with the fetus papyraceus attached.

2.27

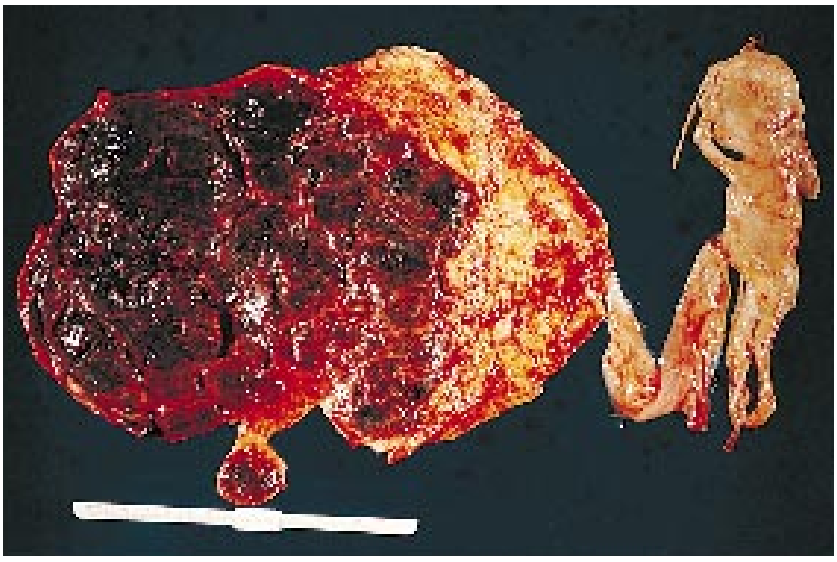

Figure 2.27. Another example of the twin transfusion syndrome. Note the maternal surface of the placenta showing the congested recipient placenta on the left and the pale donor placenta on the right with an attached fetus papyraceus.

2.28

Figure 2.28. The fetus papyraceus may calcify and result in a lithopedion ("stone child") as shown in this figure.

2.29

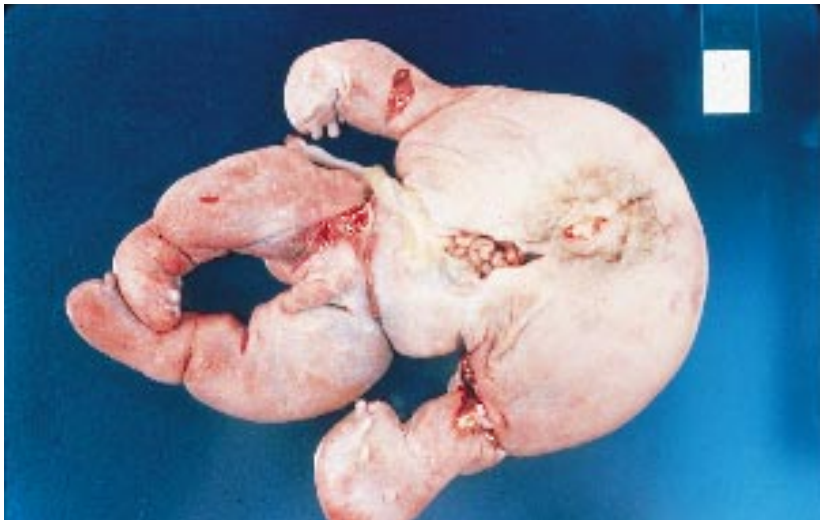

Figure 2.29. A stillborn male infant with a birthweight of 1170 g and length of 34 cm is an example of acardius acephalus. This is one of the acardiac anomalies which occurs as a consequence of abnormal umbilical artery-to-artery anastomoses between two fetuses in the presence of a fused placenta. It is sometimes referred to as the TRAP (*t*win-*r*eversed-*a*rterial-*p*erfusion) sequence. (Klima, T.)

2.30

Figure 2.30. A close-up of the abdomen of the same infant shows an omphalocele; there was also hydrops, pulmonary agenesis, and polyhydramnios. Acardiac anomalies include three groups: acephalus in 60 to 75% of cases, amorphus in 20% of cases, and a well-formed head and body in 10% of cases. (Klima, T.)

2.31

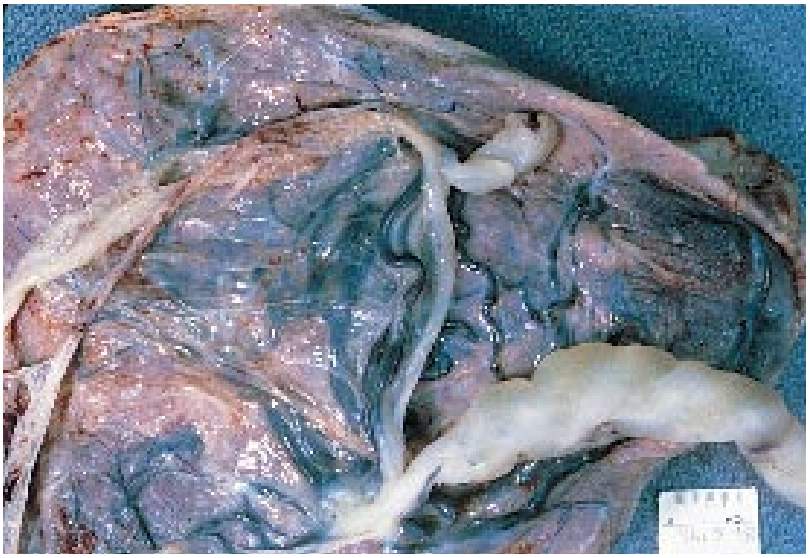

Figure 2.31. The fused placenta of the same infant with acardius acephalus shown in Figure 2.29 and 2.30. Note the large cord of the "normal" infant which had three vessels and the small cord of the infant with acardius acephalus which had two vessels. There were no separating membranes between the two cords. Note the large anastomoses between the placentas. (Klima, T.)

2.32

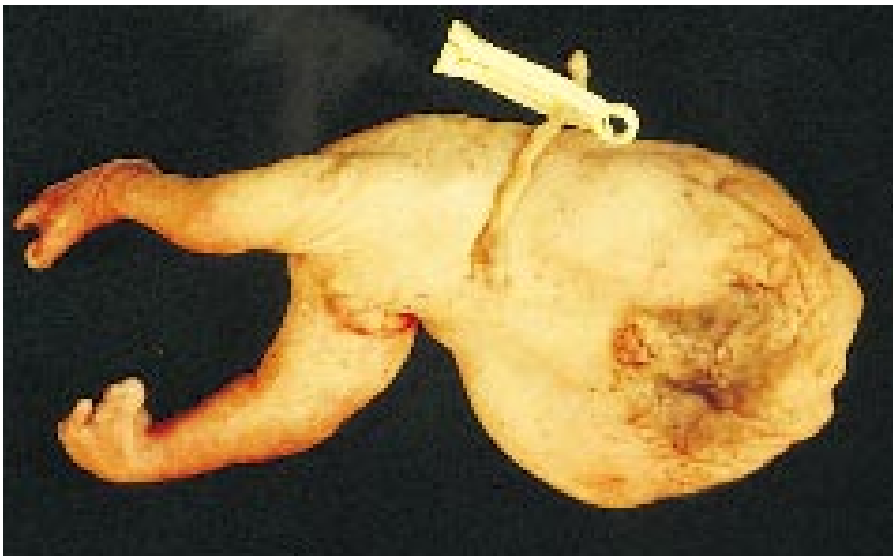

Figure 2.32. An acardius acephalus infant delivered at 30 weeks gestation. The upper body and shoulders form a fleshy mass capped by a tuft of short hairs. The lower body has two well-formed legs but has clubbed, bifid feet with two toes. (Klima, T.)

2.33

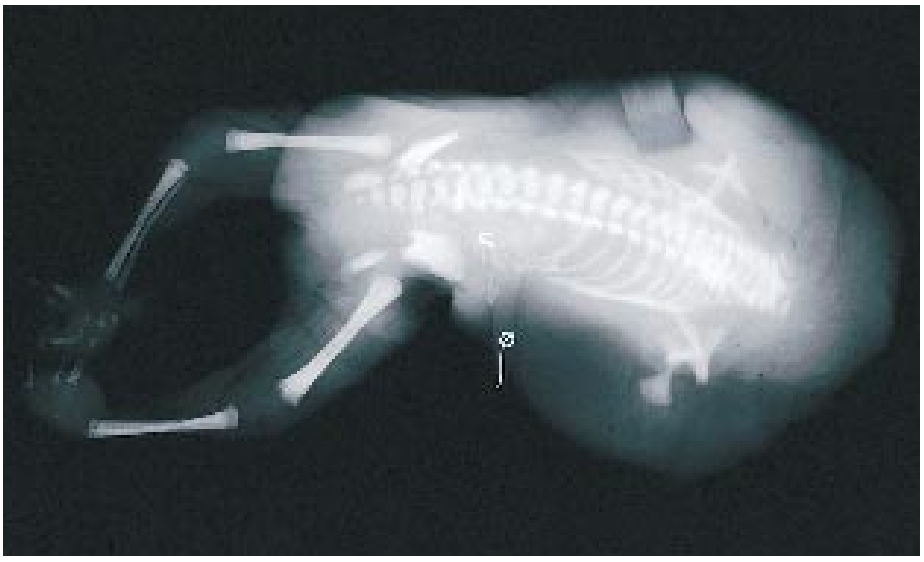

Figure 2.33. Radiograph of the infant with acardius acephalus. Note the lack of cranial development. Two clavicles and scapulae are present. The vertebral column is normal. The chest is narrow due to lack of the heart and hypoplastic lungs. The pelvis and lower extremities are well mineralized and relatively normal except for lack of some metatarsal bones.

2.34

Figure 2.34. The twin with the dominant heart of the same pregnancy often shows additional anomalies such as limb reduction defects. These have been attributed to embolic disease consequent upon stasis in the acardiac fetus. This twin had some limb anomalies which included fusion of digits of the left hand as seen in this figure.

2.35

Figure 2.35. This is the same infant showing anomalies of both feet.

2.36

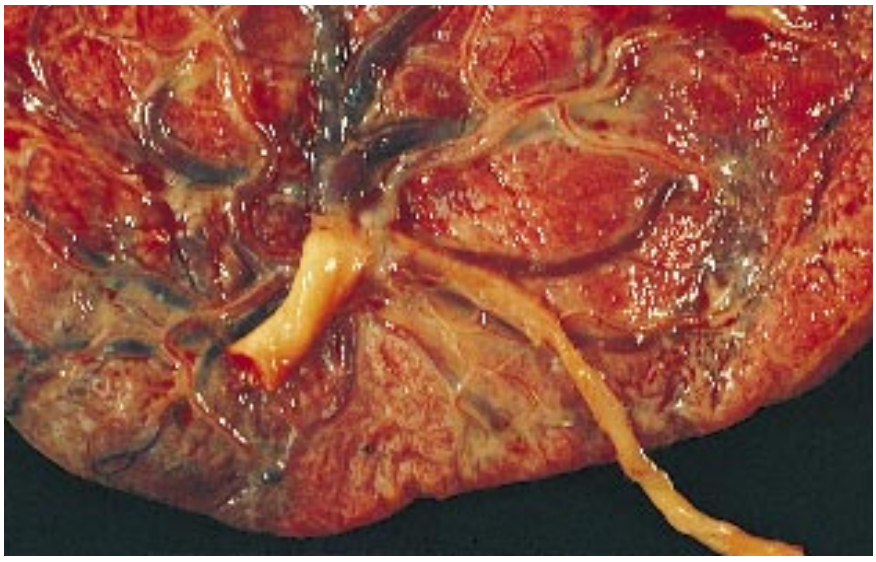

Figure 2.36. The placenta of the infants described above showing two umbilical cords with a common insertion about 5 cm from the margin of the placenta. The larger cord was approximately 10 mm in diameter and had three vessels. The smaller cord was approximately 6 mm in diameter and had two vessels. Note the congested appearance of the placental tissue and the vessels on the left and the pallor of the placental tissue and the vessels on the right. (Klima, T.)

2.37

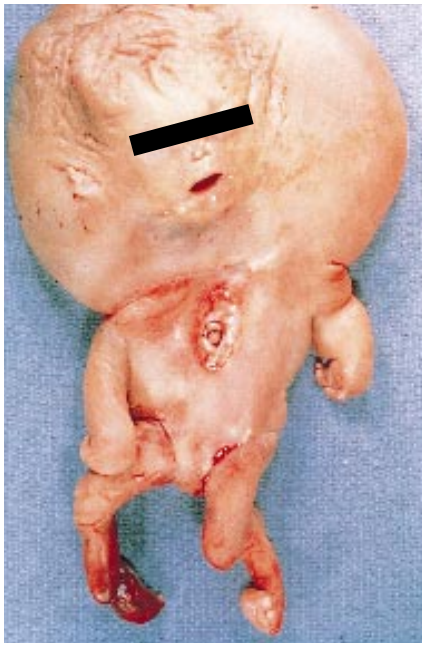

Figure 2.37. This is an example of acardius anceps (hemiacardius). The cranial portion is partially covered by hair, but no head is formed. There is a globular structure of the upper part which shows a rudimentary face with an oral opening through which a cleft palate is seen. Four extremities are present. There is a defect in the anterior abdominal wall with intestinal loops present. (Klima, T.)

2.38

Figure 2.38. Close-up of the same infant shown in Figure 2.37. The anterior wall of the abdomen is missing and the intestinal loops are exposed. There is no umbilical cord identified. (Klima, T.)

CONJOINED TWINS

Conjoined twins are rare, one per 50,000 to 100,000 live births. They result from the failure of the zygote to completely divide. This occurs in approximately 1% of monozygotic twins. The incidence of the types of fusion is as follows: The most common types are thoracopagus twins with an incidence of one per 70,000 live births (73.4%), pygopagus twins (18.8%), ischiopagus twins (5.9%), and the most rare types are the craniopagus twins with an incidence of one per 2,000,000 to 4,000,000 live births (1.7%). Conjoined twinning occurs only in monoamnionic-monochorionic pregnancies.

2.39

Figure 2.39. In thoracopagus conjoined twins, note the fusion at the thorax and upper part of the abdomen with a single site of umbilical cord insertion. The posture is typical for thoracopagus conjoined twins in that the heads are hyperextended and the backs are relatively straight.

2.40

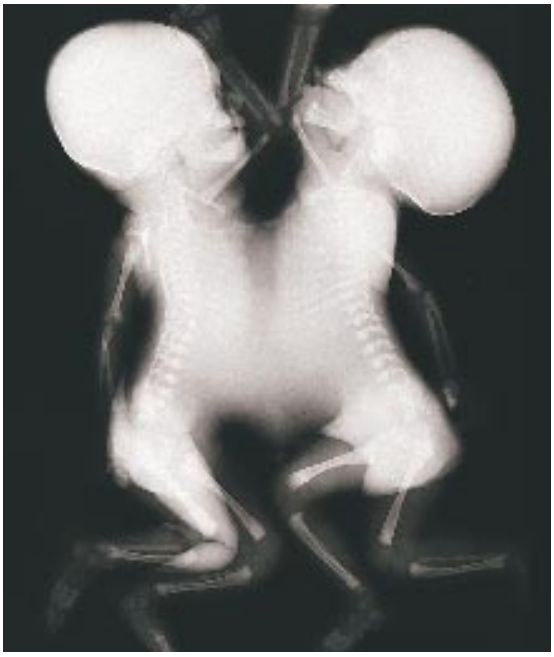

Figure 2.40. Radiograph of the conjoined twins shown in Figure 2.39 illustrates the hyperextended heads and the fusion of the thoraces and upper abdomen. On fetal radiograph, the hyperextended fetal heads at the same level were considered almost diagnostic of thoracopagus conjoined twins. With the advent of ultrasonography, the diagnosis should be made more readily.

2.41

Figure 2.41. Another set of thoracopagus conjoined twins showing the typical posture of the hyperextended heads.

2.42

Figure 2.42. Thoracopagus conjoined twins showing the fusion from the upper thorax to the midabdomen.

2.43

Figure 2.43. The same twins as shown in Figure 2.41 showing the fused upper abdomen and the fused umbilical cord.

2.44

Figure 2.44. This fused umbilical cord section from the same set of thoracopagus conjoined twins shows the presence of four vessels, two arteries and two veins. In the fused umbilical cords seen in conjoined twinning, there may be from two to seven vessels. (Singer, D.)

2.45

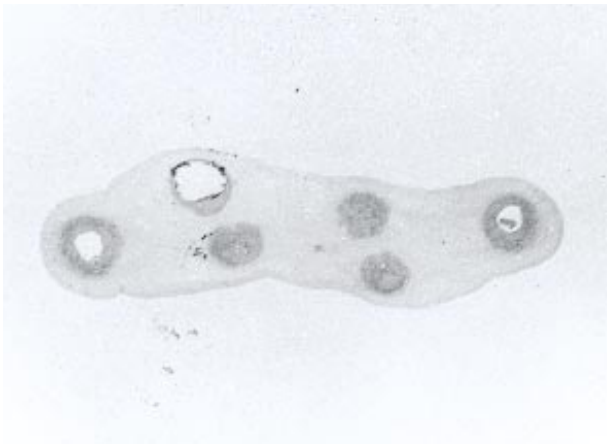

Figure 2.45. This fused umbilical cord section showing three arteries and three veins is another example from conjoined twins. (Singer, D.)

2.46

Figure 2.46. Pygopagus conjoined twins are fused at the buttocks.

2.47

Figure 2.47. The same set of pygopagus conjoined twins showing the fused genitalia.

2.48

Figure 2.48. Close-up of the fused genitalia in the same set of pygopagus conjoined twins.

2.49

Figure 2.49. The twins shown in Figure 2.46 were successfully separated. This figure shows them prior to discharge from the hospital.

2.50

Figure 2.50. Radiograph of a set of omphalopagus twins shows the fusion at the abdominal walls and hence they could be separated.

2.51

Figure 2.51. An example of craniopagus conjoined twins.

2.52

Figure 2.52. Note on the left, the vaginal delivery of prosopothoracopagus conjoined twins. On the right, note the twins following delivery. Prosopothoracopagus conjoined twins are twins united in the frontal plane with the fusion extending from the oral region through the thorax and upper abdomen. Diagnosis was not made prenatally and the twins died at delivery. Note that there are only two upper extremities (dibrachus) and four lower extremities (tetrapus). (Caberra-Meza, G.)

2.53

Figure 2.53. Cephalothoracopagus conjoined twins. Note the syncephalus.

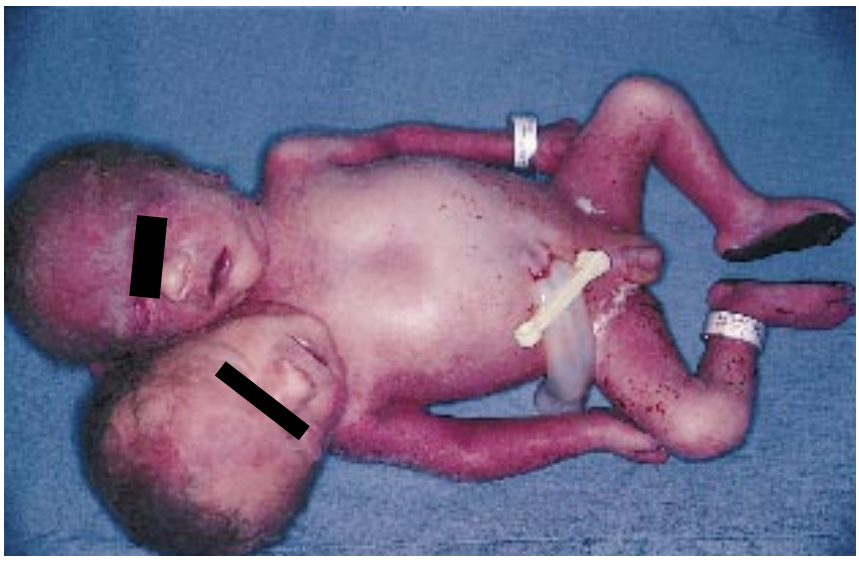

2.54

Figure 2.54. Dicephalus conjoined twins with dicephalus, three upper extremities (tribrachus), and two lower extremities (dipus). Note the two separate heads and the fused chest.

2.55

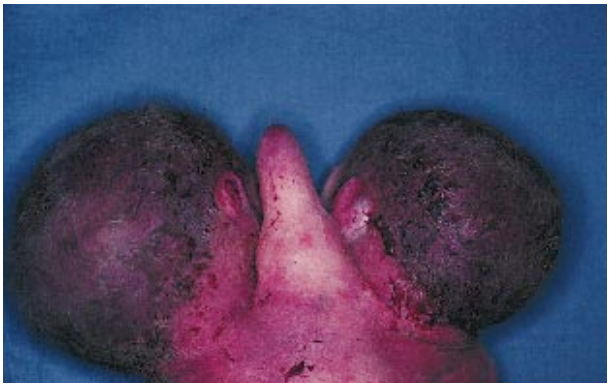

Figure 2.55. A close-up of the same twins shown in Figure 2.54 demonstrates the third upper extremity extending from the fused shoulders. There were two separate neurologic systems, two separate pulmonary systems, two gastrointestinal systems joining at the jejunum, a single genitourinary system, and conjoined hearts with complex anomalies.

2.56

Figure 2.56. Another example of dicephalus conjoined twins. Note that the head on the left of the figure is normal but that there is anencephaly of the head on the right of the figure.

2.57

Figure 2.57. Radiograph of the same conjoined twins showing the normal head on the left of the figure and the anencephalic head on the right of the figure. Note that there are fused vertebral columns with some separation at the lower thorax and upper abdomen and that there is dibrachus.

2.58

Figure 2.58. Asymmetric ischiopagus conjoined twins. Note that the twin on the right of the figure, which is attached at the ischia, is an anencephalic parasite with a partial thorax and abdomen and two upper and two lower extremities. The "normal" twin on the left of the figure had gastroschisis, imperforate anus, and rectovaginal fistula. There were two bladders, two kidneys, and two uteri present.

2.59

Figure 2.59. Close-up of the anencephalic parasite in the above asymmetric ischiopagus conjoined twins.

2.60

Figure 2.60. Radiograph of the asymmetric ischiopagus conjoined twins. Note at the bottom the severely anecephalic twin attached to the "normal" twin who has a large gastroschisis. Each twin has four extremities.

2.61

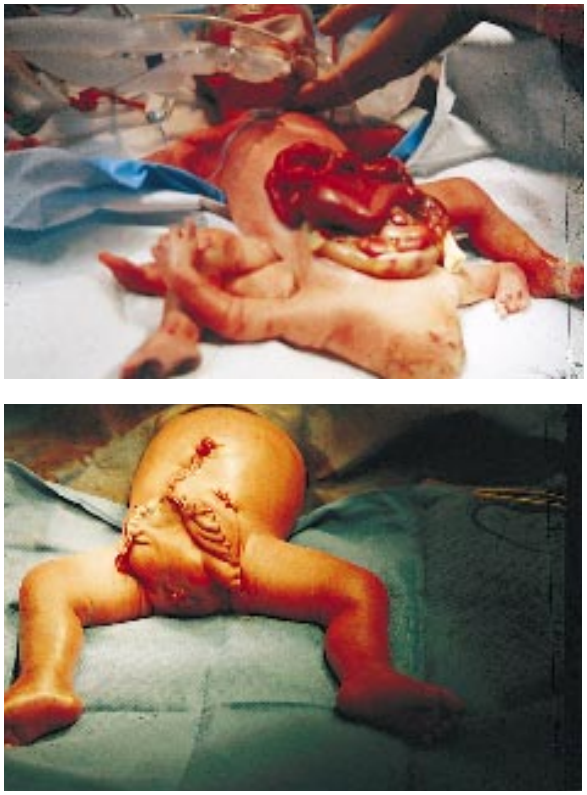

Figure 2.61. Preoperative (above) and postoperative (below) appearance of the asymmetric ischiopagus conjoined twins shown in Figures 2.58 to 2.60.

2.62

Figure 2.62. Dipygus twins. Recent work has suggested that genes are involved in establishing the body axes, metameric pattern (segmentation genes), and regional specialization (homeotic genes). This raises the possibility that many of the abnormalities of facial duplication in man are not a manifestation of incomplete twinning but may be homeotic malformations. Limb duplication may also be a result of stimulation of homeobox gene expression and thus a well-formed pair of arms and/or legs may be seen emerging.

2.63

Figure 2.63. This infant has a well-developed lower extremity emerging from the chest and has been considered to be an asymmetrical double malformation – heteroadelphia (an underdeveloped *parasite* attached to a well-developed *autosite*). With the new concept, this could be an example of a homeotic malformation. Also note the large omphalocele.

2.64

Figure 2.64. Close-up view of the same accessory lower extremity as shown in Figure 2.63.

2.65

Figure 2.65. Duplication of the right leg and foot. The question again arises as to whether this is an asymmetric double monster or a homeotic malformation. (Cabera-Meza, G.)

2.66

Figure 2.66. Discordant twins. The twin on the left is an example of a severe caudal regression syndrome. There was oligohydramnios, renal agenesis, imperforate anus, and lack of external genitalia. The twin on the right is normal. (Cabera-Meza, G.)

2.67

Figure 2.67. Another example of discordant twins. The twin on the left is an albino and the twin on the right is normal. This is the second set of discordant twins (one albino and one normal) born to this mother.

Chapter 3
Effects of Maternal Medication

During pregnancy, the average fetus is exposed to four physician-prescribed and five self-prescribed drugs. Every drug administered or taken by a pregnant woman presents the mother with both risks and benefits. The risks include the drug's potential as a teratogen or as a cause of toxicity in the fetus. Most human teratogens affect the embryo during a very narrow period of early development as illustrated by the time (24 to 33 days gestation) during which the fetus is susceptible to limb reduction defects caused by thalidomide. Several human teratogens, such as alcohol, androgens, cocaine, diphenylhydantoin, radiation, tetracycline, valproic acid, and warfarin have serious side effects beyond the period of organogenesis. These effects may include cell deletion, vascular disruption, necrosis, physiologic decompensation, organ pathology, and intrauterine growth retardation. Drugs taken in the third trimester may not have teratogenic effects, but may be toxic to the fetus. Some examples include indomethacin (causing oligohydramnios), propylthiouracil (causing fetal goiter), and erythromycin (causing cholestatic hepatitis). A detailed history of maternal drug use and abuse is essential in evaluating most malformations and diseases in the neonatal period.

3.1

Figure 3.1. This illustration contrasts the craniofacial features of a healthy child on the right to those of a child with fetal alcohol syndrome on the left. Note the microcephaly, short palpebral fissure, flat maxillary area, poorly developed philtrum and thin upper lip (Peter Shvartsman, Canadian Medical Association Journal, July 15, 1981 cover).

3.2

Figure 3.2. This infant, age 6 weeks, was born to a mother with severe, chronic alcoholism. There was failure to thrive and hypotonia. Note the microcephaly (head circumference less than the third percentile), short nose, absence of philtrum and thin vermilion border of the upper lip.

Findings in fetal alcohol syndrome include intrauterine growth retardation, microcephaly, dysplastic facial features, hypoplasia of the midface, and a hypoplastic philtrum with a thin vermilion border of the upper lip. Later there may be continued failure to thrive and developmental and behavioral disorders.

3.3

Figure 3.3. Close-up of the face of the same infant shows the short nose, absence of the philtrum, and thin vermilion border of the upper lip. Many other findings in fetal alcohol syndrome have been reported, including epicanthic folds, ptosis, hypoplastic maxilla, deep or accentuated palmar creases, and clinodactyly.

3.4

Figure 3.4. Soon after birth, this infant of a narcotic addict shows hypotonia. Note the concavity of the inner aspect of the thighs and the position of the lower extremities. This has resulted from a postural deformation in which the fetus has had its thighs flexed over its abdomen in utero. Because of the mother's narcotic habit there was minimal fetal movement in utero.

3.5

Figure 3.5. Drug withdrawal is a major problem in neonates delivered of narcotic addicted mothers. This figure stresses the fact that one should always check for signs of drug addiction in the mother. This figure shows needle tracks at both elbows of a mother.

3.6

Figure 3.6. Infants with retinoic acid embryopathy (Accutane™ embryopathy) may have craniofacial, cardiovascular, and central nervous system abnormalities. In this infant note the narrow sloping forehead, flat depressed nasal bridge, mild micrognathia, and microtia with absence of the external auditory canal. In addition there was congenital heart disease. Affected infants may have hydrocephalus, microcephaly, or thymic abnormalities. This mother was treated with retinoic acid during the first month of pregnancy.

3.7

Figure 3.7. Close-up of the ears of the same infant as shown in Figure 3.6 shows the bilateral microtia with absence of the external auditory meatus.

3.8

Figure 3.8. In infants with the fetal hydantoin (Dilantin™) syndrome there is moderate growth retardation, usually prenatal, a wide anterior fontanelle and metopic ridging. In this infant, note the growth retardation, profuse scalp hair, and short neck. Other findings included hypoplasia of the distal phalanges with small nails and a digital thumb.

3.9

Figure 3.9. Close-up of the face of the same infant. Note the marked hirsutism, low hairline, low nasal bridge with a short upturned nose ("pug" nose), and long philtrum.

3.10

Figure 3.10. Hypertrichosis in another infant with the fetal hydantoin syndrome. Mother was treated throughout pregnancy with hydantoin. The risk of fetal hydantoin syndrome in infants of treated mothers is about 10%.

3.11

Figure 3.11. Gum hypertrophy in an infant with the fetal hydantoin syndrome. Many other findings have been reported in infants with fetal hydantoin syndrome, including widely spaced nipples, rib anomalies, abnormal palmar creases, pilonidal sinus, and congenital heart disease.

3.12

Figure 3.12. This infant of an epileptic mother on hydantoin developed seizures at the age of 36 hours. He had hypocalcemia with a calcium level of 6.4 mg/dL and a phosphorus level of 11.2 mg/dL. In fetal hydantoin syndrome the digital hypoplasia may be associated with narrow distal phalanges and hypoplastic nails.

3.13

Figure 3.13. This infant with the fetal hydantoin syndrome presented with many of the findings already described. There was growth retardation, hypertelorism, small pug nose, anteverted nostrils, long philtrum, and thin vermilion border of the upper lip, and short neck.

3.14

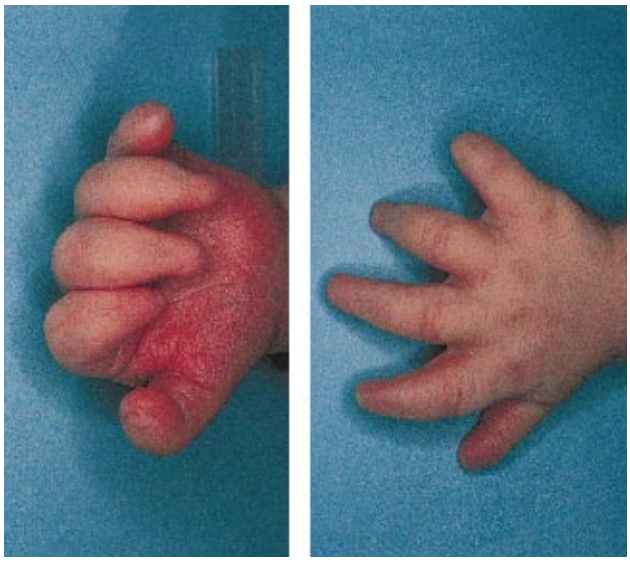

Figure 3.14. The same infant shows the characteristic changes in the fingers. Note the hypoplasia of the distal phalanges with hypoplastic or absent nails and the digital thumbs. There is mild webbing.

3.15

Figure 3.15. The same infant with fetal hydantoin syndrome shows the marked hypoplasia of the distal phalanges of the toes and absent or hypoplastic nails.

3.16

Figure 3.16. Postnatal growth deficiency and microcephaly are present in two-thirds of children exposed to valproic acid in combination with other anticonvulsants. It does not occur with monotherapy with valproic acid. This infant with the fetal vaproate syndrome shows the typical craniofacial abnormalities. Note the trigonocephaly with a prominent metopic ridge, bifrontal narrowing, outer orbital ridge deficiency, midface hypoplasia, epicanthic folds, small short upturned nose, and long flat philtrum.

3.17

Figure 3.17. A cranial view of the same infant shows the trigonocephaly due to premature closure of the metopic suture, bifrontal narrowing, and outer orbital ridge deficiency.

3.18

Figure 3.18. Lateral view of the head and face of the same infant shows the marked metopic ridge, small flat short nose, micrognathia and "square" ears.

3.19

Figure 3.19. The same infant with fetal valproate syndrome as shown in Figures 3.16 to 3.18, had distal phalangeal hypoplasia and tapering of the fingers. Note the abnormal creases on the fingers and palm due to lack of fetal movement in utero. Other changes reported in infants with this syndrome include tracheomalacia, congenital heart defects, and urogenital anomalies.

3.20

Figure 3.20. Yellow staining of the teeth in a child exposed to maternal tetracycline in utero.

3.21

Figure 3.21. A Wood's filter shows the fluorescence of the nails in an infant exposed to maternal tetracycline. If young infants are given tetracycline after birth the staining of the teeth and nails also occurs.

3.22

Figure 3.22. Drug-induced pseudohermaphroditism in a female infant who was virilized by progestational agents during the first trimester of pregnancy. The incidence of this condition has decreased because, with recognition of this iatrogenic cause of virilization of the fetus, there has been a decreased use of incriminating drugs such as progestational agents or androgens during the first trimester. There may be fusion of labioscrotal folds with formation of a urogenital sinus and clitoromegaly. (See Volume V, chapter 5).

3.23

Figure 3.23. The thalidomide syndrome in twin infants born to a mother who took thalidomide early in gestation. Maternal ingestion of thalidomide between the 25th to 44th day after conception may cause malformations. In the thalidomide syndrome the limbs are usually asymmetrically involved and the malformations of the extremities are of all grades of severity (digits are usually present). There may be microphthalmia, ear deformities, and cardiac, renal and intestinal malformations.

3.24

Figure 3.24. Phocomelia in another infant born to another mother who took thalidomide in early gestation. Note the asymmetric phocomelia.

3.25

Figure 3.25. This infant with the fetal warfarin syndrome (Coumadin™ embryopathy) was born to a mother who was being treated with warfarin during the first trimester of pregnancy. These infants typically are low birthweight and have facial and skeletal abnormalities. Less commonly they may have central nervous system and eye abnormalities. In this baby note the typical facial features of a broad flat face and nasal hypoplasia with a low nasal bridge, a prominent philtrum, and micrognathia.

3.26

Figure 3.26. The lateral view of the face strikingly demonstrates the marked nasal hypoplasia resulting in a very flat face. Because of the marked nasal hypoplasia these infants often present with upper airway obstruction.

3.27

Figure 3.27. Radiograph of the lower extremities of the same infant shows the stippling of the epiphyses at the proximal femora. Stippling of the epiphyses may occur along the vertebral column and the tarsal bones. The stippling disappears in the first few years of life. Coumadin™ embryopathy is phenotypically similar to hereditary chondrodystrophia punctata and it must thus be distinguished from the different hereditary forms of Conradi-Hünermann syndrome.

Chapter 4
Birth Trauma

Birth trauma refers to those injuries sustained during labor and delivery. Despite skilled and competent obstetric care, some may be unavoidable. Factors predisposing infants to injury include macrosomia, prematurity, cephalopelvic disproportion, dystocia, prolonged labor, and abnormal presentation. In 1988, birth injuries ranked eight as major causes of neonatal mortality and caused 4.6 deaths per 100,000 live births. The clinician who cares for newborn infants must be familiar with the conditions caused by birth injury. Injuries are known to occur to the soft tissues, head, eyes, ears, vocal cords, neck and shoulder, spine and spinal cord, intra-abdominal organs, extremities, and genitalia. Although many are mild and self limited, others are serious and potentially lethal.

4.1

Figure 4.1. Severe molding of the head following an occipitoposterior presentation. The mobile skull bones and brain deform to comply with pressure in the birth canal. Note the flattened forehead and long occiput. It resolves spontaneously and needs no intervention.

4.2

Figure 4.2. Persistent occipitoposterior presentation with marked molding and a caput succedaneum. A caput succedaneum occurs as a result of the presenting part pressing against the partly dilated cervix whose constricting rim obstructs the return flow of venous flood and lymph from the scalp leading to edema. The distribution crosses suture lines (compare with cephalhematoma) and is usually present at birth.

4.3

Figure 4.3. Caput succedaneum with prolonged labor. In a caput succedaneum the tissues involved are those encircled by the "girdle of contact" formed by the maternal passages. The location indicates the intrauterine lie of the fetus. In breech delivery there may be similar edema and bruising of the perineum, buttocks, or genitalia. These are really an equivalent of caput succedaneum.

4.4

Figure 4.4. "Blisters" of the skin following prolonged labor over a caput succedaneum in an infant at the age of 1 day following prolonged labor. Aspiration of the material was sterile.

4.5

Figure 4.5. A large caput (chignon) following vacuum extractor delivery. The word "chignon" refers to the localized area of scalp edema caused by the suction of the cup of the vacuum extractor. Most cases resolve spontaneously but if associated with perinatal asphyxia there may be necrosis of the chignon leading to ulceration of the scalp.

4.6

Figure 4.6. "Caput ring." In rare cases with persistent strong contractions and a slowly dilating cervix, necrosis of the scalp may occur in the area of a caput due to pressure ischemia occurring during a prolonged labor.

4.7

Figure 4.7. Cephalhematoma over the right parietal bone. A cephalhematoma is a subperiosteal hemorrhage occurring as a result of vessel rupture at birth. It is generally not apparent at birth but is noted in the first day or two of life. It should be distinguished from a caput succedaneum. It is most commonly seen over the parietal bones and more commonly over the right parietal than the left. A caput succedaneum and cephalhematoma may occur concurrently.

4.8

Figure 4.8. Large left parietal cephalhematoma. Note that the cephalhematoma is limited by suture lines because it is a subperiosteal hemorrhage. Cephalhematoma occurs more commonly after prolonged primigravida labor or forceps delivery especially in post term infants where suture fusion makes the skull hard and unyielding.

4.9

Figure 4.9. Bilateral cephalhematomas in this infant demonstrate very clearly the limitation of the cephalhematoma by suture lines. Complications of cephalhematomas include anemia, jaundice, infection, and underlying skull fracture. In general, cephalhematomas resolve spontaneously over a period of weeks to months.

4.10

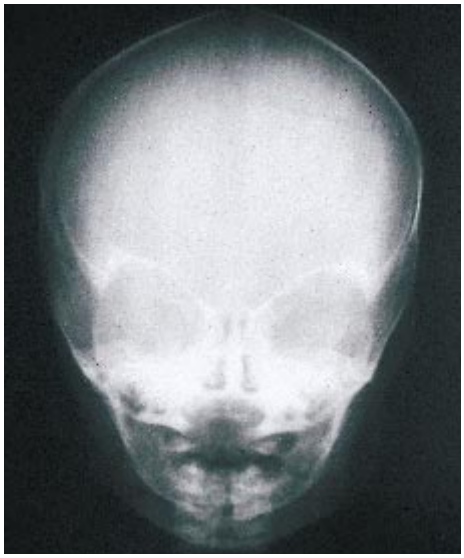

Figure 4.10. Cephalhematoma with linear fracture of the skull. This occurs in 4 to 5% of infants with a cephalhematoma.

4.11

Figure 4.11. Calcification in a cephalhematoma giving the lesion an "egg shell" feel occurs as a result of deposition of calcium in the organizing blood. Periosteal new bone forms around the perimeter of the cephalhematoma and this rim of calcification may be noted for several months.

4.12

Figure 4.12. Infected cephalhematoma in an infant with *Escherichia coli* sepsis. Osteomyelitis of the underlying parietal bone was present.

4.13

Figure 4.13. The same infant as in Figure 4.12 with pus being drained from the infected cephalhematoma (pyocephalhematoma). The pus grew pure *E. coli* in culture. In general it is recommended that cephalhematomas not be aspirated, but on rare occasions, if the infant develops sepsis due to any organism, infection may occur in the cephalhematoma requiring drainage.

4.14

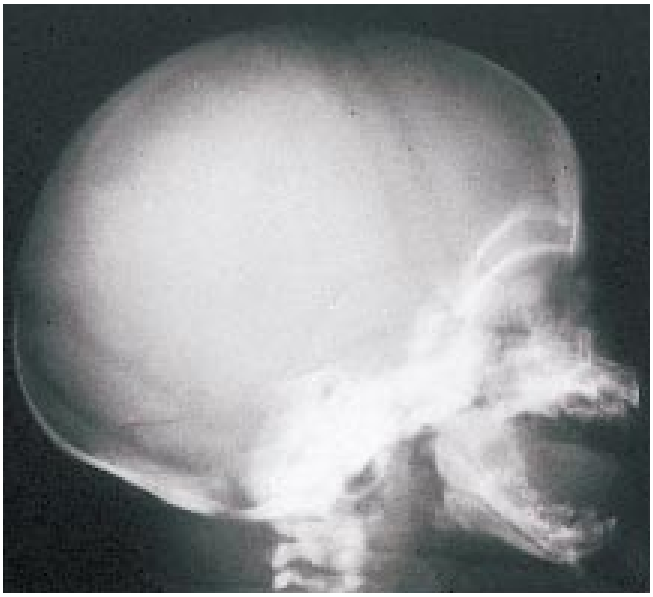

Figure 4.14. Radiograph of the skull of the same infant showing osteomyelitis of the parietal bone.

4.15

Figure 4.15. Massive scalp hemorrhage of the newborn (subgaleal hemorrhage). When there is rupture of the capillaries in the subaponeurotic area, there may be massive scalp hemorrhage with spread over the entire scalp and massive blood loss. Disseminated intravascular coagulopathy may ensue rapidly. This condition may occur as a result of a precipitous delivery or poor application of a vacuum extractor. Note the massive soft tissue swelling.

4.16

Figure 4.16. Frontal view of the same infant who had a massive scalp hemorrhage with a skull fracture. Note the ecchymoses of the upper eyelids and marked swelling from the bridge of the nose extending over the scalp. This is characteristic of a subgaleal hemorrhage as the aponeurosis of Galen attaches at the upper eyelids and has no attachment to the scalp until the nape of the neck and the sternocleidomastoid muscle on the sides, hence the massive hemorrhage in the subgaleal area of the head.

4.17

Figure 4.17. A massive scalp hemorrhage following vacuum extractor delivery. Note the limitation of bleeding at the nape of the neck and the sternocleidomastoid muscle. The bleeding into the subaponeurotic space may result in massive blood loss leading to hypovolemia and shock.

4.18

Figure 4.18. Hematoma of the right cheek and mouth which occurred during a difficult spontaneous delivery.

4.19

Figure 4.19. Trauma from a forceps delivery. Forceps marks on the cheek are fairly common. Rarely, a transient facial palsy may be associated with this type of trauma and occasionally the forceps may actually traumatize the skin, leading to ulceration.

4.20

Figure 4.20. Forceps mark following delivery. The pressure of the forceps blade may result in damage to the underlying tissue and, as in this infant, subcutaneous fat necrosis may occur.

4.21

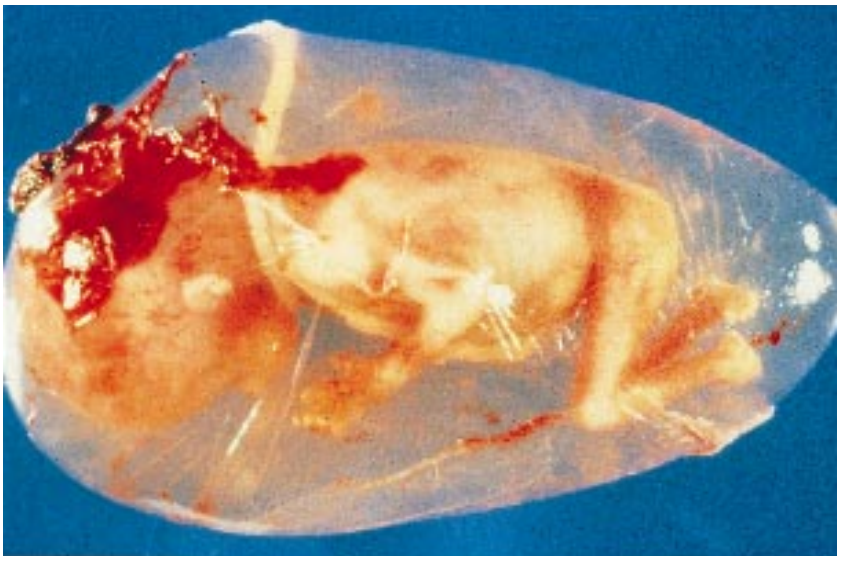

Figure 4.21. Fetus born in a caul with a nuchal cord. Cord around the neck once is present in about 20% of deliveries and, in about 2% of deliveries, there is a cord around the neck twice. This common finding generally does not cause problems unless the cord constricts the neck tightly. (Klima, T.)

4.22

Figure 4.22. Facial suffusion due to a nuchal cord.

4.23

Figure 4.23. Cord around the neck interfering with circulation. Note the petechiae of the face and head and the subconjunctival hemorrhages. Petechiae are also seen in infants in whom there is abnormal delay following delivery of the head and neck before the trunk and shoulders are delivered. In subconjunctival hemorrhage a linear or lunar hemorrhage is often seen to the side of the iris. Petechiae and subconjunctival hemorrhages do not have the same ominous significance as those on the trunk or limbs and usually fade in the first few days of life.

4.24

Figure 4.24. Marked suffusion and bruising of the face as a result of a face presentation. This could be considered the equivalent of a caput with the face as the presenting part. There is deep blue discoloration and swelling of the face and there may be considerable disfiguration of the face which is of short duration.

4.25

Figure 4.25. Face presentation in a premature infant of 34 weeks gestation. Note the very marked ecchymotic appearance of the face.

4.26

Figure 4.26. Face/brow presentation. Note the marked edema and ecchymoses over the face and brow, particularly the left eye.

4.27

Figure 4.27. A brow presentation with hyperextension of the head. This is the classic "militaristic attitude" with head back and chin out. Opisthotonos is excluded by lack of arching of the back. As this is the baby's "position-of-comfort" in utero, during the first few days postnatally the infant will be unhappy if an attempt is made to flex the head. After several days the infant will adopt a normal posture.

4.28

Figure 4.28. In this infant who was a breech presentation note the edema, bruising, and ecchymosis. In breech presentations the perineum, buttocks, and thighs may be severely bruised.

4.29

Figure 4.29. This infant is another example of a breech presentation. Note the extended legs and the equivalent of a caput over the right buttock, which was the presenting part.

4.30

Figure 4.30. Bruising of male genitalia due to a breech presentation. Note the marked swelling of the scrotum and penis. In rare cases testicular trauma may occur.

4.31

Figure 4.31. Breech presentation in a female infant with marked bruising and swelling of the genitalia. Note the swollen labia majora and bruised labia minora.

4.32

Figure 4.32. Petechiae following a breech delivery are frequently seen in otherwise normal infants. They are of no consequence and improve spontaneously in a few days.

4.33

Figure 4.33. Typical position-of-comfort of an infant who was a frank breech presentation. Note the mild genu recurvatum. This infant kept her legs in extension with the knees flexed for several days. "Position-of-comfort" deformations are common in breech presentations and improve in a few days. These infants should all be checked for congenital dislocation of the hip.

4.34

Figure 4.34. The characteristic molding of the head of an infant in a breech presentation. The frontal view shows the occipitofrontal head elongation along with a prominent occipital shelf and the neck appears long.

4.35

Figure 4.35. Lateral view of the head of the same infant shows the flattening of the vertex and the prominent occipital shelf. The plane of flattening is directed upward and forward from the occipital protuberance, which is quite prominent. The characteristic head results from prolonged pressure of the flexed head against the fundus of the uterus in breech presentation.

4.36

Figure 4.36. "Hanging neck" contusion in a difficult delivery of a breech presentation. The infant was extremely depressed and required ventilatory support.

4.37

Figure 4.37. Double footling breech presentation. The right leg presented through the cervical os for 6 hours prior to delivery. Note the marked ecchymoses and edema. This resolved spontaneously but the infant developed hyperbilirubinemia.

4.38

Figure 4.38. This mother had a history of a difficult previous abortion. With this pregnancy she had a spontaneous rupture of the uterus. On laparotomy a large perforation was noted in the uterus through which the infant's lower extremities presented. Note the compression edema and ecchymoses of the left leg and the gangrene of the right foot.

4.39

Figure 4.39. A close-up view of the gangrene of the right foot in the same infant.

4.40

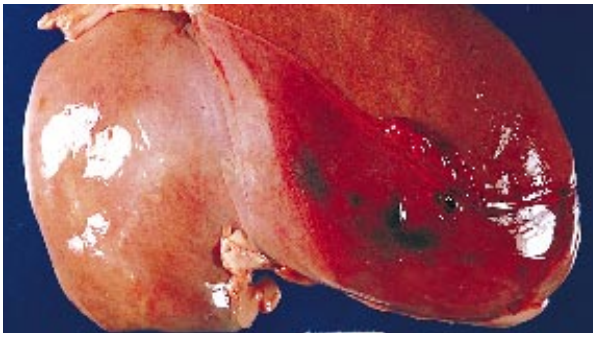

Figure 4.40. Subcapsular hematoma of the liver is generally a pathologic finding. It occurs most commonly with breech delivery especially in premature infants. Occasionally, if bleeding persists, the capsule of the liver ruptures and there is massive hemorrhage into the peritoneal cavity. This usually occurs on the third or fourth day of life. The same may occur in the course of mismanaged artificial cardiopulmonary resuscitation. Rupture of the spleen is very rare and is more common with a transverse lie.

4.41

Figure 4.41. Transverse lie with a shoulder presentation. Note the marked swelling and ecchymoses of the right shoulder and upper extremity.

4.42

Figure 4.42. Compound presentation of the right arm, hand and vertex. Note the depression in the skull.

4.43

Figure 4.43. The same infant with the arm and hand placed in its in utero position. Note the marked edema of the right forearm and hand compared to that of the left arm and hand. This occurred as the result of the compound presentation.

4.44

Figure 4.44. In this infant the membranes ruptured 10 days prior to delivery which was by cesarean birth for chorioamnionitis. There was difficulty in delivering the right arm which presented at the elbow. The hand is normal; therefore this was not due to an amniotic band.

4.45

Figure 4.45. Intrauterine skull fracture (congenital molding of the skull) which occurs in cases of infants with poor mineralization of the skull where the mother has a prominent sacral promontory and has a prolonged labor or delivers precipitously. It results in a greenstick or depressed fracture of the skull.

4.46

Figure 4.46. Radiograph of the skull of the infant shown in Figure 4.45 showing a depressed fracture in a poorly mineralized skull after a spontaneous vertex delivery. In these infants the fracture may improve spontaneously but there is a question as to whether treatment should be passive or surgical lifting of the fracture is indicated.

4.47

Figure 4.47. Another example of an intrauterine skull fracture (also called congenital molding of the skull).

4.48

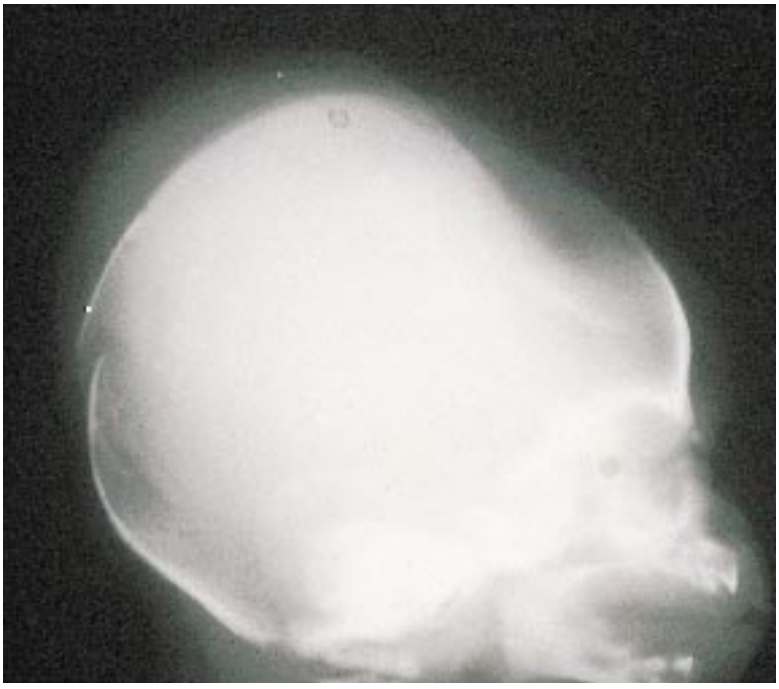

Figure 4.48. Radiograph of a depressed fracture of the skull following forceps trauma. A linear skull fracture may be seen underlying a cephalhematoma or may occur from postnatal trauma such as in an infant falling from the bed to the floor.

4.49

Figure 4.49. This infant had depression on both sides of its skull from its intrauterine position. Note that this is not traumatic and requires no treatment.

4.50

Figure 4.50. Cervical cord injury. This very rare complication is invariably associated with breech delivery. Note the crying infant lying flat on the bed in the "pithed-frog" position with abdominal distention due both to lack of muscle tone and to an enlarged bladder.

4.51

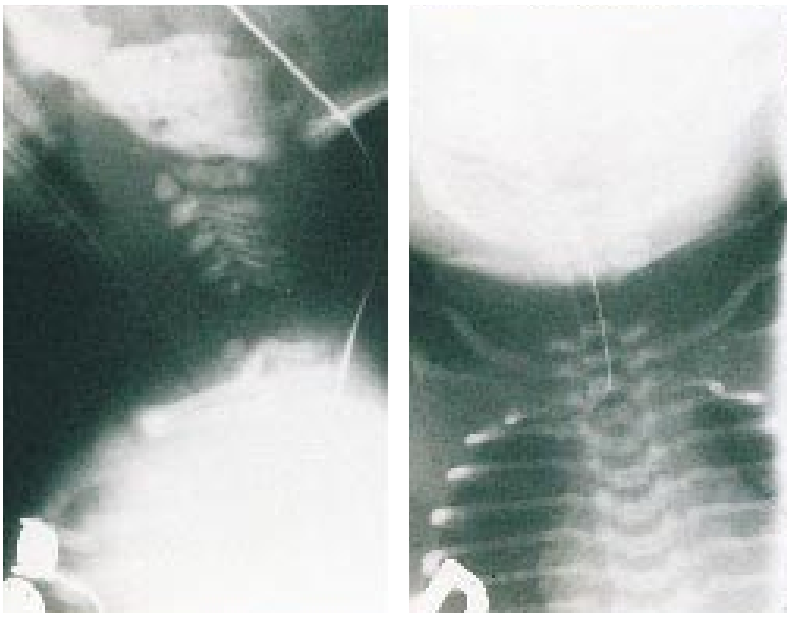

Figure 4.51. Radiograph of the neck showing the cervical cord and spinal injury following breech delivery. Note the fracture dislocation and separation involving C5 and C6.

4.52

Figure 4.52. Congenital torticollis is usually not apparent at birth but within the first week a swelling is noted over the sternocleidomastoid muscle (stenomastoid tumor). This is thought to occur as a result of spasm, hemorrhage or fibrosis. It results in shortening of the sternocleidomastoid muscle and tilting of the head. It is important to recognize since it may cause astigmatism.

4.53

Figure 4.53. Fracture of the right clavicle in an infant at the age of 3 days. There was soft tissue swelling but not much callus formation. The baby may be asymptomatic and the first clinical sign may be a swelling over the clavicle from callus formation or there may be pseudoparesis of the upper limb on the affected side.

4.54

Figure 4.54. This infant did not have the fracture of the left clavicle diagnosed until the age of 10 days but the nurses had noted that the infant was irritable and restless especially when handled. Examination revealed the excessive callus due to a fracture of the left clavicle. In any infant with a fracture of the clavicle one should also check for injury to the brachial plexus, phrenic nerve, recurrent laryngeal nerve, and the sympathetic chain.

4.55

Figure 4.55. A radiograph of the chest showing a fracture of the right clavicle. The clavicle is the site of the most common fracture during delivery especially if shoulder dystocia is present. Healing is rapid because of the speed with which callus formation occurs and it is rare to have any permanent deformity.

4.56

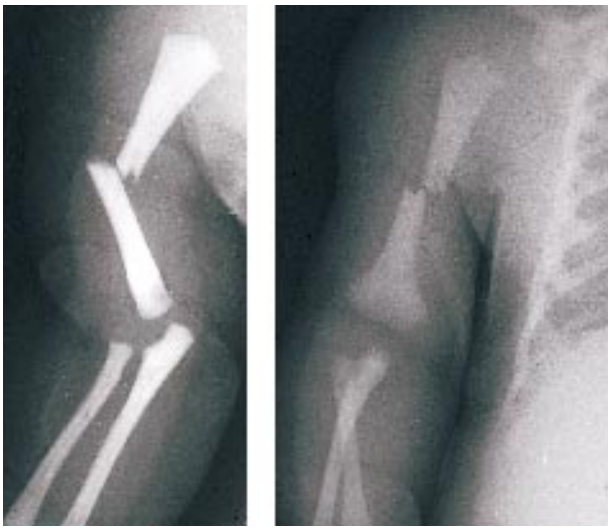

Figure 4.56. A radiograph of a fracture of the middle third of the right humerus following a difficult delivery. This commonly arises with shoulder dystocia and may be associated with lesions of the brachial plexus due to traction on the shoulder girdle. The upper arm is immobile, painful and may be swollen.

4.57

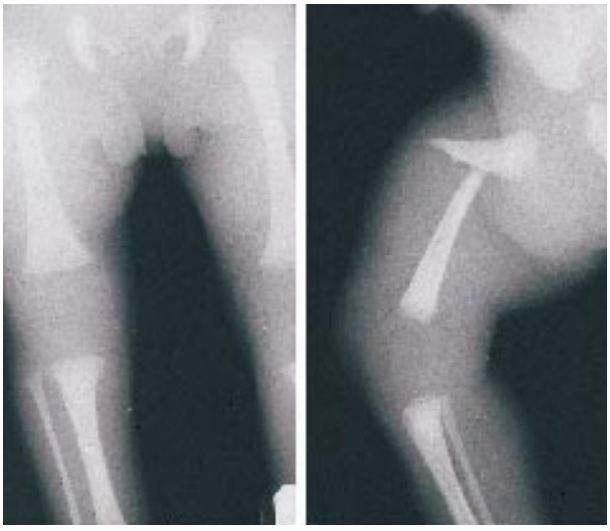

Figure 4.57. A radiograph of a fracture of the right femur occurring as a result of birth injury following breech extraction.

4.58

Figure 4.58. A radiograph of a fracture of the left femur with marked soft tissue swelling. Note the large right inguinal hernia.

4.59

Figure 4.59. Facial nerve palsy occurred in this infant as a result of application of forceps. It may also occur following prolonged labor in a mother with a prominent sacral promontory. Note the ptosis and drooping mouth on the right side.

4.60

Figure 4.60. This shows the same infant crying. The facial palsy becomes readily apparent. This demonstrates how easily the diagnosis may be missed in a quiet or sleeping infant. There is diminished movement of the affected side of the face, the eye frequently but not always remains partly open, the nasolabial fold is absent and the mouth droops, being drawn over to the healthy side when the infant cries. Note that the forehead is smooth on the affected side. Restoration of normal function and disappearance of the paresis may be complete in a few days or usually within a few weeks. Permanent paralysis is exceptional and suggests a central lesion.

4.61

Figure 4.61. Facial palsy of the left side in an infant. This infant shows the typical findings in that he is unable to close his eye or contract the lower facial muscles and has loss of the nasolabial fold on the affected side. In traumatic facial paresis frequently only the mandibular branch of the facial nerve is affected. With central facial paresis the two lower branches are affected allowing for movement of the forehead. Facial paresis in Möbius syndrome is usually bilateral and incomplete and the face is expressionless.

4.62

Figure 4.62. Congenital hypoplasia of the depressor anguli oris muscle (angular depressor muscle). The localized facial weakness in which the lower lip on one side fails to be depressed on crying results in an "asymmetric crying facies." The resulting facial asymmetry when the child cries may be misinterpreted. There is a weakness of the muscles controlling movement of the mouth but not those of the upper face. The nasolabial folds are normal and the affected side will not move when the infant cries. The normal side of the face is assumed to be abnormal because the lower lip on the intact side appears to be pulled down and everted. This is a benign condition and is *not* facial palsy. It lessens as the child gets older. It may be associated with other anomalies, particularly those of the cardiovascular system.

4.63

Figure 4.63. Erb's palsy (upper brachial plexus injury) occurs as a result of traction on the brachial plexus (most often the upper nerve roots, C3, C4, and C5). This type of injury occurs most commonly in cases of shoulder dystocia. It presents with the infant lying with the affected upper extremity adducted and internally rotated, the elbow extended, and the hand partially closed with the palm directed outwards and posteriorly resulting in the typical "waiter's tip" position. The majority of these injuries resolve spontaneously in 3 to 4 weeks.

4.64

Figure 4.64. Bilateral involvement of the upper brachial plexus resulting in the typical position in both upper extremities. In the rare event of a bilateral palsy the possibility of damage to the spinal cord has to be considered. Note that infants with Erb's palsy may lack a Moro response on the affected side.

4.65

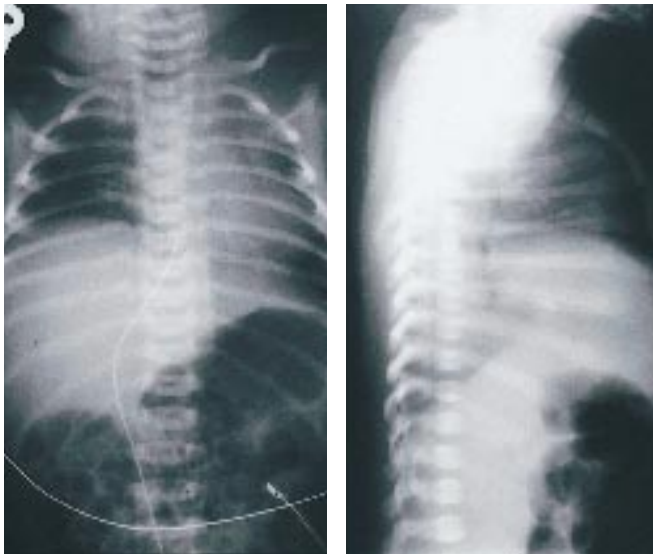

Figure 4.65. Anteroposterior and lateral radiograph of the chest in an infant with a right Erb's palsy. Note the ipsilateral paralysis of the right diaphragm due to phrenic nerve palsy which may occur in association with upper motor brachial plexus trauma. A rare complication associated with Erb's palsy is a Horner's syndrome on the same side, due to involvement of the cervical sympathetic nerves. If Horner's syndrome persists, the infant may develop heterochromia iridis caused by failure of development of secondary pigmentation in the affected eye.

4.66

Figure 4.66. Left radial nerve palsy in a neonate presents as a typical wrist-drop. The condition probably results from interference with blood supply to the nerve if there is abnormal compression or traction during a difficult labor. With the wrist-drop there is ability to grip with the fingers and voluntary extension of the fingers. A similar appearance may occur in an infant with a postural deformity, or a pseudo "wrist-drop" may be seen in a floppy, hypotonic infant hence it is important to check for voluntary wrist extension.

Chapter 5
Deformations and Disruptions

A structural abnormality or anomaly may be a malformation, deformation, or disruption. Deformations and disruptions are the result of mechanical forces affecting normal tissue, while malformations are the result of a primary problem in morphogenesis. A deformation is a physical change in form, shape, or position caused by mechanical forces secondary to restricted intrauterine motion (e.g., clubfoot secondary to constraint of the foot). Most of these have an excellent prognosis once the fetus is released from the constraining environment. In some instances, application of an opposite force may be needed to correct the deformation. Some deformations are caused by a problem intrinsic to the fetus and are not reversible (clubfoot secondary to neuromuscular disorder). A clear distinction between deformation and malformation is important when educating parents on prognosis, management and recurrence risk. A disruption is a congenital defect resulting from an extrinsic interference with an originally normal developmental process (e.g., abnormality caused by an amniotic band). Disruptions usually result in cell death and are not correctable.

DEFORMATIONS (Congenital Postural Deformities, "Position-of-Comfort" Anomalies) and DISRUPTIONS (Amniotic band disruption complex–The Early Amnion Rupture Spectrum (TEARS))

Autoamputation of digits, furrows due to amniotic bands, and syndactyly may develop between the affected digits. Amniotic bands may cause major disruptions that lead to constriction or amputation or to craniofacial disruption. Lack of symmetry of the lesions differentiate disruption caused by amniotic bands from genetic causes of craniofacial or limb anomalies.

5.1

Figure 5.1. The infant in the following five figures was referred to hospital with a diagnosis of multiple congenital malformations. It should be noted that these "malformations" represent examples of congenital postural deformities. Note the position of the hands, lower extremities and the feet occurring as a result of this infant's position in utero.

5.2

Figure 5.2. A close-up of the postural deformities involving the feet.

5.3

Figure 5.3. This figure demonstrates the congenital postural scoliosis and pseudo "wrist-drop."

5.4

Figure 5.4. This figure of the same infant shows a skin dimple over the left hip. Skin dimples are not uncommon in association with deformations (postural deformities or "position-of-comfort" deformities).

5.5

Figure 5.5. The infant has been placed into her in utero position. This demonstrates clearly how the above changes occurred as a result of the infant's "position-of-comfort" in utero. If placed in a normal position, infants with deformations will be uncomfortable and will cry, but will quiet down rapidly when allowed to return to their "position-of-comfort."

5.6

Figure 5.6. Abdominal pregnancy is associated with multiple congenital postural deformities as there is no cushion of amniotic fluid.

5.7

Figure 5.7. Asymmetry of the face and head in an infant at birth due to a deformation.

5.8

Figure 5.8. The same infant demonstrating that this occurred as a result of the right upper extremity lying in apposition to the face and head on the right side in utero.

5.9

Figure 5.9. This normal infant presented at birth with a depression over its left temporal area. This occurred as a result of an in utero positional deformity.

5.10

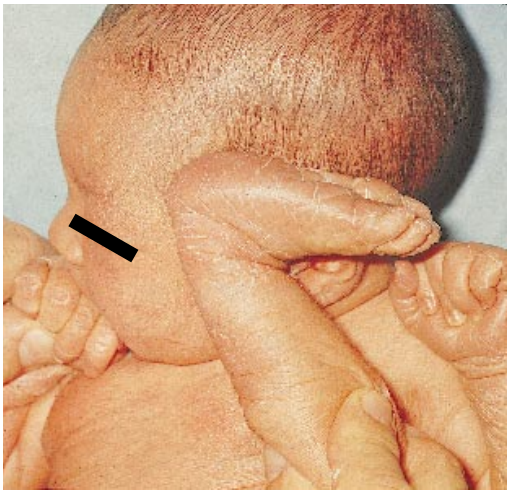

Figure 5.10. In the same infant as shown in Figure 5.9 the left temporal depression was due to pressure of the baby's left foot on the fetal skull in utero.

5.11

Figure 5.11. This very common finding of folding of the ear lobe occurs as a result of a postural deformity.

5.12

Figure 5.12. In this infant the same type of postural deformity is noted demonstrating that this occurs as a result of the shoulder pressing up against the ear lobe in utero. In general, over 90% of congenital postural deformities correct spontaneously.

5.13

Figure 5.13. In rare cases marked pressure of the shoulder on the fetal head in utero can result in a depression over the temporal area. Note the ear is pushed forward.

5.14

Figure 5.14. The same infant in its "position-of-comfort" shows that the shoulder caused the depression and abnormal appearance of the ear.

5.15

Figure 5.15. This infant with asymmetry of the jaw at birth was noted to have some abrasions on the neck. Skin abrasions can occur in relation to a postural deformity.

5.16

Figure 5.16. The same infant showing its "position-of-comfort" in utero.

5.17

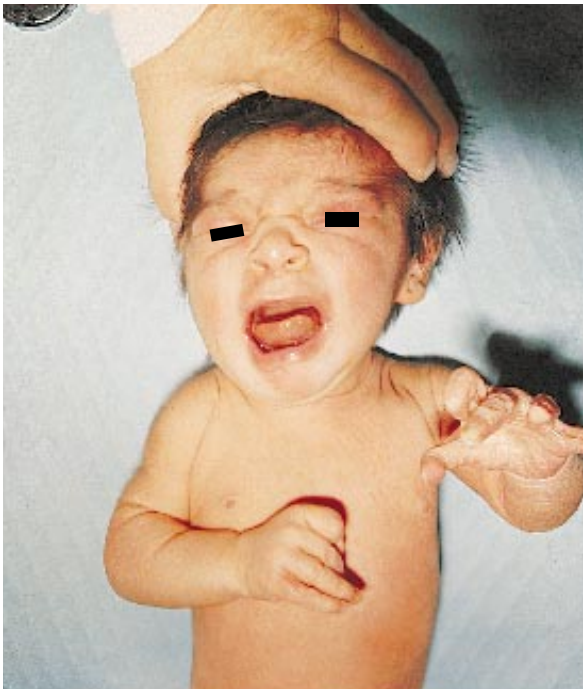

Figure 5.17. There is marked asymmetry of the face in this infant. When the face and head are straightened, the infant is very uncomfortable and cries.

5.18

Figure 5.18. The same infant quiets down immediately when allowed to go into its "position-of-comfort" in utero. This also demonstrates the reason for the asymmetry of the face.

5.19

Figure 5.19. Positional deformity showing asymmetry of the face and jaw.

5.20

Figure 5.20. Asymmetry of the face occurring as a result of a "position-of-comfort" deformity.

5.21

Figure 5.21. The same infant shows that the asymmetry is due to its left foot being placed up against the side of the face and jaw. Another example of "position-of-comfort" deformity.

5.22

Figure 5.22. Malocclusion of the jaw may occur if there is a marked and prolonged positional deformity. Infants with malocclusion should be followed as the malocclusion may require treatment at a later date.

5.23

Figure 5.23. There is asymmetry of the nostrils in this infant. Note the vertical left nostril and horizontal right nostril. This can occur as a result of a postural deformity or dislocation of the nasal cartilage.

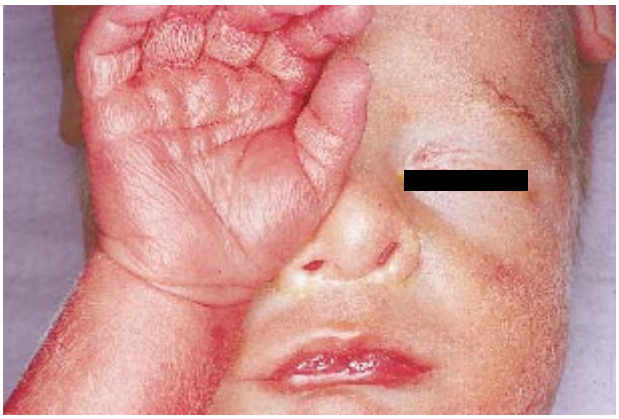

5.24

Figure 5.24. The same infant shows that the asymmetry was associated with a postural deformity due to pressure of the right hand on the nose in utero. This invariably corrects spontaneously.

5.25

Figure 5.25. In this infant note the asymmetry of the nostrils and ecchymosis due to a dislocation of the triangular cartilage of the nasal septum, which may occur during delivery, especially if the mother has a prominent sacral promontory. When the septum is manually moved toward the midline the asymmetry persists confirming the dislocation. These infants require an otolaryngology evaluation.

5.26

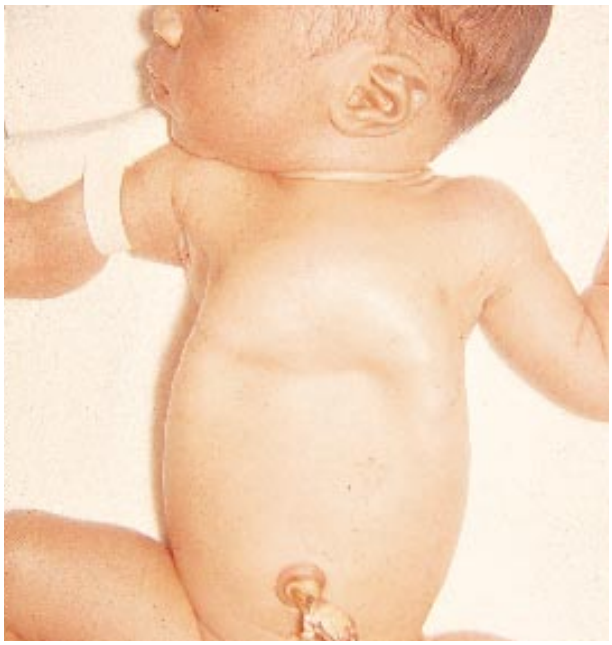

Figure 5.26. Note the subcostal depression on either side of the xiphoid in an infant who was a breech presentation.

5.27

Figure 5.27. This figure shows the same infant with both knees fitting well into the depressions. This is a fairly common example of a "position-of-comfort" deformity.

5.28

Figure 5.28. Another example of a positional deformity on both sides of the subcostal area resulting from position in utero in a breech presentation. This should not be confused with subcostal retraction in this premature infant who had respiratory distress.

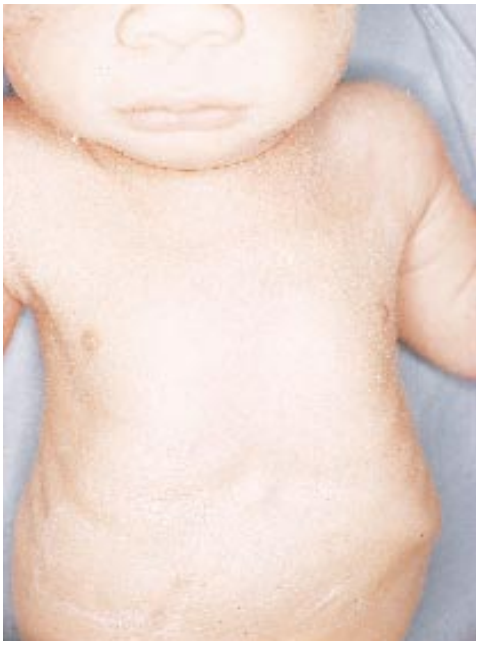

5.29

Figure 5.29. In this infant the chest appears to be narrow compared with the rest of the body.

5.30

Figure 5.30. The same infant shows the arms lying along side the chest wall compressing the thorax. This is a fairly common postural deformity and should not be confused with a narrow thorax observed in cases of dwarfism.

5.31

Figure 5.31. In this infant it appeared that there was a left wrist-drop and the diagnosis of radial palsy was considered. However, with stimulation the left hand moved normally and the postural deformity resolved completely in a few days.

5.32

Figure 5.32. In breech presentation there may be a marked concavity of the inner aspect of the thigh. The lower extremities in a frank breech may lie up against the fetal abdomen causing a "position-of-comfort" deformity.

5.33

Figure 5.33. The same infant showing its "position-of-comfort." A similar concavity of the inner aspect of the thighs may occur in infants who have lack of movement in utero.

5.34

Figure 5.34. Radiograph of an otherwise normal infant with the uncommon finding of bilateral bowing of the femora occurring as a result of a "position-of-comfort" deformity. Bowing of one or both tibiae in which they curve gently toward the midline may have the soles of the feet face each other. Femoral bowing is rare but is occasionally present in babies born after prolonged breech presentation. Congenital bowing of the forearm and humerus almost never occur. These tend to improve gradually as with all deformations.

5.35

Figure 5.35. Posterior view of an infant showing congenital postural scoliosis which occurred as a result of position in utero.

5.36

Figure 5.36. The same infant demonstrating the postural scoliosis. Postural scoliosis in the newborn is rare. If a true congenital scoliosis is present it is usually associated with a structural anomaly of the vertebral column.

5.37

Figure 5.37. This infant has a fairly common congenital postural deformity – genu recurvatum. This "position-of-comfort" deformity gives the impression that there is a dislocation at the knees. Note the hyperextensibility at the knees and note that the creases on the thighs which are normally seen posteriorly are anteriorly placed.

5.38

Figure 5.38. The same infant with genu recurvatum in its "position-of-comfort." When it occurs, genu recurvatum ("back knee") is almost invariably associated with breech presentations and the incidence is much more common in females. The majority correct spontaneously; in severe cases posterior splinting may be necessary.

5.39

Figure 5.39. Another example of genu recurvatum in an infant with a neural tube defect. Note the bilateral clubfeet that are also considered to be postural deformities. Genu recurvatum may occur in neurologic disorders and in syndromes with generalized joint laxity and hypermobility, such as Ehlers-Danlos syndrome.

5.40

Figure 5.40. This infant has a congenital dislocation of the right knee. This uncommon finding has the same appearance as genu recurvatum. Congenital dislocations of the knee rarely occur as an isolated condition but may be seen in Larsen's syndrome, a condition in which there are multiple joint dislocations. It may be confirmed by radiography and requires treatment.

5.41

Figure 5.41. Another view of the congenital dislocation of the right knee in the same infant.

5.42

Figure 5.42. Metatarsus adductus (metatarsus varus) is a common postural deformity which requires no treatment. The forefoot is turned medially so that the lateral border of the sole is quite convex. The heel is in a neutral position and the foot can be dorsiflexed normally. If intrauterine constraint has been prolonged a deep plantar crease will be seen on the medial side.

5.43

Figure 5.43. The position of the feet in utero in the same infant as shown in Figure 5.42 demonstrates how the midfoot becomes adducted.

5.44

Figure 5.44. Talipes calcaneovalgus is the most common of the congenital postural deformities. The foot is dorsiflexed on the fibular side of the ankle and everted with the sole facing anterolaterally. As implied by the name, the calcaneus also is deviated laterally. A deep skin crease is often present in the plane of abnormal flexion and the subcutaneous tissue is diminished over the anterolateral region of the foot.

5.45

Figure 5.45. In this infant with talipes calcaneovalgus, note the marked dorsiflexion of the foot which is lying against the anterior part of the leg. Talipes calcaneovalgus may occur as a result of abnormal intrauterine posture or may be associated with lower motor neuron defects such as spina bifida. Spontaneous correction usually occurs. This anomaly is more common in babies born in the breech position, especially if the knees were flexed in utero.

5.46

Figure 5.46. The same infant showing the flattening of the dorsum of the foot and marked concavity of the lateral side of the ankle joint.

5.47

Figure 5.47. An infant with severe talipes calcaneovalgus with marked bowing of the tibia and fibula. Osseous changes such as these are uncommon. This infant required surgical correction.

5.48

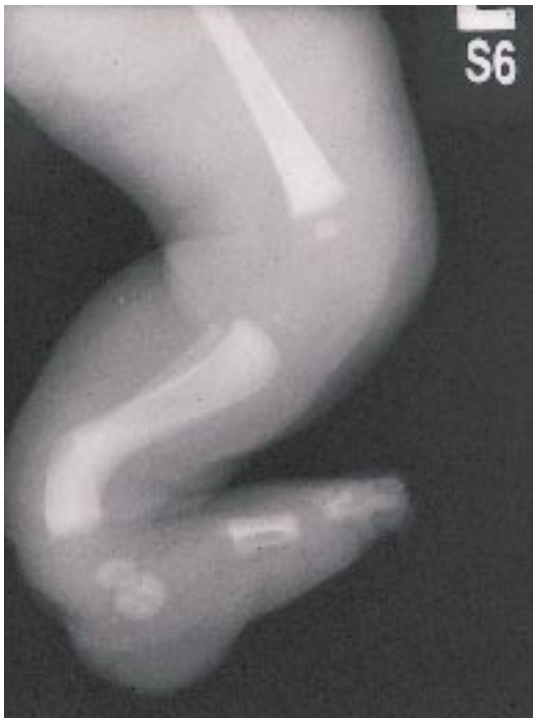

Figure 5.48. Radiograph of the same infant showing the marked bowing of the distal ends of the tibia and fibula.

5.49

Figure 5.49. Bilateral clubfoot (talipes equinovarus). Talipes equinovarus causes the foot to be sharply plantar flexed and inverted so that the sole is toward the median plane. Note the "tip toe" position with the soles of the feet nearly facing each other. The calcaneus is in varus position and some degree of metatarsus adductus is almost always present. The skin and subcutaneous tissue over the lateral part of the joint may be thin and dorsiflexion is minimal or absent.

5.50

Figure 5.50. Bilateral clubfoot. The occurrence of club feet has been considered to be the result of a congenital malformation or a postural deformity. If the legs and feet are subjected to mechanical stress during the last weeks in utero, especially if the fetus is in the breech position, a clubfoot may develop. If the constraint has been relatively mild or brief, the deformity is usually flexible in that the foot can be manipulated into normal position. A fixed deformity implies either severe, prolonged immobilization with contractures of the ligaments and capsules of the joints or an intrinsic skeletal anomaly. This type is resistant to conservative treatment, and casting or surgery is the treatment of choice.

5.51

Figure 5.51. The same infant with the feet in their "position-of-comfort." Note the dimples at the ankles suggesting that this occurred as a result of a postural deformity. Some authors have suggested that the presence of dimples at the ankles in an infant with clubbing of the feet indicates that it has occurred as a result of a postural deformity.

5.52

Figure 5.52. Congenital curly toes (overlapping toes) are a common finding in newborn infants. There is often a family history of the same finding in parents or siblings. Treatment is not necessary.

5.53

Figure 5.53. Another infant with congenital curly toes. The abnormality becomes less obvious as the infant grows.

5.54

Figure 5.54. Twins with asymmetrical heads occurring as a result of an in utero positional deformity. Both infants were vertex presentations. Note how the heads "fit" together.

5.55

Figure 5.55. The same infants as shown in Figure 5.54 with their heads together (in utero position). As the infants grew the asymmetry improved.

5.56

Figure 5.56. This infant with arthrogryposis demonstrates the severe congenital joint contractures. These occur as a result of lack of intrauterine movement and may be associated with muscle or neurologic pathology. Such severe contractures may be accompanied (or produced) by joint webbing (e.g., multiple pterygium syndrome or popliteal pterygium syndrome).

5.57

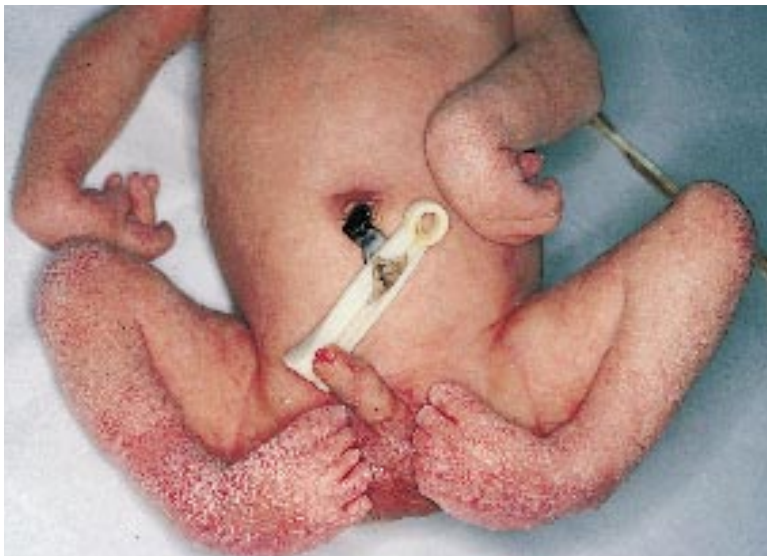

Figure 5.57. Frontal view of another infant with arthrogryposis. Extreme intrauterine compression over an extended period of time can produce such severe distortion in multiple joints that supporting ligaments become contracted and opposing tendons stretch. The muscles acting across these joints may atrophy, creating a picture indistinguishable from the intrinsic forms of arthrogryposis multiplex congenita.

5.58

Figure 5.58. Posterior view of the arthrogryposis in the same infant as in Figure 5.57.

5.59

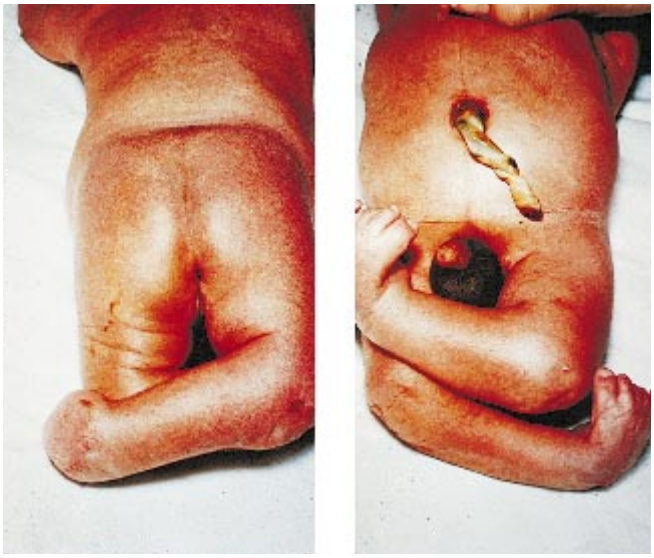

Figure 5.59. This infant is an example of arthrogryposis with joint contractures involving the lower extremities only. The upper extremities were normal. This may occur in infants with neural tube defects, caudal regression syndrome and muscle disease.

5.60

Figure 5.60. An infant with the caudal regression syndrome resulting in arthrogryposis. Note the marked underdevelopment of the hips and the webbing at the joints. There is also talipes calcaneovalgus.

5.61

Figure 5.61. Lateral view of the same infant shows the marked underdevelopment of the hips, the arthrogryposis, webbing, and the dimples at the joints due to lack of movement. Note the talipes calcaneovalgus.

5.62

Figure 5.62. An infant with an amyoplasia congenita disruptive sequence. In this condition the elbows are usually in extension with the wrists and hands flexed.

5.63

Figure 5.63. The same infant showing a close-up of the right wrist and hand. Note the dimples at the contracture site. In this condition there may be cord wrapping of the limb and amniotic bands.

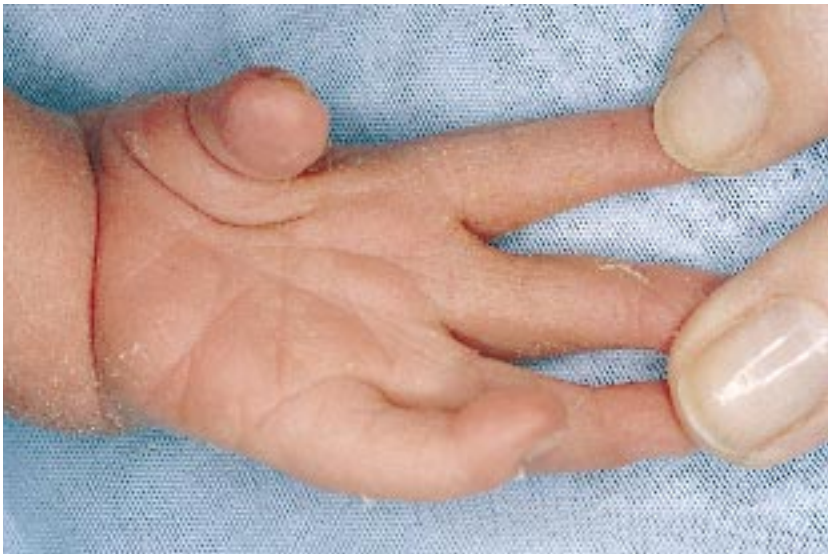

5.64

Figure 5.64. This figure shows the left hand of the same infant. Note the lack of development of the finger and hand creases. Lack of development of the creases indicates lack of fetal movement of the fingers occurring before the 10th to 12th week of gestation.

5.65

Figure 5.65. There is an intrauterine constriction band at the right wrist in this infant. Shallow constricting rings can encircle a limb at any level and destroy subcutaneous tissue sometimes producing distal edema. Amniotic bands may result in constriction or amputation (partial or complete) of extremities and are thought to occur as a result of an active fetus pushing an extremity through and tearing the amnion. This represents an example of *T*he *E*arly *A*mnion *R*upture *S*pectrum (TEARS).

5.66

Figure 5.66. The congenital anomaly of the fourth finger of the left hand in this infant is due to an amniotic band. Also note the collodion appearance of the skin of this postmature infant. The hands and feet (and especially the digits) are the most common sites of damage from amniotic bands. If there is mild constriction, distal edema is produced; with more severe compression there can be disruption of tissue down to the periosteum with eventual loss of the distal avascular portion – a congenital amputation. The findings in such infants are bizzare and very variable.

5.67

Figure 5.67. An infant with amputation of the second, third and fourth fingers occurring as a result of intrauterine constriction bands. At birth, the amputation site will be scarred and sometimes bands of fibrous tissue still will be attached to the injured area. The damage is usually asymmetric with digits affected at different levels and, occasionally, several digits will be bound together at the tips by scar tissue producing a form of pseudosyndactyly.

5.68

Figure 5.68. The amniotic band syndrome in this infant resulted in amputated fingers, intrauterine constriction bands and fusion of the amputated digits.

5.69

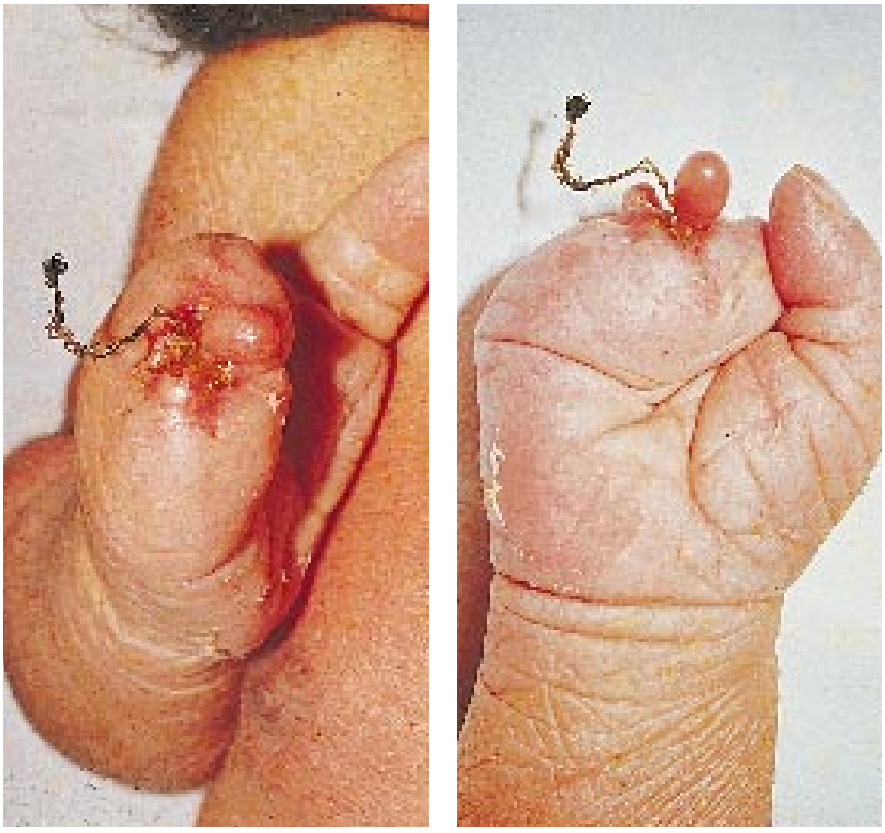

Figure 5.69. Another example of the amniotic band syndrome in which the amputated digits, raw areas and strand of amnion on the right hand can be seen.

5.70

Figure 5.70. This figure of the same infant as shown in Figure 5.69 shows the involvement of the left hand as a result of the amniotic band syndrome.

5.71

Figure 5.71. Amniotic bands involving the fingers of an infant. Note the amputated fourth finger and the constriction involving the base of the third finger resulting in gangrene.

5.72

Figure 5.72. An intrauterine constriction band at the right wrist resulted in marked obstruction of circulation to the hand. Note that at the site of constriction a band has been removed, but because of the distal involvement of the circulation, the condition worsened and the infant eventually required amputation.

5.73

Figure 5.73. In this infant there is a disruption of the right hand due to constriction bands resulting in amputations of the second, third, and fourth fingers. Note the congenital absence of the thumb in the left hand, which was not a disruption but occurred as a result of a true congenital malformation.

5.74

Figure 5.74. There is a minimal amniotic band at the distal part of the right foot of this infant. It should be noted that this type of finding could easily be missed on examination.

5.75

Figure 5.75. In this same infant shown in Figure 5.74 there were severe amniotic bands of the fingers and toes. Note the strands of amnion.

5.76

Figure 5.76. Intrauterine constriction bands (amniotic bands) may disrupt tissue growth and result in partial or complete amputation. In this infant there was amputation of the toes but a severe constriction band interfered with circulation of the left leg. Note the marked distal swelling of the left leg.

5.77

Figure 5.77. Radiograph of the same infant shown in Figure 5.76, showing marked bowing and fracture of the tibia and fibula of the left leg as a result of the constriction band. Also note the severe tissue swelling of the foot.

5.78

Figure 5.78. An intrauterine amputation of the right leg and a constriction band of the left leg were noted in this infant at birth. If there is a congenital amputation, consideration should be given to whether the amputation is a primary or secondary limb reduction defect. This is an example of a secondary limb reduction defect.

5.79

Figure 5.79. A radiograph of the same infant as shown in Figure 5.78 showing the amputation of the right leg. Note the soft tissue constriction of the distal left leg.

5.80

Figure 5.80. Another example of congenital amputation of the left leg and the toes of the right foot by amniotic bands. In primary limb reduction defects, the skin at the amputation is smooth and there is underlying subcutaneous tissue. In secondary limb reduction deformities, the skin shows ulceration or scarring and has no underlying subcutaneous tissue. Radiography shows the stump of the bone is smooth in primary limb reduction defects and the stump of the bone is jagged in secondary defects.

5.81

Figure 5.81. A radiograph of the same infant shown in Figure 5.80 showing the congenital amputation of the left leg at the site of the amniotic band.

5.82

Figure 5.82. Congenital amputation of the right hand. This is a primary limb reduction defect.

5.83

Figure 5.83. This infant presented with multiple anomalies including a bilateral cleft lip and palate, partial amputation of the right arm, and a congenital scalp defect.

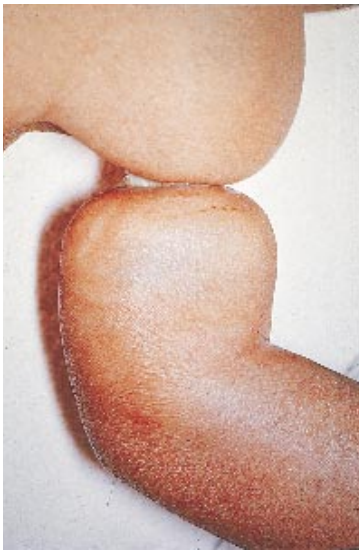

5.84

Figure 5.84. In the same infant shown in Figure 5.83, note the amniotic band constriction down to the bone almost resulting in amputation of the right arm.

5.85

Figure 5.85. The same infant as in Figures 5.83 and 5.84 showing the congenital scalp defect in the occipital area. Note the strand of amnion attached to the defect.

5.86

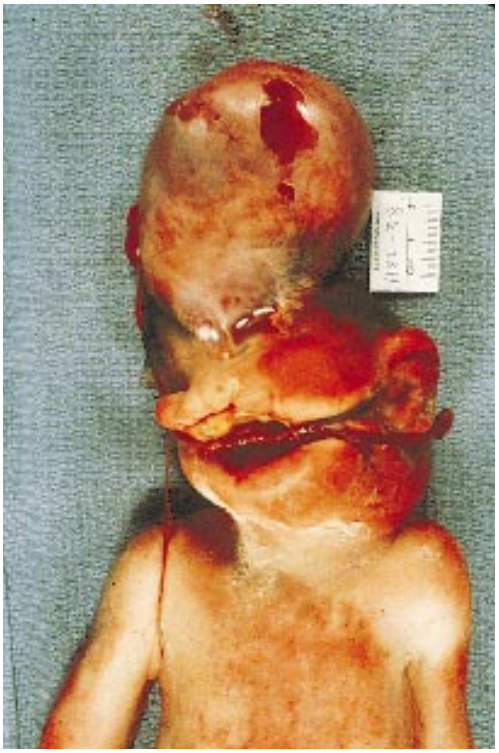

Figure 5.86. The early amnion rupture spectrum (TEARS) in this infant shows the bizarre findings involving the face and head. There is a skin defect of the scalp with an encephalocele and gross malformation of the face. The ADAM complex is an example of TEARS. The complex includes *A*mniotic *D*eformities, *A*dhesions, and *M*utilations. Findings in the ADAM complex include cleft lip, bizarre midfacial clefts, central nervous system abnormalities (hydrocephalus, microcephaly, asymmetric encephalocele), gastrointestinal abnormalities (omphalocele, gastroschisis), and ocular abnormalities (coloboma, anophthalmia, corneal opacity).

5.87

Figure 5.87. This infant is another example of the early amnion rupture spectrum. Note the asymmetric encephalocele in addition to the bizarre anomalies of the face and eye. In general, encephaloceles are midline and an asymmetric encephalocele is always suggestive of a disruption.

5.88

Figure 5.88. This infant with TEARS has bizarre facial clefting, a central nervous system defect, an abdominal wall defect, and limb defects.

5.89

Figure 5.89. A close-up of this infant showing the bizarre facial clefting and a strand of amnion extending from the right eye to the scalp defect. Also note the severe defect of the mouth and palate. In general, bizarre facial clefting (oblique facial clefting) is noted in disruptions whereas lateral or transverse facial clefts occur in infants with syndromes (e.g., Goldenhar's syndrome).

5.90

Figure 5.90. The same infant showing the abdominal wall defect (omphalocele) and strands of amnion extending from this to the central nervous system malformation.

5.91

Figure 5.91. The early amnion rupture spectrum caused a limb/body wall deficiency with spine and central nervous system defects in this infant. Note the hydrocephalus.

5.92

Figure 5.92. The limb/body wall deficiency in this infant caused a severe thoracoabdominal wall defect. Note the severe scoliosis and kyphosis and the short umbilical cord with the placenta attached to the abdominal viscera.

5.93

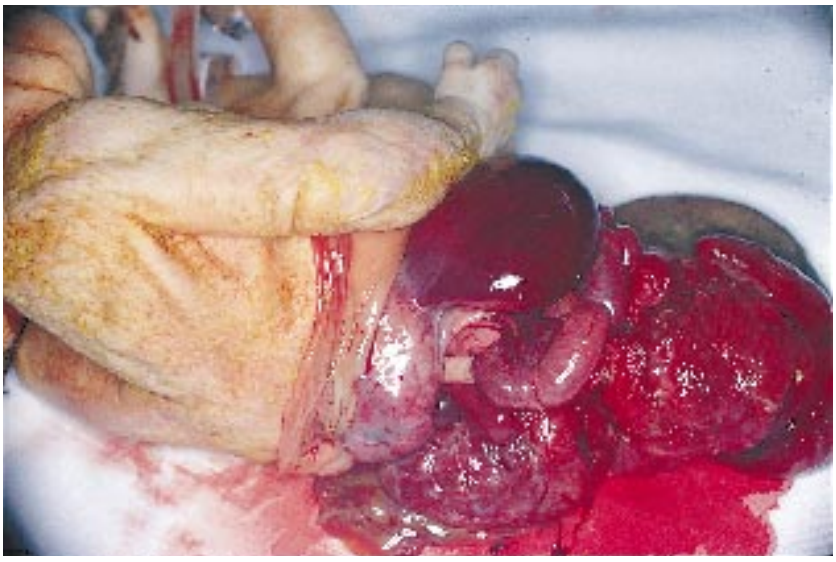

Figure 5.93. A close-up showing the right lung and the eviscerated abdominal organs with the placenta attached.

5.94

Figure 5.94. Another view showing the short umbilical cord.

5.95

Figure 5.95. In this infant with disruption, there is severe scoliosis and the placenta was attached to the right leg. The striking difference between this infant and the other examples of disruption is that this infant also had congenital malformations.

5.96

Figure 5.96. In the same infant, note that the disruption involved the lower extremities and the right hand but the infant also had an imperforate anus, lumbar spine defect and dextrocardia, plus a patent ductus arteriosus. Congenital anomalies include malformations, disruptions, and deformations. This figure should alert one to the fact that any combination of these can occur.

5.97

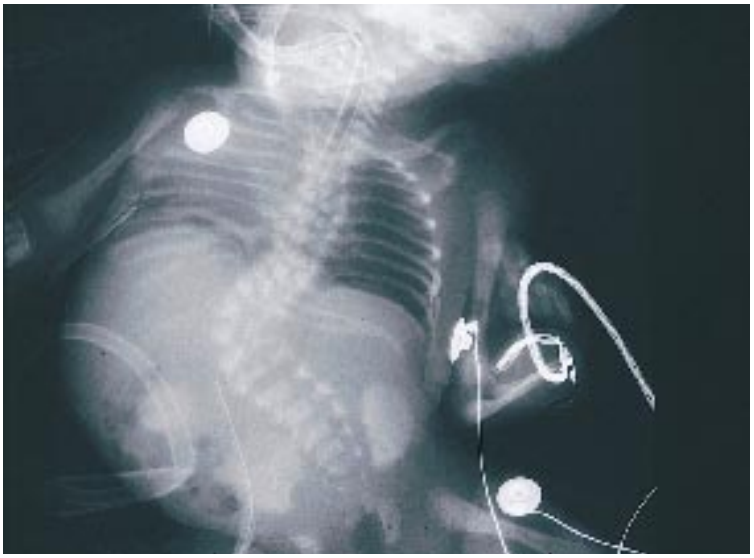

Figure 5.97. A radiograph of the same infant as in Figures 5.95 and 5.96 shows the dextrocardia, abnormalities of the ribs, and abnormal segmentation of the thoracolumbar vertebrae. In this infant the kyphosis and scoliosis was caused by both the malformation of the spine and the disruption.

5.98

Figure 5.98. The typical reduction sequence of limb reduction anomalies and scalp and skin defects are noted in this infant with Adams-Oliver syndrome.

5.99

Figure 5.99. Close-up of the skin defect of the abdominal wall in the same infant.

5.100

Figure 5.100. Close-up of the scalp defect in the same infant as in Figures 5.98 to 5.99.

5.101

Figure 5.101. The early amniotic rupture spectrum in an infant with a cervical meningomyelocele and an omphalocele. Note the amniotic band extending across the right shoulder. There was an amniotic band 1 cm proximal to the left ankle.

5.102

Figure 5.102. A close-up of the cervical meningomyelocele in the same infant. Note the amniotic band extending across the right shoulder.

5.103

Figure 5.103. A close-up of the amniotic tissue band over the right shoulder in the same infant as shown in Figures 5.101 and 5.102.

Chapter 6
Fetal Growth and Assessment of Gestational Age

The normal term infant has completed a gestation of ≥ 37 weeks and has a birth weight ≥ 2500 g. Accurate dating of pregnancy is important in evaluating the abnormally grown infant at birth. There are two different populations of low birthweight infants, those who are 1) born premature in gestation (i.e, at < 37 weeks); or 2) small for gestational age (SGA). Infants are SGA for one of two reasons: 1) a normal intrauterine environment but abnormal development due to fetal factors (i.e., chromosomal abnormalities); or 2) an abnormal uterine environment (i.e., maternal toxemia, heart disease, etc.) leading to abnormal growth.

Many criteria have been used to estimate gestational age. Obstetrical factors employed to determine age include date of last menstrual period, auscultation of fetal heart tones (audible by Doppler at 10 weeks, and stethoscope at 20 weeks), quickening (first maternal perception of fetal movement usually occurring at 18 to 20 weeks), and fundal height (used to estimate fetal size during the first trimester). Ultrasonography with first trimester measurements of crown-rump length accurately estimates gestation ± 3 days. Up to 30 weeks gestation, measurements of the fetal biparietal diameter, femur length, and abdominal circumference are a reliable index of fetal size (body weight) and gestational age, but afterwards may be quite variable. Physical examination may also be used in assessing gestational age. Gestational age only indirectly measures maturity, and other measurements are needed to determine organ-specific maturity (e.g., amniotic fluid lactase/sucrase ratio > 2 for fetal lung maturity).

6.1A

	6 months 28 weeks	6½ months 30 weeks	7 months 32 weeks	7½ months 34 weeks	8 months 36 weeks	8½ months 38 weeks	9 months 40 weeks
1. Posture	Completely hypotonic	Beginning of flexion of thigh at hip	Stronger flexion	Frog-like attitude	Flexion of the four limbs	Hypertonic	Very hypertonic
2. Head to ear maneuver							
3. Popliteal angle	150°		110°	100°	100°	90°	80°
4. Dorsiflexion angle of foot			40–50°		40–50°		Premature reached 40wk 40° Full term
5. 'Scarf' sign	'Scarf' sign complete with no resistance		'Scarf' sign more limited		Elbow slightly passes midline		Elbow almost reaches midline
6. Return to flexion of forearm	Upper limbs very hypotonic lying in extension			Flexion of forearms begins to appear, but very weak	Strong 'return to flexion.' Flexion tone inhibited if forearm maintained 30 seconds in extension	Strong 'return to flexion.' Forearm returns very promptly to flexion after being extended for 30 seconds	

Passive tone. Increase of tone with maturity illustrated by means of six clinical tests. (From Amiel-Tison, C.: Arch. Dis. Child.,*43*:89,1968.)

6.1B

Gestational age	32wk	34wk	36wk	38wk	40wk
Lower extremity	Brief support	Excellent straightening of legs when upright			
Trunk	–	+ –	Transitory straightening	Good straightening of trunk when upright	
Neck flexors	No movement of the head.	[face view] Head rolls on the shoulder	Brisk movement head passes in the axis of trunk	Head maintained for a few seconds	Maintained in axis for more than a few seconds
Neck extensors	Head begins to lift but falls down	[profile view] Brisk movement head passes in the axis of trunk	Good straightening but not maintained	Head maintained for a few seconds	Maintained in axis for more than a few seconds

Active tone. Increase of tone with maturity illustrated by means of four tests of righting reactions. (From Amiel-Tison, C.: *In* Gluck, L. (ed.), Modern Perinatal Medicine, Chicago, Year book Medical Publishers, 1974, p. 347.)

Figure 6.1A & B. Many scoring systems have been devised to assess by exam the gestational age of infants at birth. The originals are shown here in figures A & B, published by Amiel-Tison. The Dubowitz examination is one of the most complete systems, combining the general physical examination performed in the first hours of life with the neurologic evaluation carried out when the infant is at least 24 hours old. The Ballard Method abbreviates the Dubowitz scoring system and uses only 12 physical and neurologic criteria. Statistically, however, the Ballard is as accurate in assessing gestation age (± 2 weeks) as more thorough examinations and is most useful in the busy clinical setting.

6.2

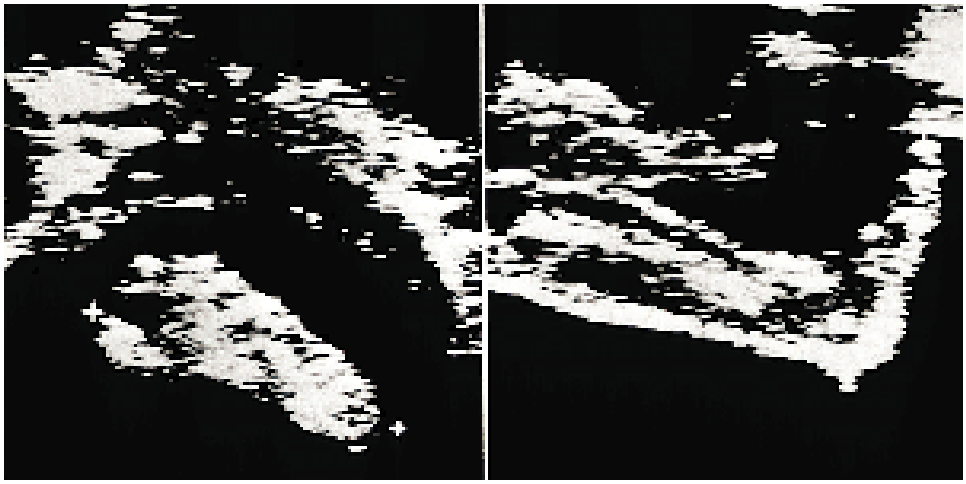

Figure 6.2. A prenatal ultrasound examination showing a view of a foot. Foot length on prenatal ultrasound has been shown to correlate well with gestational age.

6.3

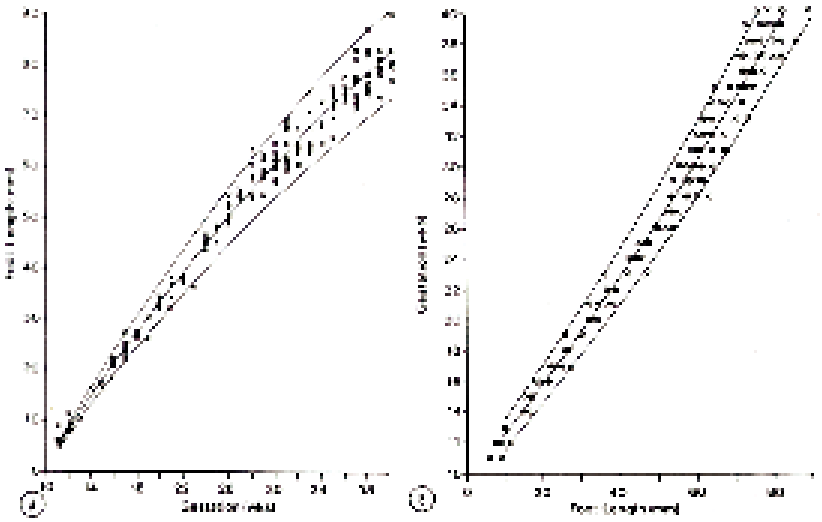

Figure 6.3. Graphic representation of the correlation between fetal foot length and gestational age. (Mercer et al. Scatter plots of ultrasonic feetus. gestational age. AM J Obstet Gynecol 1987; 156:350 Mosby Year Book, used with permission)

6.4

Figure 6.4. The premature infant has a large head in relation to body size and the eyes are protruding due to disproportion between the size of the eyeballs and the orbital cavity. The skin is red to pink, shiny due to edema, transparent with highly visible arterioles and venules, and is covered by lanugo. Subcutaneous tissue is poorly developed. Scalp hair is sparse and straight. Vernix is not formed and no nipples or areolae are seen. Note that the infant lies flat on the bed, in a frog-leg position with shoulders, elbows, and knees all touching the mattress. The head is to one side or other, not in line with the trunk.

6.5

Figure 6.5. The postmature infant appears long and skinny due to decreased subcutaneous fat stores with advancing gestation near term. The skull is hard because the sutures have started to fuse. Note the wizened facies and alert expression typical of the post-term baby. These infants tend to be wakeful and have desquamation of the skin. The hands are like a washerwomen's, dry and wrinkled, with long fingernails. Meconium staining may be seen on the umbilical cord and fingernails more commonly in the post-term infants.

6.6

Figure 6.6. When a fetus is undergrown due to intrauterine dysfunction, the sequence begins with loss of fat and muscle mass as noted in this growth-retarded infant. This is followed by loss of mass of less essential organs (liver, thymus, spleen, adrenals), loss of mass of more essential organs (heart), and finally loss of brain mass. If head circumference is compromised, it indicates that malnutrition must have been very severe, and it carries a poor prognosis.

6.7

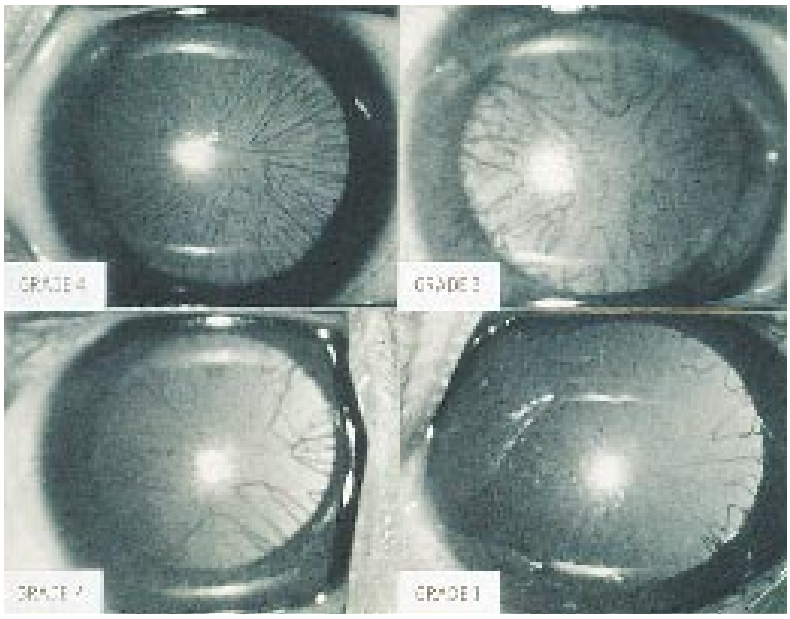

Figure 6.7. Two systems are useful clinically to determine gestational age by examination of the eye. First, examination of the anterior eye for the presence of the tunica vasculosa lentis, apparent generally from 27 to 34 weeks. Note in this composite figure the tunica vasculosa lentis Grade IV at 27 to 28 weeks completely covers the anterior surface of the lens and then gradually decreases to Grade I by 33 to 34 weeks when only peripheral remnants of the vessels are visible on the anterior surface of the lens.

6.8

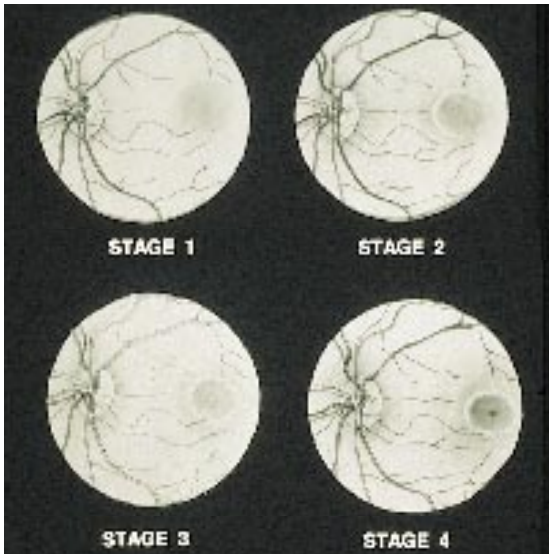

Figure 6.8. The second system used to determine gestational age involves examination of the fundus to assess macular development from 34 weeks to term. This composite figure shows Stage I – dark red pigmentation appearing, 34 to 35 weeks gestation; Stage II – the annular reflex is partially evident, 36 weeks gestation; Stage III – the complete annular reflex is present, 37 weeks gestation; Stage IV – the foveolar pit can be seen, 38 weeks gestation.

6.9

Figure 6.9. Because calcium is preferentially deposited in the last few weeks before birth, the stiffness of the baby's ear cartilage provides another test of maturity. In premature infants, the ear cartilage is deficient and the soft pinna does not spring back. On release it remains crumpled against the side of the head. At term the cartilage is more rigid similar to the adult ear.

6.10

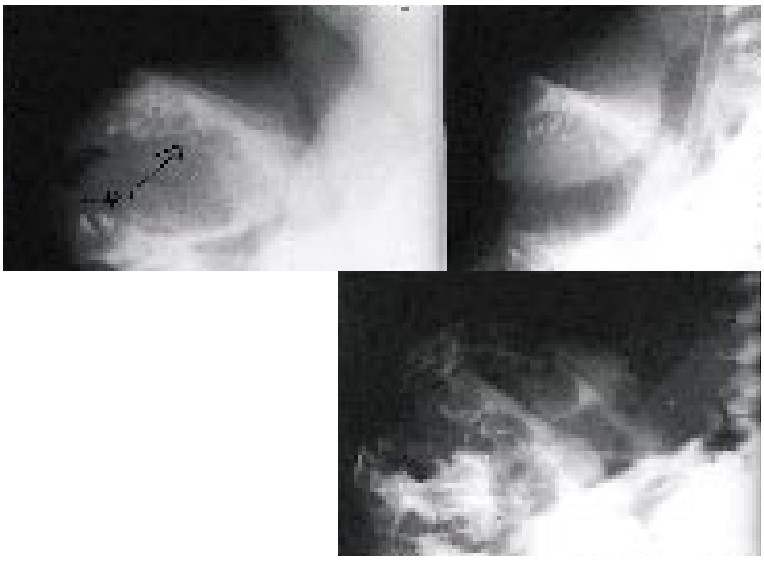

Figure 6.10. The presence of teeth seen by radiography in the jaw is a relatively accurate method of assessing gestational age. In the figure on the top left, incisors and cuspids have appeared but no molars, indicating a gestational age of less than 33 weeks. In the top right is shown the appearance of incisors and first deciduous molars consistent with 33 to 37 weeks gestation. On the bottom, the second deciduous molar and follicle of first permanent molar are present, indicating a gestation of greater than 37 weeks. This method is not useful in assessing infants with anhydrotic ectodermal dysplasia who have adentia.

6.11

Figure 6.11. Hair, particularly on the head, is a reliable marker of maturity. Premature hair is fuzzy and the hair ends tend to clump together. In the term infant the hairs are distinct, coarse and silky. Lanugo is absent prior to 20 to 22 weeks gestation, but by 30 to 32 weeks becomes diffuse over the body. By term, lanugo has mostly disappeared. There are marked racial differences among babies with respect to lanugo characteristics. Hispanic infants, in general, have considerably more body hair persisting to term and black infants often have less than average lanugo.

6.12

Figure 6.12. The breast analog does not respond to hormonal stimulation until near the 35th week and thus the size of the nodule can be correlated with development. Before 34 weeks the nipple and areola are identifiable, although they are immature-looking and non-pigmented. Between 34 and 36 weeks the nipple becomes erectile and a small nubbin of breast tissue can be felt under the areola. By 36 to 38 weeks, there is usually a palpable nodule and, by term, the nodule has enlarged to 5 to 10 mm in size.

6.13

Figure 6.13. In the preterm male infant the testes are undescended and the scrotum empty, as pictured here. In the preterm female infant the clitoris is relatively large, and the vulva gapes due to separation of the labia majora and minora.

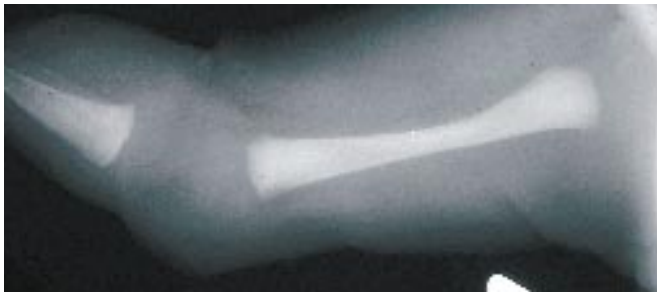

6.14

Figure 6.14. Looking for epiphyseal centers in long bone radiographs is useful in the assessment of gestational age. The lower extremity radiographs show the proximal tibial epiphyseal center, which generally appears by 36 weeks gestation, being followed by the distal femoral epiphyseal center at 38 weeks gestation. In this patient no epiphyseal centers are seen, consistent with the infant's gestational age of 35 weeks. Conditions that may alter the normal appearance of the centers include hypothyroidism, congenital viral infections, and congenital syphilis.

6.15

Figure 6.15. At 30 weeks or less the soles of the baby's feet are smooth. At 34 weeks, creases have started to appear on the anterior third of the plantar surface. By term, the entire plantar area is noticeably creased. In the post-term infant shown here, the soles show excessive creasing on the plantar surface together with dry peeling skin.

6.16

Figure 6.16. Meconium staining, as noted in this post-term infant, is a potential sign of fetal distress and is more common in the post-term infant. Meconium staining of the fingernails, as noted in this figure, suggests exposure to meconium of at least 4 to 6 hours, duration. Presence of meconium in the amniotic fluid may be helpful in assessing gestational age. In general, the fetus does not pass meconium before 34 weeks gestation; hence, the presence of meconium may either increase the estimated gestation of a premature infant or suggest that other causes of discolored amniotic fluid (such as *Listeria monocytogenes*) be considered.

6.17

Figure 6.17. Meconium staining of the umbilical cord of the same post-term infant.

Chapter 7
Iatrogenesis

All interventions, whether intended as therapy or as monitoring, are inherently invasive and therefore have associated risks. The task of weighing risks and benefits would be simple if both were quantitatively known. Estimating the frequency of complications is difficult except for the most frequent and even those vary widely. Complications due to mechanical trauma, accidents, technique errors, or faulty equipment are potentially preventable. Complications due to interaction of the intervention with the patient (e.g., infection, thrombosis) may not be preventable until new techniques, equipment, or methods are developed. This section provides a catalogue of complications associated with intensive care in the neonate. Clinicians must continue to be vigilant and mindful of potential iatrogenic complications so that these problems may be prevented when possible and otherwise rapidly recognized and managed.

7.1

Figure 7.1. Ultrasound examination of the abdomen of a pregnant mother (gestational age 35 weeks) who was shot with a BB gun. Note the shadow from the BB pellet located in the soft tissue above the fetal femur. (Moise, K.)

7.2

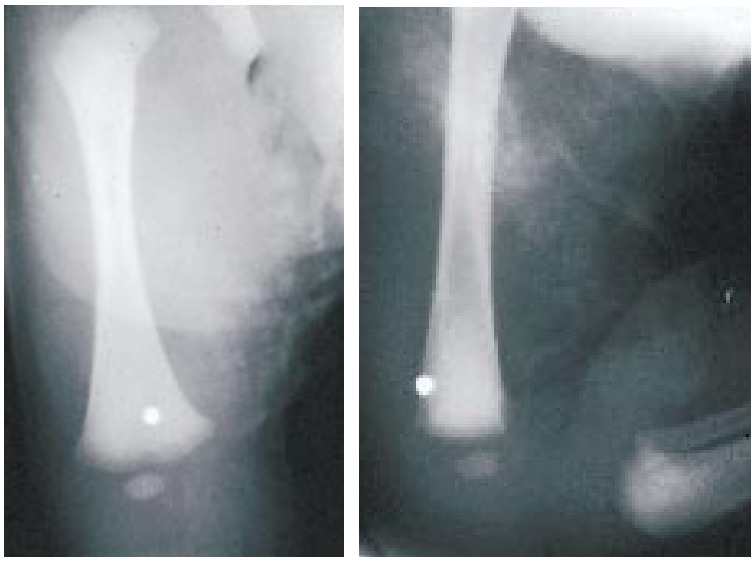

Figure 7.2. After delivery of the infant, radiography showed the presence of the BB pellet at the distal end of the femur. The infant had a normal course.

7.3

Figure 7.3. This infant developed swelling and some erythema over the frontal area. Radiography of the skull shows periosteal elevation of the frontal bone. This resulted from the application of a fetal scalp electrode.

7.4

Figure 7.4. Skin incisions on the buttocks of an infant delivered by cesarean birth. It is not uncommon for infants to have iatrogenic trauma, such as facial abrasions from forceps delivery, and trauma from diagnostic-therapeutic procedures such as amniocentesis. (Landers, S.)

7.5

Figure 7.5. Circular lesions on the back of an infant as a result of skin burns from a faulty transcutaneous pO_2 electrode. With the advent of pulse oximetry the transcutaneous electrodes are rarely used nowadays.

7.6

Figure 7.6. Purpuric lesions on the chest of a very small premature infant following vigorous physiotherapy.

7.7

Figure 7.7. Hypopigmentation of the skin of the lower abdomen as a result of scarring from application of tape in the newborn intensive care unit. Trauma to the skin from adhesive tape is not uncommon, especially in very low birth weight infants. The hypopigmentation improves over time. (Landers, S.)

7.8

Figure 7.8. This infant developed necrosis and discoloration of the toes as the result of burns from the heater in an incubator at the time Gordon-Armstrong incubators were in use for management of premature infants. In our nursery, several infants developed burns over a short period of time. It was determined that the physician examining the infant would place the infant on top of the incubator and the burn would result from contact with a metallic instruction guide which was normally present on the incubator cover. Once the cause was determined, this problem was eliminated. The reason for including a historic figure is that in care and management of a sick neonate one should always be on the alert for possible iatrogenic problems.

7.9

Figure 7.9. Percutaneous alcohol absorption with resultant erythema and burns to the buttocks of a premature infant. During placement of an umbilical arterial catheter, alcohol or iodine may track down the sides of the abdomen and soak the underlying sheet. Evaporation is restricted from the skin in contact with the underlying sheet and this may result in irritation, erythema, and severe burns, especially in a premature infant with very sensitive skin.

7.10

Figure 7.10. In this premature infant with a birth weight of 1000 g and severe hyaline membrane disease, it was elected to do medical management of the omphalocele. Mercurochrome was applied three times a day to the sac of the omphalocele as a topical solution. Treat-ment with organic mercurial antiseptics is controversial, since infants may develop potentially toxic levels of mercury because of the reduced skin barriers. The infant developed acute mercurial poisoning with the typical findings of acrodynia. Other preparations, such as silver nitrate, hexachlorophene, etc., have also been used with success in medical management of an omphalocele. One should always be on the alert for problems which may arise from excess absorption.

7.11

Figure 7.11. Decubitus ulceration of the back of the neck of an infant who was placed in the supine position and was on muscle relaxants for 8 days while being treated for septic shock. This stresses the importance of nursing care in these infants. (Landers, S.)

7.12

Figure 7.12. This infant had a lumbar puncture performed to exclude possible meningitis. Four days later these nodular erythematous lesions developed on the back over the sites of the lumbar puncture attempts. The lesions were those of subcutaneous fat necrosis. The possibility of infection should remain in the differential diagnosis.

7.13

Figure 7.13. Slightly fluctuant erythematous midline back lesion in an infant with a staphylococcal abscess following lumbar puncture.

7.14

Figure 7.14. Appearance of the heels of a low birth-weight premature infant after repeated "heel-sticks." This can be avoided by warming of the heel and more gentle squeezing of the heel when collecting blood. Miscalculation of the water temperature when warming a heel may cause scalding and a skin burn. (Landers, S.)

7.15

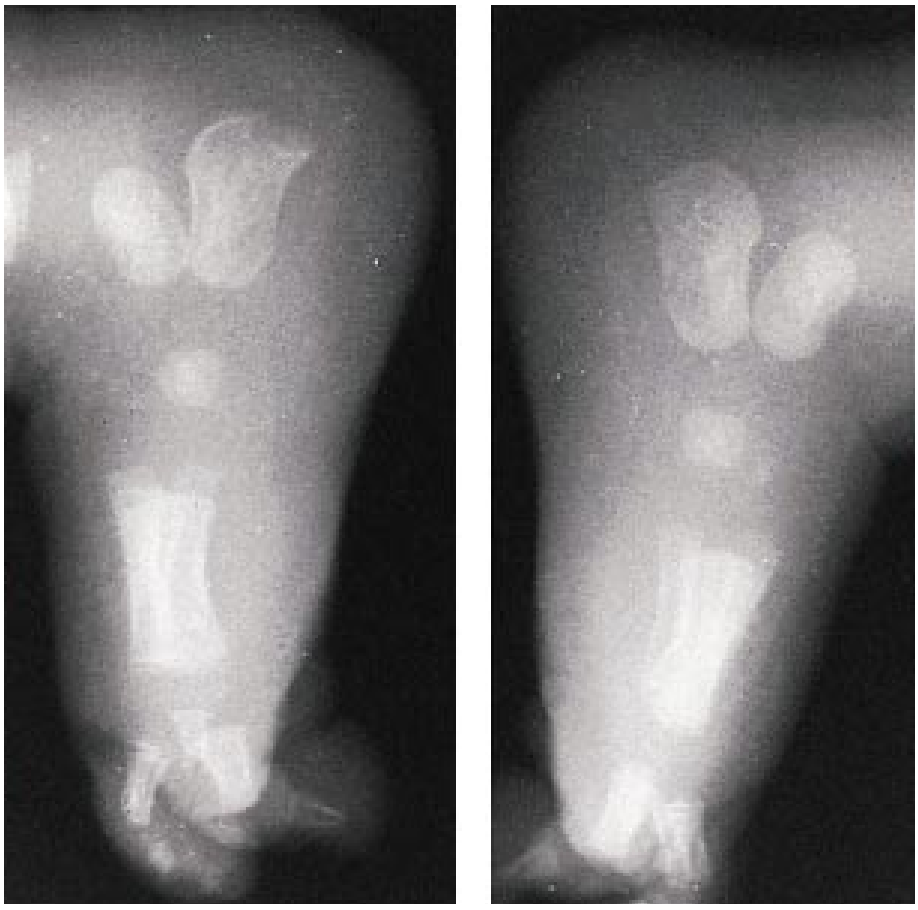

Figure 7.15. Radiograph of the feet of an infant with osteomyelitis of the calcaneus (on the left) following "heel-stick" trauma. The other heel is normal (on the right). One of the most common methods in infants of collecting laboratory blood specimens for analysis is by "heel-stick."

7.16

Figure 7.16. Radiograph of an infant with a spiral fracture of the distal end of the tibia. This fracture is the result of increased angulation with force applied by a technician collecting a "heel-stick" blood specimen. On the left, note the fresh fracture. On the right, note the healing fracture 3 weeks later. This infant had congenital syphilis. On initial radiographs there were growth arrest lines in the proximal tibia and distal femur, but the tibia was otherwise normal.

7.17

Figure 7.17. Edema, bullous excoriation and discoloration of the foot of an infant following dislodgment of the needle from an infusion pump. Ulceration due to extravasation of intravenous infusion fluid may follow subcutaneous leakage of any hypertonic solution, but those containing calcium are particularly irritating.

7.18

Figure 7.18. Soft tissue infiltration following continuous infusion with a needle displaced out of the vein. If these areas are large, they may subsequently require a skin graft.

7.19

Figure 7.19. Calcification of the scalp veins following intravenous infusion of sodium bicarbonate and calcium gluconate. Deep areas of necrosis may occur following infiltration from intravenous solutions containing calcium.

7.20

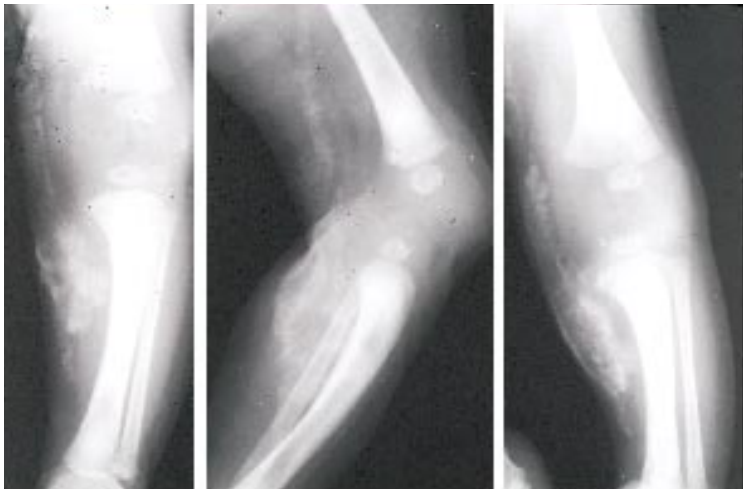

Figure 7.20. Radiographic series of an infant's leg with soft tissue and intravascular calcifications. This infant received calcium gluconate through a "cut-down" in the ankle. There are two patterns of calcification: amorphous ("bulky") and vascular (going up through the thigh).

7.21

Figure 7.21. Soft tissue swelling and erythema in this infant with *Staphylococcus aureus* bacteremia and abscess. Abscess formation can occur frequently alone or in association with bacteremia at old venipuncture sites.

7.22

Figure 7.22. Infant with staphylococcal scalp infection following scalp vein infusion.

7.23

Figure 7.23. This scalp defect occurred as the result of a staphylococcal infection with an underlying osteomyelitis of the skull.

7.24

Figure 7.24. Transillumination of the scalp of an infant following infiltration of fluid from an intravenous scalp infusion. Extravasation of fluid in the scalp or scalp edema will transilluminate.

7.25

Figure 7.25. Hypopigmentation, alopecia and scarring on the scalp of a former very low birth weight premature infant (birth weight 700 g) following multiple scalp vein infiltrations.

7.26

Figure 7.26. Scalp infiltration of total parenteral nutrition fluid and intralipid in an infant at the age of 7 days. This healed without residual hypopigmentation or scarring.

7.27

Figure 7.27. Soft tissue nonerythematous swelling of this infant's right side of neck, arm and chest occurred as the result of extravascular extravasation of central total parenteral nutrition. Note the facial palsy on the left side.

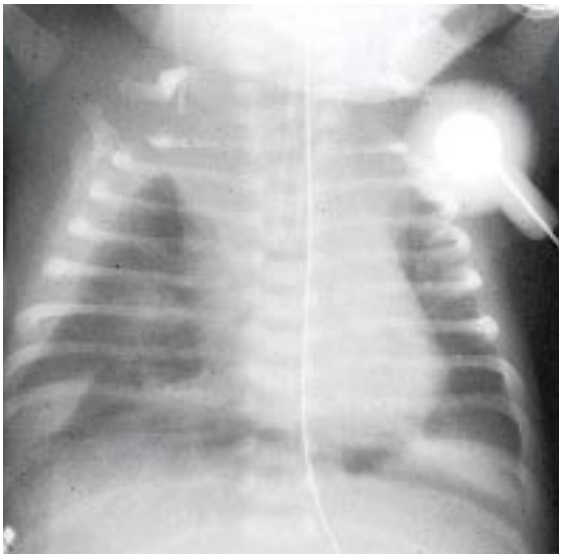

7.28

Figure 7.28. In this radiograph of the neck and chest, note the right-sided soft tissue swelling in the neck, a widened mediastinal shadow, and a large pleural effusion. These findings are the result of perforation of the vein by the central total parenteral nutrition catheter.

7.29

Figure 7.29. Patchy discoloration of the skin of an infant as the result of a bolus infusion of Prostaglandin E.

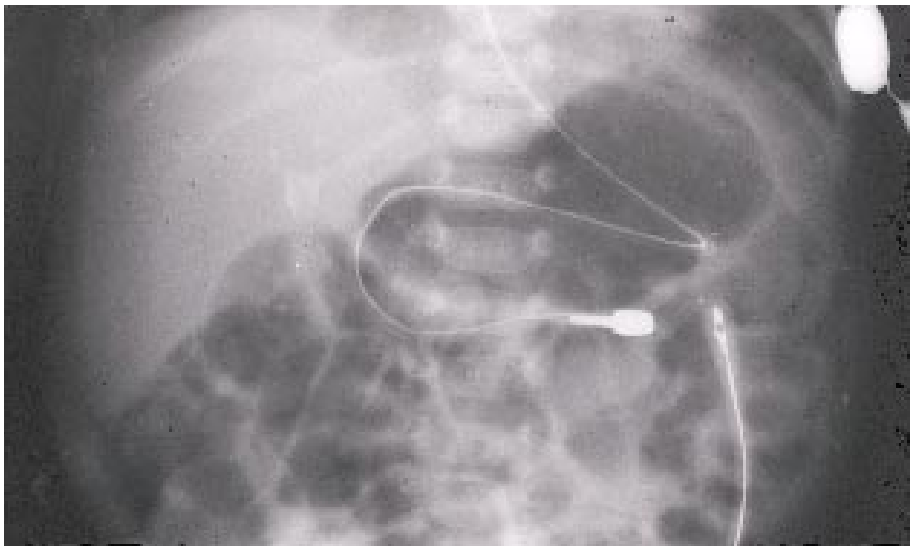

7.30

Figure 7.30. Abdominal radiograph of an infant with a gold-tip transpyloric feeding tube. Note the right upper quadrant vascular calcification of the portal vein. This is the result of sodium bicarbonate and calcium gluconate infusion given together through an umbilical venous catheter.

7.31

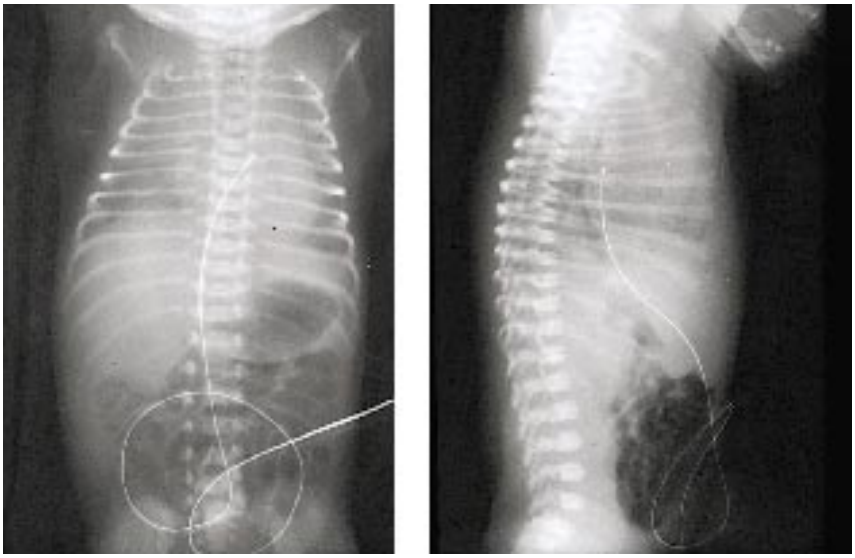

Figure 7.31. Anteroposterior and lateral radiographic views of an umbilical venous catheter placed high in the heart. It is possible to sample oxygenated left atrial blood when the catheter passes across the patent foramen ovale.

7.32

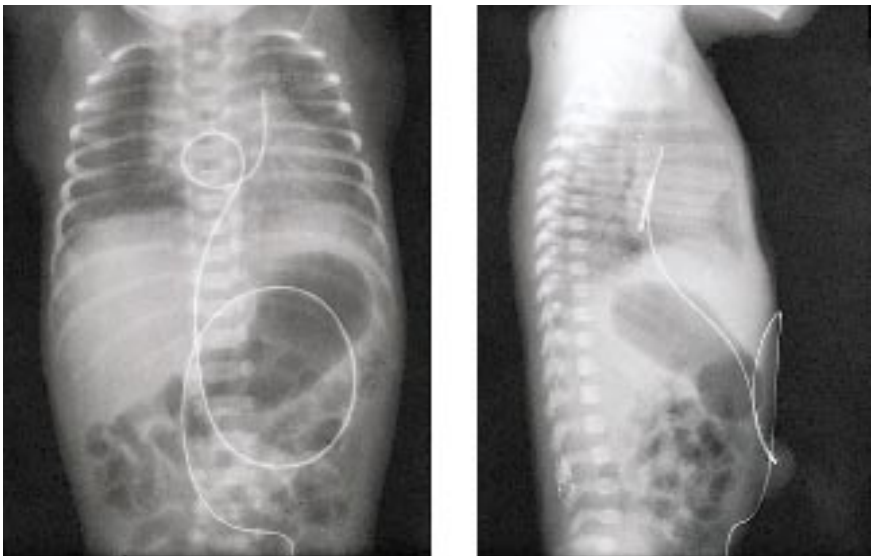

Figure 7.32. Anteroposterior and lateral radiographic views of an infant with an umbilical venous catheter placed in the left pulmonary artery. The previous figure and this figure stress the importance of checking placement of umbilical catheters following their insertion. When they are placed in such abnormal positions they should be withdrawn.

7.33

Figure 7.33. Chest and abdominal radiograph of an infant after placement of an umbilical venous catheter. Note the placement of the catheter in the liver with air outlining the portal venous system.

7.34

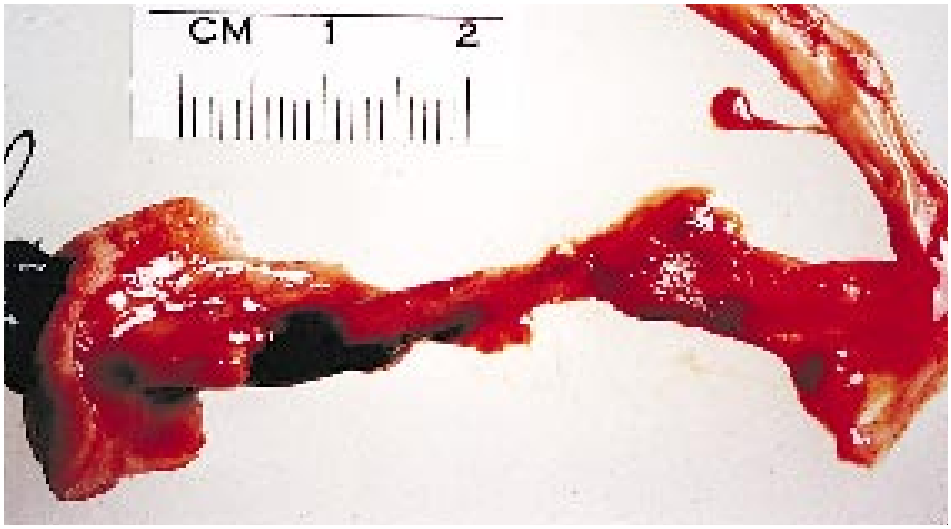

Figure 7.34. Autopsy specimen of the umbilical vessels with umbilical vein perforation from a catheter during umbilical vein placement.

7.35

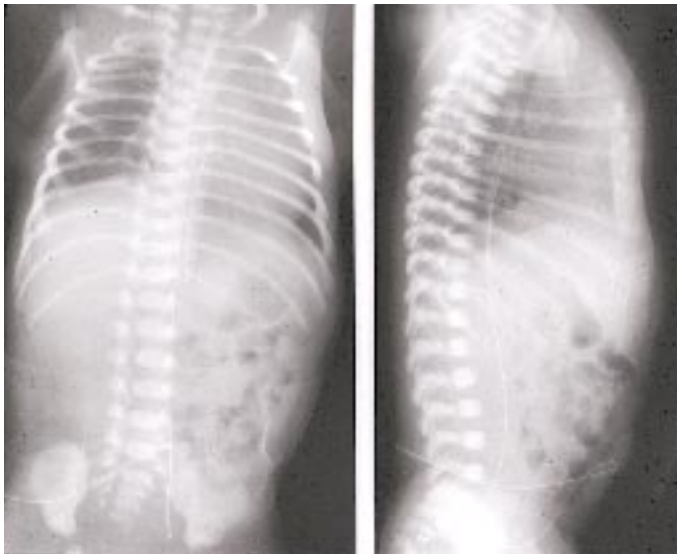

Figure 7.35. Anteroposterior and lateral radiographs in an infant showing an umbilical artery catheter which is placed high in the thoracic aorta curving on itself.

7.36

Figure 7.36. Anteroposterior and lateral radiographs of the same infant showing repositioning of the umbilical artery catheter after its initial high aortic placement. These follow-up films show the location of the catheter in the superior mesenteric artery. The infant developed abdominal distention and vomiting and had a large segment of gangrenous bowel which was removed.

7.37

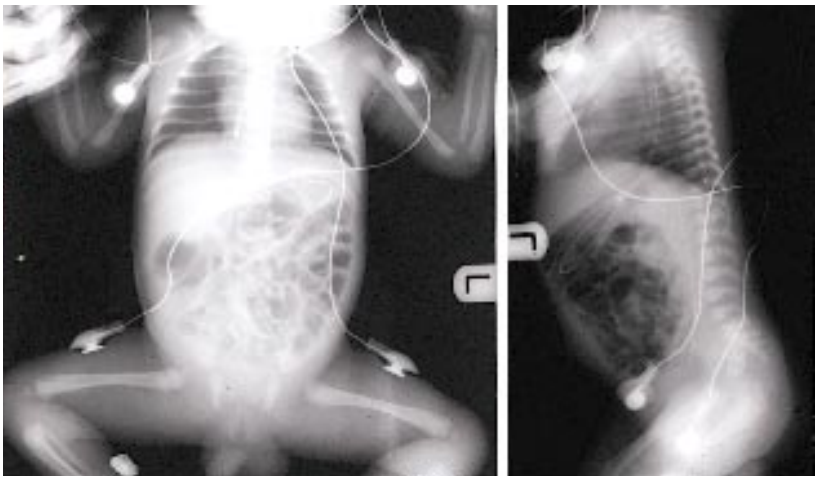

Figure 7.37. Anteroposterior and lateral radiographic views of a "free," broken umbilical artery catheter lying in the abdominal and thoracic aorta. The catheter broke at the insertion site during planned removal. The remaining catheter had to be surgically removed.

7.38

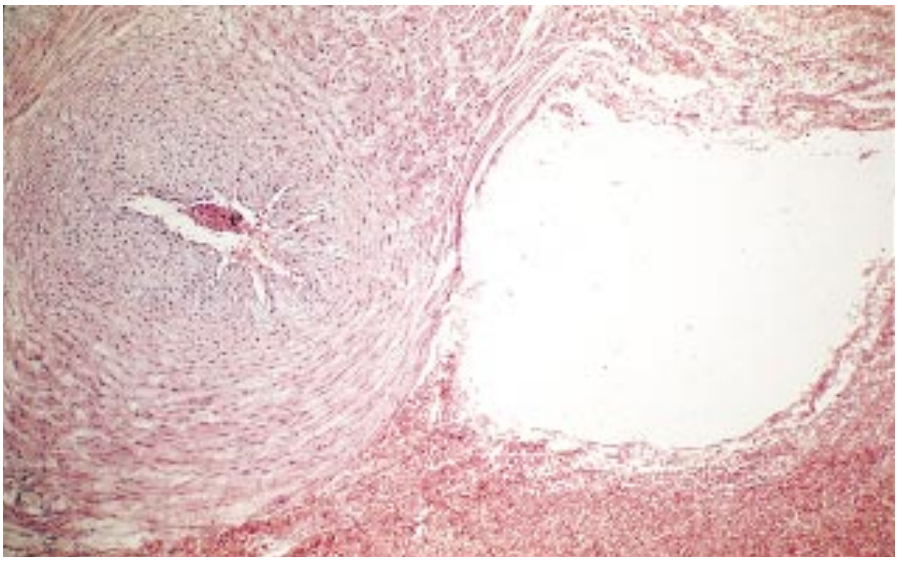

Figure 7.38. Histologic view showing on the left the umbilical artery and on the right the juxtaposed "false" catheter passage. The possibility of creating a false passage should always be considered when there is difficulty with placement of an umbilical catheter.

7.39

Figure 7.39. Discoloration of the great toe and little toes of the left foot in this infant followed umbilical artery catheter placement. With removal of the catheter, vasospasm subsided with subsequent normal circulation and appearance. Umbilical artery catheterization may be associated with thrombotic complications.

7.40

Figure 7.40. On the left, note the discoloration of the toes in an infant 4 hours after placement of an umbilical arterial catheter. There was no significant improvement after catheter removal. On the right, note the gangrenous and atrophied appearance of the same foot 15 days later.

7.41

Figure 7.41. Severe atrophy and gangrene of the left lower extremity in an infant as a result of umbilical artery catheter placement. This can occur as a result of vasospasm or clot formation in a major vessel with inadequate collateral support in a very low birthweight infant.

7.42

Figure 7.42. Discoloration and necrosis of the buttocks as a result of umbilical artery catheter placement in an infant at the age of 4 days. This occurs from spasm and thrombosis of the internal obturator artery which supplies the muscles of the buttock. Intra arterial injection of alkali may also be followed by gangrene of the buttock.

7.43

Figure 7.43. Discoloration with gangrene of the right buttock following umbilical artery catheter placement.

7.44

Figure 7.44. The same infant 10 days later showed marked improvement of the buttock.

7.45

Figure 7.45. Gangrene of the left buttock following umbilical artery catherization. The umbilical artery catheter was positioned in the iliac artery radiographically. There is a well-known association between injection of medications into the umbilical artery and necrosis and gangrene of the buttock and sciatic nerve palsy.

7.46

Figure 7.46. The same infant with unilateral gangrene of the buttock also had a sciatic nerve palsy as a result of the umbilical catheter being positioned in the iliac artery. Note the "foot drop."

7.47

Figure 7.47. Radiograph of the lower extremities in an infant with leg length discrepancy. The soft tissue mass and bone growth of the left leg are decreased in comparison to the right. These postnatal changes were the result of femoral artery thrombosis after umbilical artery catheter placement.

7.48

Figure 7.48. Placement of an umbilical artery catheter was difficult in this infant. On the first and second attempts the catheter went down each leg. On the third attempt the catheter was placed in the aorta. It remained in place for 4 hours when blood was noted in the urine and the legs were both noted to have some discoloration.This figure shows the status 19 hours after the catheter was removed. The infant continued to improve.

7.49

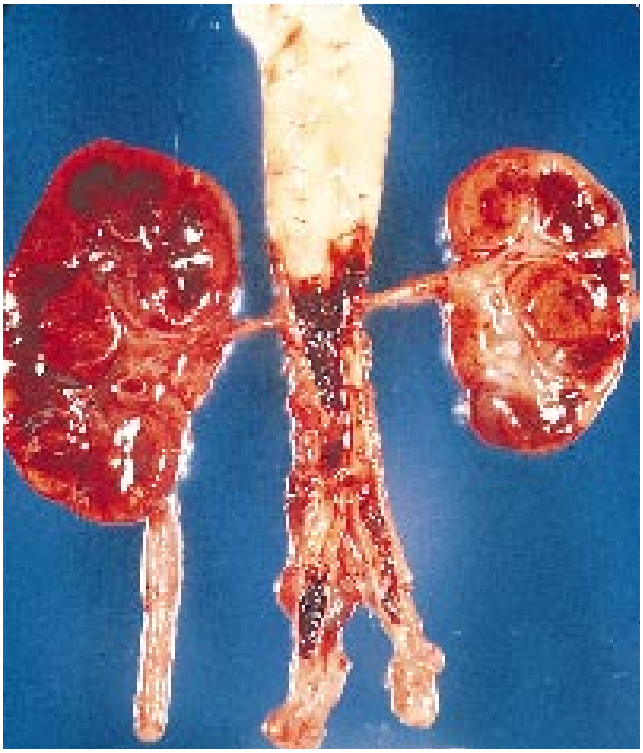

Figure 7.49. Autopsy specimen demonstrating thrombosis involving the aorta, iliac arteries and renal arteries following umbilical artery catheterization at birth. The infant died at the age of 12 days.

7.50

Figure 7.50. Autopsy specimen of the aorta with periumbilical artery catheter thrombosis.

7.51

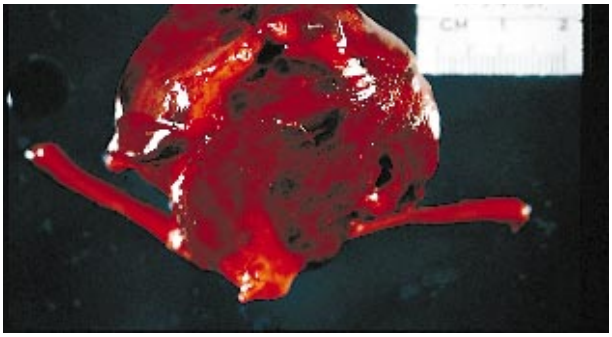

Figure 7.51. Autopsy specimen of the bladder. Note the engorged hemorrhagic bladder wall which was the result of an umbilical artery catheter perforation.

7.52

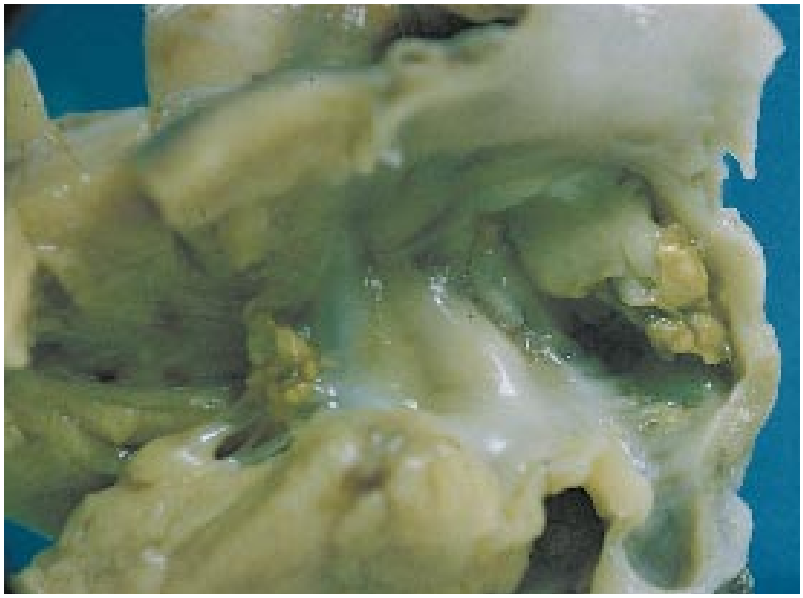

Figure 7.52. Autopsy specimen of the heart in an infant who developed vegetations as a result of prolonged umbilical venous catheter placement. Note the verrucous vegetations due to staphylococcal endocarditis.The condition was diagnosed antemortem by echocardiography. In cases of prolonged sepsis in small premature infants, the diagnosis of endocarditis should always be excluded.

7.53

Figure 7.53. Gangrene resulting in amputation of the right arm following an infusion of 10% dextrose in the right radial artery.

7.54

Figure 7.54. This infant developed obstruction to the circulation of the distal right forearm and hand following attempts at right radial artery catheterization. Subsequently, a cut-down was placed in the right brachial artery, resulting from thrombosis. Note the white discoloration and atrophy of the hand and distal forearm with gangrene of the distal fingertips. A sharp demarcation line separated the normal from the abnormal circulation.

7.55

Figure 7.55. Close-up of the right hand of the same infant 2 weeks later shows the atrophy and gangrene of the right hand.

7.56

Figure 7.56. The same infant, in addition to the thromboses, had embolization from the same site which resulted in discoloration and impaired circulation of the right lower extremity. This improved.

7.57

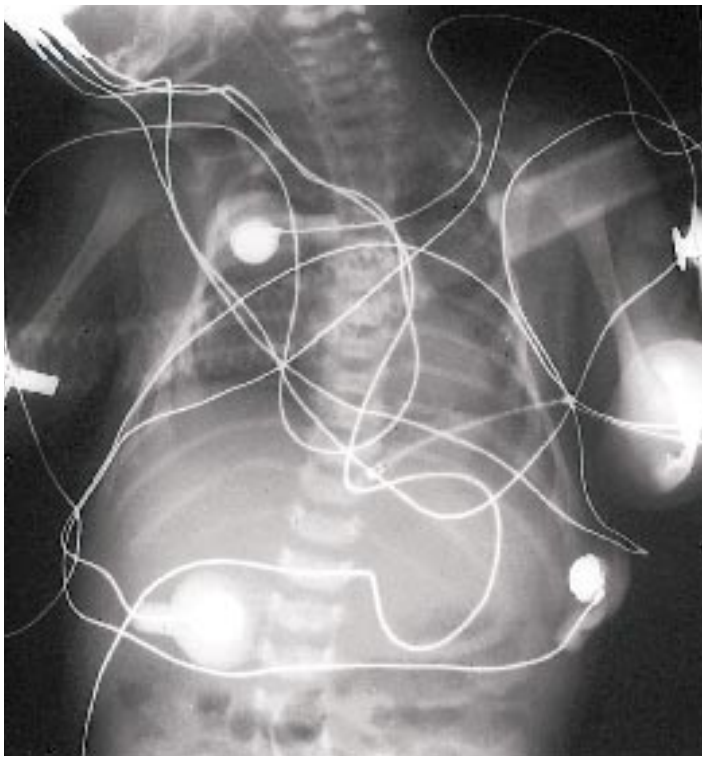

Figure 7.57. Radiograph of the chest of an infant admitted to the neonatal intensive care unit. Note the excessive neonatal equipment interfering with evaluation of the status of any cardiorespiratory pathology. When doing radiographic evaluation it is extremely important that an attempt be made to clear all the excess tubes and leads to obtain as clear a field as possible.

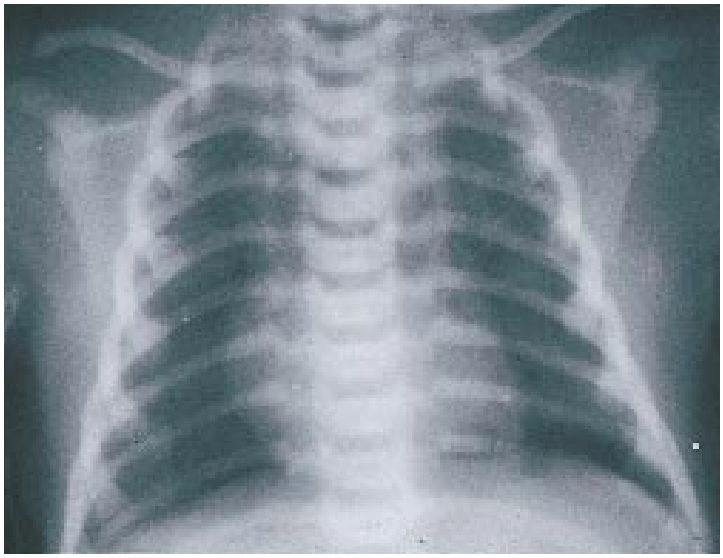

7.58

Figure 7.58. Radiograph of the chest of an infant with a translucent circular mediastinal shadow. If the radiograph is taken through the top of the incubator, it may give artifactual shadows such as this one caused by the hole in an Isolette™ .

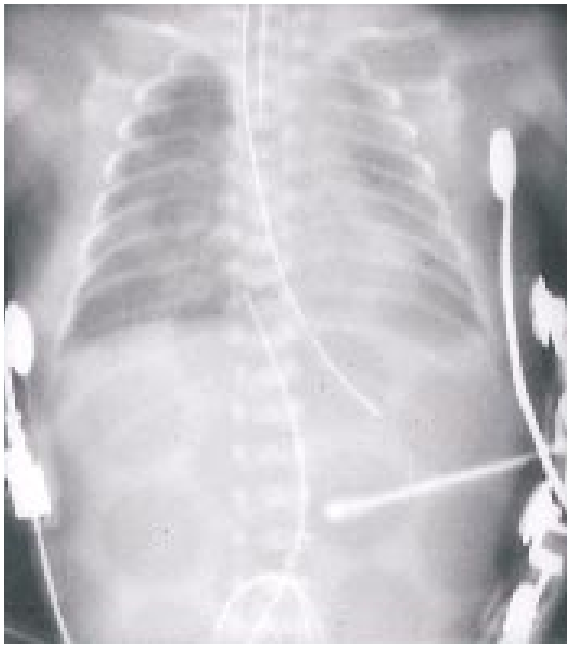

7.59

Figure 7.59. Radiograph of chest and abdomen showing artifactual shadows from placement of the infant on an air mattress. It is important to be aware of these possible artifacts when reviewing radiographic films.

7.60

Figure 7.60. An infant with respiratory distress developed acute deterioration. It was noted that there was poor movement of air into the lungs. On removing the nasotracheal tube a blood clot was found to be obstructing the tube. With replacement of the tube there was rapid improvement.

7.61

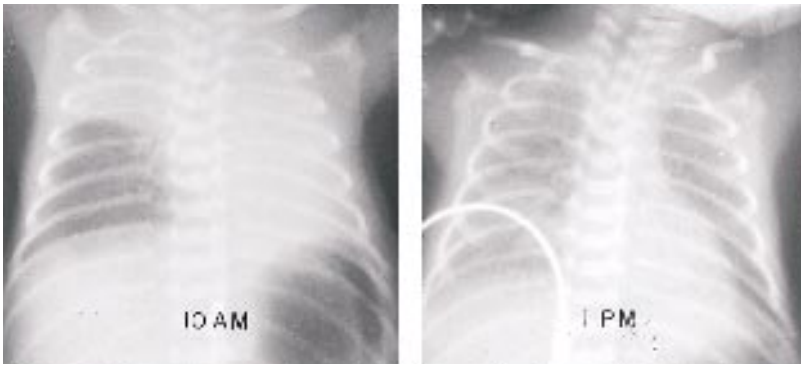

Figure 7.61. Serial chest radiographs of an infant with left lung and right upper lobe opacification as the result of right mainstem bronchus intubation (left). After repositioning the endotracheal tube there was rapid resolution of the atelectasis (right).

7.62

Figure 7.62. Lateral view of the chest and abdomen in an infant who has a "swallowed endotracheal tube." Note that the endotracheal tube is a cuffed tube which is rarely used at the present time. During resuscitation instead of endotracheal intubation the esophagus was inadvertently intubated and the tube was swallowed. This was successfully removed without any complication.

7.63

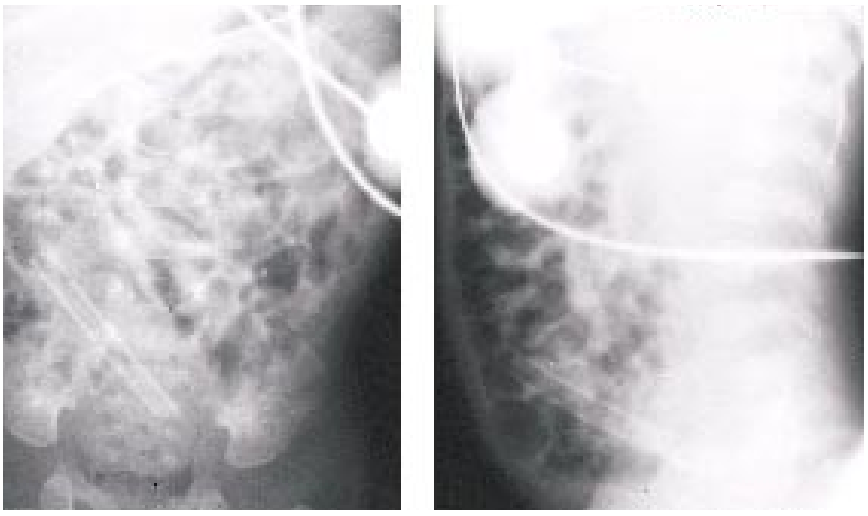

Figure 7.63. Abdominal radiographs of an infant who "swallowed a nasal CPAP tube." The tube was recovered in the stool 11 days later. (Singleton, E.)

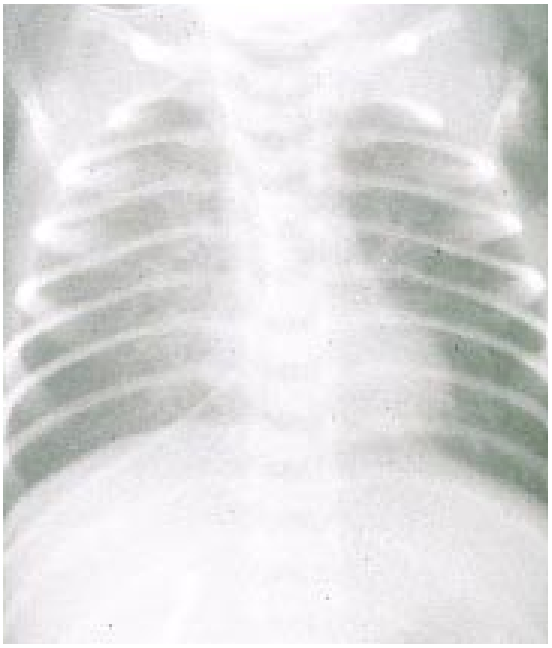

7.64

Figure 7.64. This infant developed increasing respiratory distress. Radiography of the chest showed abnormal placement of the feeding tube that tracks into the right thorax. Associated with this are increased infiltrates, most prominent in the right lung. The abnormal placement of the feeding tube occurred as a result of esophageal perforation.

7.65

Figure 7.65. Radiograph of the chest of the same infant 24 hours later showing a right-sided pneumothorax and placement of the nasogastric feeding tube in the left thorax as the result of esophageal perforation. It should be noted that the feeding tube may pass either to the right or left side of the chest. Spontaneous perforation of the esophagus (Boerhaave's syndrome) does occur, but would be extremely rare in a neonate. Neonatal perforation is usually associated with trauma such as from a feeding tube.

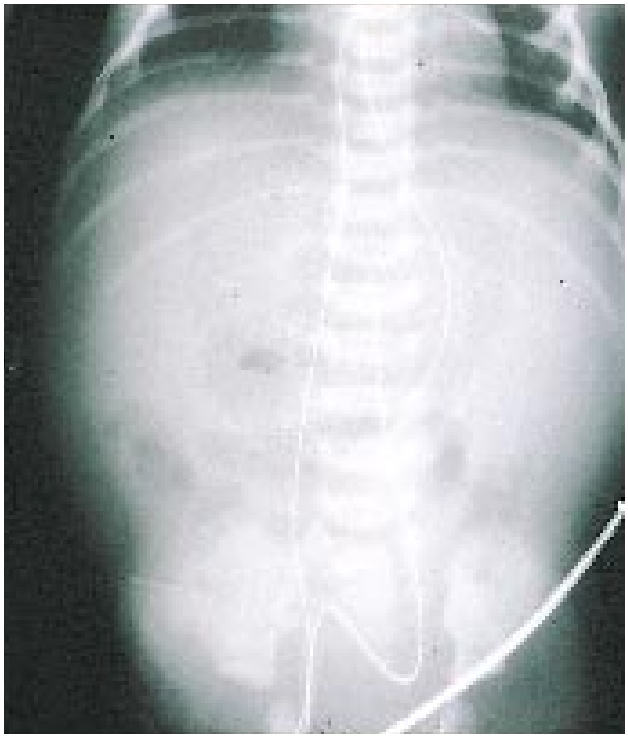

7.66

Figure 7.66. Abdominal radiograph of an infant with pneumoperitoneum as a result of nasogastric tube perforation of the stomach. Note the midline lucency, the "football sign," with visible falciform ligament. Perforation of the stomach may occur spontaneously as a result of a weakness in the wall of the stomach. It is also reported from placement of feeding catheters. Application of suction, especially if the catheter tip is up against the stomach wall, can cause damage. (Singleton, E.)

7.67

Figure 7.67. Soft tissue swelling of the neck was crepitant to palpation. This infant developed subcutaneous emphysema as a result of resuscitation. The subcutaneous emphysema absorbs spontaneously.

7.68

Figure 7.68. Radiograph of the chest and abdomen in an infant showing massive left pneumothorax and pneumomediastinum with displacement of the heart to the right side. On the right side some air is noted between the diaphragm and the upper border of the liver. This is a mild pneumoperitoneum from tracking down of air from the pneumomediastinum. This iatrogenic pathology occurred with vigorous bag and mask resuscitation using excessive pressures.

7.69

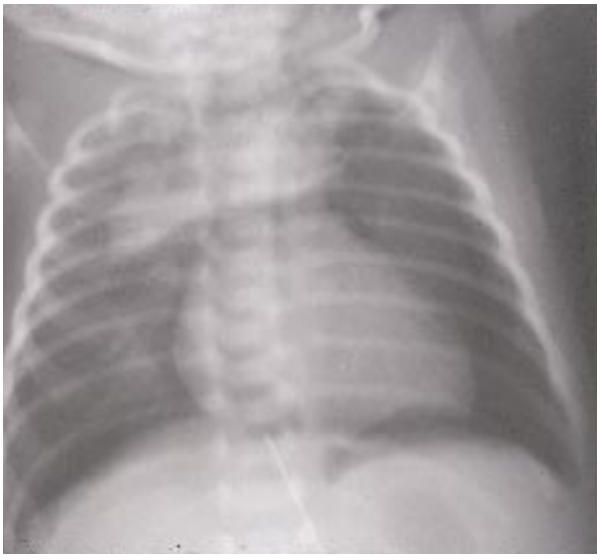

Figure 7.69. Radiograph of the chest in an infant requiring resuscitation at delivery. Note the pneumomediastinum with the lobes of the thymus gland being very prominent bilaterally ("butterfly wing" appearance) as a result of the air in the pneumomediastinum lifting up the lobes of the thymus.

7.70

Figure 7.70. Radiograph of the chest in an infant with severe respiratory distress who developed a pneumopericardium causing cardiovascular instability.

7.71

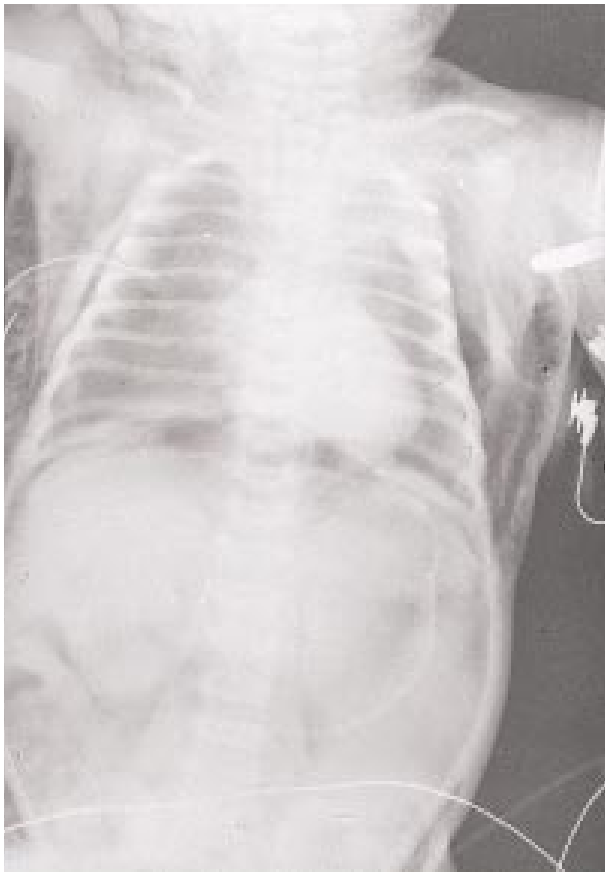

Figure 7.71. Chest and abdominal radiograph in an infant with massive air leak. Note the pneumothorax, pneumomediastinum, pneumoperitoneum and subcutaneous emphysema. This problem occurred as a result of the use of excessive pressures in ventilating the infant.

7.72

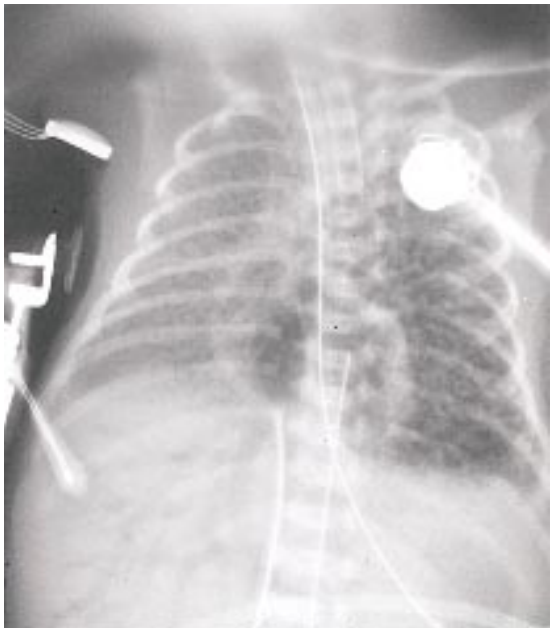

Figure 7.72. Radiograph in an infant with massive air embolism. Note the presence of air in the heart and in the vascular bed of the liver.

7.73

Figure 7.73. A plain radiograph of the skull in the same infant with massive air embolism shows air in the ventricular collecting system. There was also an associated large intraventricular hemorrhage. Massive air embolism is a rare complication of excessive positive pressure resuscitation or ventilation.

7.74

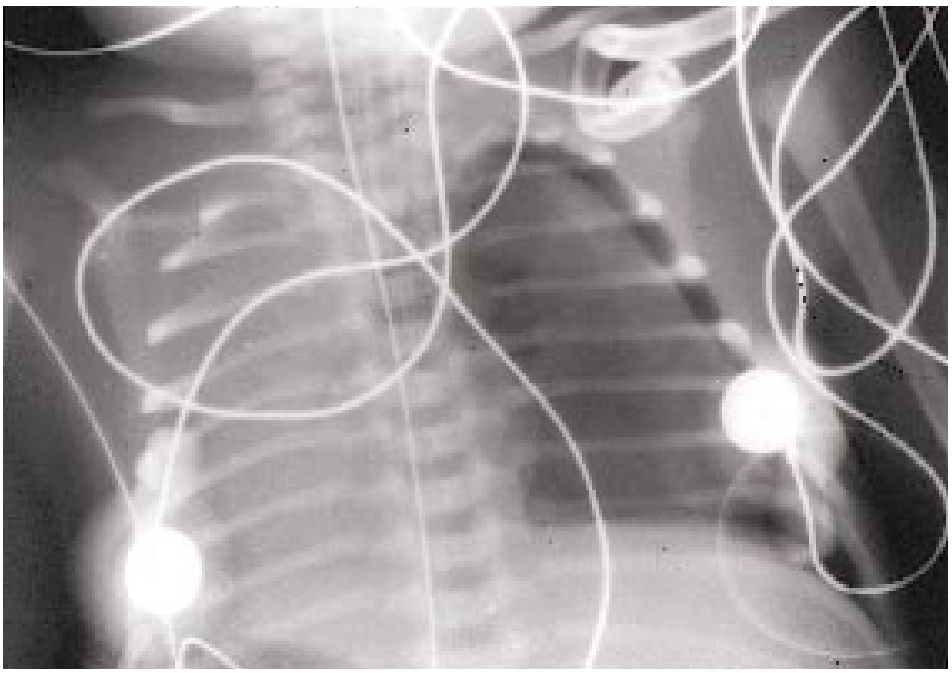

Figure 7.74. Radiograph of the chest of an infant with a left-sided pneumothorax. Note the superior location of the improperly placed chest tube which is lying outside the left thorax.

7.75

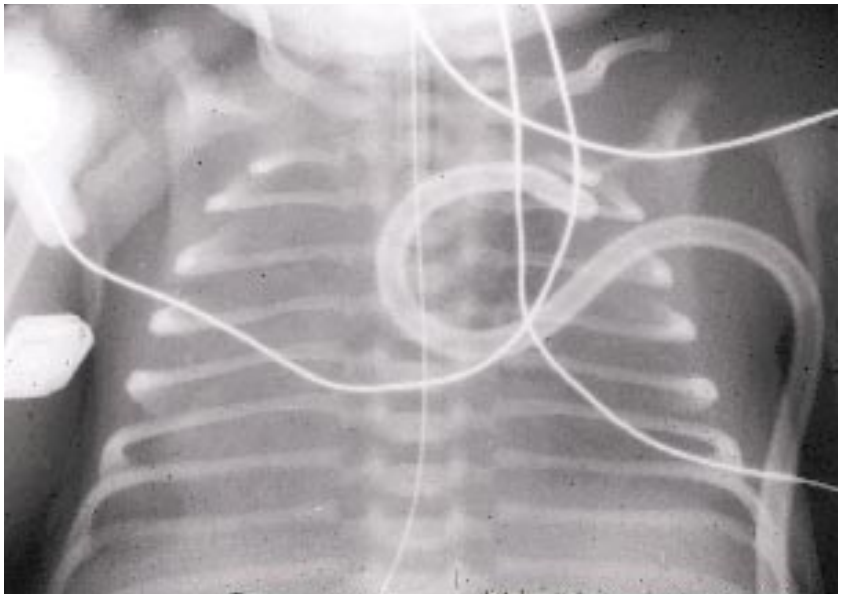

Figure 7.75. Radiograph of the chest of the same infant with rapid resolution of the pneumothorax after proper placement of the chest tube into the left thorax.

7.76

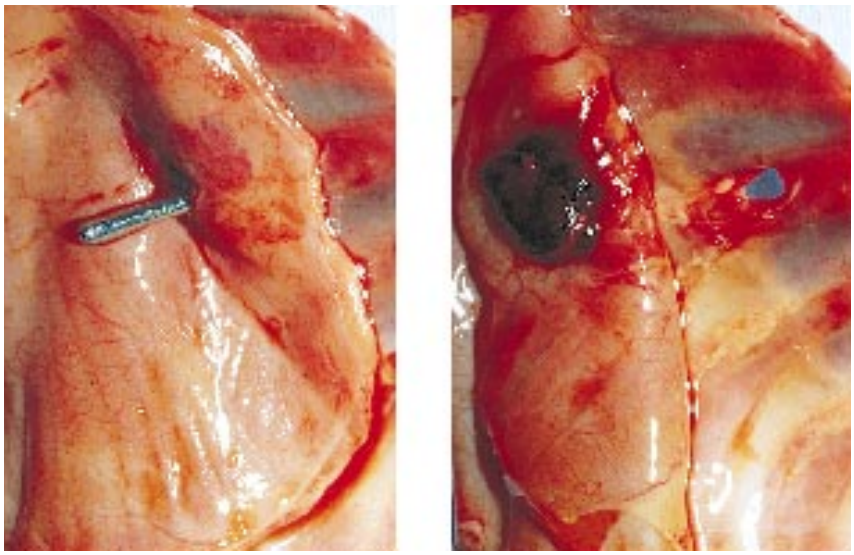

Figure 7.76. This low birth weight infant (birth weight 1440 g) developed a large pneumothorax on the right side. A chest tube was placed in the right sixth intercostal space in the anterior axillary line. The tube perforated the diaphragm and liver resulting in massive hemorrhage from the liver. At autopsy the figure on the left shows the placement of the tube through the chest wall with damage to the diaphragm. The figure on the right shows the perforation of the diaphragm which then resulted in damage to the liver and hemorrhage.

7.77

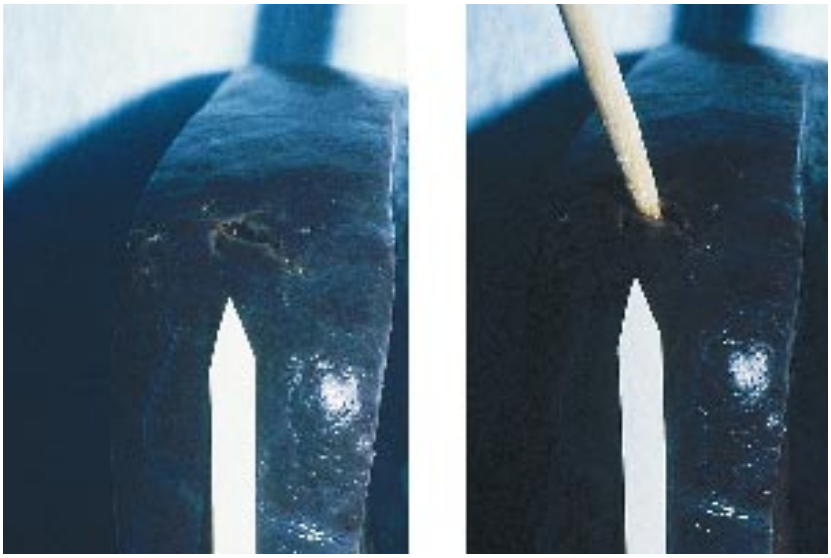

Figure 7.77. Autopsy specimen of the liver from the same infant. Note the laceration of the liver which resulted in the hemorrhage.

7.78

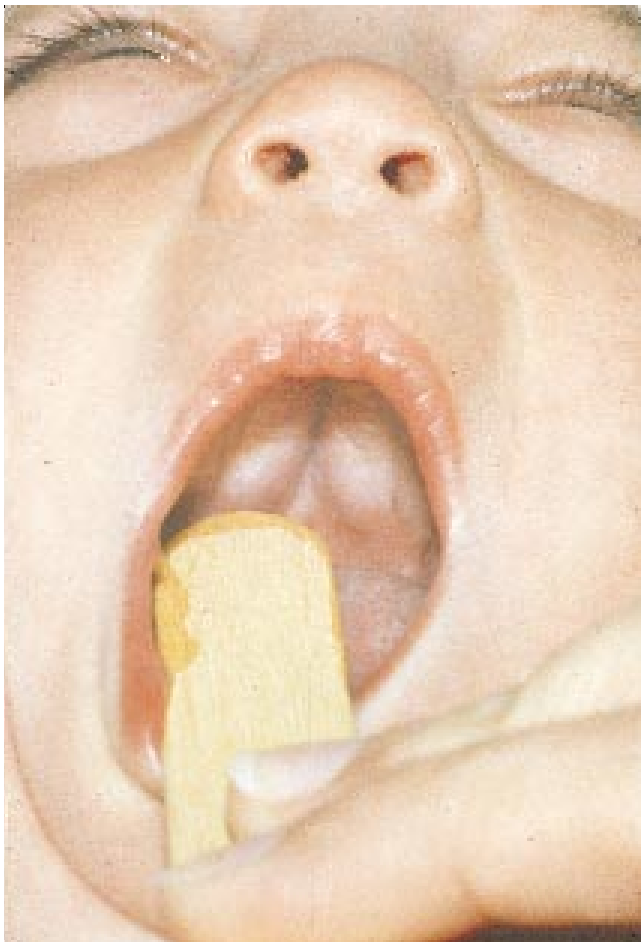

Figure 7.78. As the result of prolonged endotracheal tube intubation this infant developed ridging of the hard palate with a subsequent high arch.

7.79

Figure 7.79. Radiographs of the chest in an infant with (on the left) an apparently normal chest soon after birth. On the right, 2 weeks later, note the fracture of the right humerus and fractures of the ribs. The etiology was obscure but was thought to be iatrogenic.

7.80

Figure 7.80. Radiograph of the lower extremities in an infant with bronchopulmonary dysplasia who developed rickets. Note the poor mineralization of the bones with metaphyseal flaring and cupping.

Index